Synthesis Gas Fermentation

in Membrane Biofilm Reactors

by

Diana Calvo Martinez

A Dissertation in Partial Fulfillment
of the Requirements of the Degree
Doctor of Philosophy

Approved April 2021 by the
Graduate Supervisory Committee:

Bruce E. Rittmann, Co-Chair
Cesar I. Torres, Co-Chair
Rosa Kralmajnik-Brown

ARIZONA STATE UNIVERSITY

May 2021

ABSTRACT

The increasing concentrations of greenhouse gases into the atmosphere call for urgent measures to use non-fossil feedstock for fuels and chemicals. Synthesis gas (or syngas) is a mixture of three gases: hydrogen (H_2), carbon monoxide (CO), and carbon dioxide (CO_2). Syngas already is widely used as a non-fossil fuel and a building block for a variety of chemicals using the Fischer-Tropsch process. Recently, syngas fermentation has attracted attention as a more sustainable way for the conversion of syngas to chemicals, since its biocatalysts are self-generating, are resilient, and can utilize a wide range of syngas compositions. However, syngas fermentation has technical and economic limitations. This dissertation, by contributing to the understanding of syngas fermentation, helps to overcome the limitations. A bibliometric analysis showed the topic's landscape and identified that mass transfer is the biggest challenge for the process. One means to improve syngas mass transfer is to use the membrane biofilm reactor, or MBfR, to deliver syngas to the microorganisms. MBfR experiments delivering pure H_2 demonstrated that the H_2:IC ratio (IC is inorganic carbon) controlled the overall production rate of organic compounds and their carbon-chain length. Organic chemicals up to eight carbons could be produced with a high H_2:IC ratio. A novel asymmetric membrane dramatically improved mass transfer rates for all syngas components, and its low selectivity among them made it ideal for high-rate syngas fermentation. MBfR experiments using syngas and the asymmetric membrane, as well as a conventional symmetric membrane, confirmed that the key parameter for generating long-chain products was a high H_2:IC ratio. The fast mass transfer rate of the asymmetric membrane allowed a very high areal production rate of acetate: 253 $g.m^{-2}.d^{-1}$, the highest reported to

date. Since the membrane delivered H_2 and C from the syngas feed, the relatively low selectivity of the asymmetric membrane favored acetogenesis over microbial chain elongation. A techno-economic analysis of the MBfR showed that the cost to produce acetate was less than its market price. All results presented in this dissertation support the potential of syngas fermentation using the MBfR as a means to produce commodity chemicals and biofuels from syngas.

ACKNOWLEDGEMENTS

This dissertation is the work of so many people that were on my side during all these years, that it would be unfair to say this is only mine. I am forever thankful with everybody that some way or another, helped me to conclude this amazing journey.

I distinctly remember when I wrote that email to Dr. Rittmann. I never imagined that under that prodigious name, there was such a caring person that takes the time to reply an email to a Colombian student looking to pursue a Ph.D. I have learned to be a better researcher, a better thinker, a much better writer, and a better person. I still cannot believe that I was one of the lucky ones that pursued her Ph.D. with him.

I met Dr. Torres in 2009, when I visited the lab. He was so kind that I was even more encouraged to come to ASU. Dr. Torres is the most intelligent person I have ever met, empathic, and easy-going. I thank him for his endless support, for going to the lab when I felt stuck, for the great data discussions, and for his extraordinary taste in music!

I owe a lot to my third committee member, Dr. Rosy, who has been supportive and has selflessly shared her knowledge. She gave me the opportunity to be her TA. It was such a pleasure, that I did it twice! We had the most amazing discussions. I thank her for everything she has done for me. She is an example for all Latinas in academia.

I had wonderful mentors through my Ph.D. Aura taught me the building block for my dissertation: membrane biofilm reactors. We built a strong friendship that has survived time and distance. Anca was the other fundamental piece I needed for my Ph.D. She taught me microbiology techniques, including the extreme sport of making anaerobic media. Her analytical power surpasses research, a great characteristic to have when you are a parent. I thank Anca for her support, her kindness, her hospitality and her amazing

friendship. I could not ask for a better company in this motherhood journey. To my other mentors, Prathap, Sudeep, and Andrew, I thank them for sharing their knowledge.

I also learned from my peers and built friendships with them. With Sofia, we developed methods together, had great discussions, went to trips, laugh, and had hard times as well. All these was the foundation of a wonderful friendship. I also learned a lot from Esra, eager to help everybody. She taught many how to run Quiime, including myself. She was and still is a key support. I thank Blake for his support and his knowledge in the late stages of my Ph.D. I also thank Michelle for all the years together, advising and encouraging. I thank Burcu for her support, friendship and kind soul.

I was very fortunate to have the most amazing mentees in my team: Anderson, Kadmiel, Omar and Vineet. Their hard work was a foundation for my Ph.D.

I must thank Diane Hagner, Sarah Arrowsmith and specially Carole Flores (our "lab mom") for her support. I also thank Ultraworking for their support in work cycles.

I had the fortune to stablish strong collaborations that were essential to produce this dissertation. Hector and Jineth taught me and help me analyze and process the bibliometrics data. Robert Stirling selflessly shared his abundant knowledge in economics, and he was a fundamental piece in our TEA. Other pieces I thank in this economic puzzle were Ellen Stechel and Ivan Ermanoski. Finally, I must acknowledge our collaboration with Ryan Lively and Hye-Youn Yang from GeorgiaTech, whom we shared discussions and who successfully synthetized outstanding membranes.

I also thank our sponsors during my Ph.D.: Minciencias (Colombia) through the fellowship for doctoral studies Francisco Jose de Caldas No 529, the U.S. National Science Foundation - Award Number 1603656, ASU LightWorks, and the Swette family.

Before coming to ASU, I got into teaching and research thanks to Manuel Rodriguez, who was my academic dad in my infancy. I thank him for all his knowledge, his support, his sense of humor, his huge heart, his good soul, and his faith in me.

To my friends, I thank them for baring with me during these years. Lina has helped in all ways possible, from research to babysitting. She was a key piece and I thank her for her friendship. I thank Vanessa for her love beyond frontiers, and beyond generations. I thank my friends here and in Colombia, the "ten", Mily, and Suarez, for their support. I also thank everybody that helped us taking care of Bella during this Ph.D.

Thanks to my relatives, especially Dario and Lucelly, Pops and Madre, Abuelita Concha and Tia Claudia. They have been there with intact faith and unconditional help.

Lastly, I must thank the most special piece I have in my life: My family. My mom is so full of love, that she goes above and beyond without hesitation. I cannot express in words the gratitude I feel towards her. I must thank my dad, whom I owe my love of learning and teaching, for all his hard work to give us a better life, for all his lessons and for his unconditional love. I thank my brothers for always being there, giving me strength. Special thanks to Alejo and Aleja, whose came several times to help me, even with graphs. Finally, I thank my amazing husband and my daughter. Juan is my rock, my counselor, my confidant. He keeps me going and has the biggest faith in what I can do for the world. I cannot imagine this journey without him. To Bella, my beautiful daughter, my inspiration, my everything. She is the sparkle every day, the laugh when I need it the most, the innocence when I feel overwhelmed with the world, the hope of a better future. She is my motor, today and always. I dedicate this dissertation to her.

TABLE OF CONTENTS

Page

LIST OF TABLES

LIST OF FIGURES

Figure Page

Figure Page

CHAPTER 1

INTRODUCTION

Increases of global greenhouse emissions demand urgent measures to reduce climate change (Naik et al., 2010). Non-fossil fuels and sustainable production of chemicals are key steps toward slowing and ultimately reversing climate change. One material that can help achieve both steps is syngas (short for synthesis gas), a mixture of carbon dioxide (CO_2), carbon monoxide (CO), and hydrogen (H_2). Syngas can be a carbon-neutral biofuel and a building block for more complex biofuels and chemicals (Henstra et al., 2007; Wender, 1996). Syngas provides a means to utilize carbon from sources such as lignocellulosic biomass, other organic wastes, natural gas, coal, and even water and CO_2 from the atmosphere (Agrafiotis et al., 2014; Wender, 1996).

Syngas production is mainly associated with lignocellulosic biomass, which represents a large renewable feedstock that is highly resistant to biodegradation by most microorganisms (Latif et al., 2014; Phillips et al., 2017). Syngas is produced by thermochemical conversion, in which the syngas components are generated through gasification (Alonso et al., 2010). This pathway offers several advantages over direct biochemical conversion of biomass to biofuels, as direct conversion requires pretreatment and hydrolysis processes, which are technical and economic bottle-necks in biofuel production (Arantes and Saddler, 2010; Yang and Wynman, 2012).

A recent renewed interest has fallen in solar technologies to produce syngas (Andrei et al., 2020; Falter and Pitz-Paal, 2018). Classic feedstocks include natural gas,

biogas, or even biomass, but the use of "zero-energy chemicals", i.e., water and carbon dioxide, is more attractive for their availability and non-existent carbon footprint (Agrafiotis et al., 2015). The limited efficiency of carbon dioxide splitting with solar power and the inability to control the H_2:CO ratio in the syngas produced has been the bottleneck for the expansion of the technology, but redox-paired oxide systems used for water splitting have proven to be adaptable for carbon dioxide splitting in the last decade (Agrafiotis et al., 2015; Marxer et al., 2017).

Syngas is in fact one of the main building blocks for liquid chemicals and liquid fuels (Agrafiotis et al., 2015). Further conversion of syngas to these products current relies on the Fischer-Tropsch process (FTP), where a metal catalyst is used to hydrogenate carbon monoxide. However, the process represents a major economic hurdle due to its poor conversion and thermal efficiencies (Wilhelm et al., 2001).

The biological conversion of syngas to liquid biofuels is an attractive alternative to the FTP (Munasinghe and Khanal, 2010). While the FTP requires high temperature, pressure, and costly metal catalysts, microorganisms work with ambient conditions and are self-generated (Mohammadi et al., 2011).

The biological conversion of syngas to liquid chemicals and fuels, *i.e.*, syngas fermentation, is made possible by the metabolism of acetogens, a group of microorganisms that produce valuable organic chemicals from CO_2 (Diekert and Wohlfarth, 1994). Acetogens are anaerobic bacteria that utilize the Wood-Ljungdahl pathway to convert H_2 and CO_2, syngas, and a variety of sugars to predominantly acetate, along with ethanol (Drake et al., 1997; Fuchs, 1986; Henstra et al., 2007; Phillips et al.,

2017). Metabolic engineering has been used to shift the distribution of the products towards higher acids and alcohols (Daniell et al., 2012; Lan and Liao, 2013). One example is *Clostridium ljungdahlii*, which normally is able to produce acetate and ethanol, but is genetically amenable for production of ethanol only or even butanol directly (Köpke et al., 2010; Richter et al., 2013).

Biochemically converting syngas to liquid fuels has generated significant interest in the past few years, but several challenges are evident. With collaborators, I performed a bibliometric analysis (Chapter 3) to identify trends in the field, its main challenges, and how the challenges are being addressed. From the bibliometric analysis, I identified that one main challenge is having a bioreactor that allows high rates of gas delivery to the syngas-consuming microorganisms (Abubackar et al., 2012; Mohammadi et al., 2011). This challenge stems from the low aqueous solubility and, consequently, slow interfacial gas-liquid mass transfer of the gaseous substrates (H_2 and CO). Various laboratory versions of continuous stirred tank reactors (CSTRs), trickling filters, and gas-lift bioreactors have been tried to improve mass-transfer rates (Haddad et al., 2014; Mohammadi et al., 2012; Orgill et al., 2013), but none is economically feasible for industrial-scale production, because the mass-transfer rates in these conventional bioreactors remain far too low, even with significant energy input.

The membrane biofilm reactor (MBfR) is a relatively new process that overcomes problems stemming from the low solubility of gaseous substrates. The MBfR delivers a low-solubility gas directly to a biofilm that grows on the outer surface of a hollow-fiber membrane and utilizes the gas as a substrate (Rittmann, 2018). This translates not only in

better mass transfer between gas and liquid, but also high retention of biomass in the biofilm and higher substrate concentrations encountered by the microorganisms.

I am part of a team that is deeply experienced using MBfRs for water treatment, for which H_2 is delivered to the biofilm to reduce a broad spectrum of oxidized contaminants in water: e.g., nitrate, nitrite, perchlorate, selenate, arsenate, chromate, uranium, dibromochloropropane, chloroform, tetrachloroethene (PCE), trichloroethene (TCE), and N- nitrosodimethylamine (NDMA) (Chung et al., 2008, 2007a, 2006; Lee and Rittmann, 2000, 2002; Martin and Nerenberg, 2012; Ontiveros-Valencia et al., 2013; Rittmann, 2018, 2006; Van Ginkel et al., 2008; Zhao et al., 2013a; Zhou et al., 2014; Ziv-El et al., 2012; Ziv-El and Rittmann, 2009). I studied the MBfR as a novel process for high-rate and low-cost microbiological conversion of syngas to organic chemicals.

Key to my success for the conversion of syngas, as well as other possible future applications, is achieving rates of gas delivery much greater than attained with traditional bioreactor types, as well as with MBfRs used today for water treatment. Therefore, I worked with collaborators on optimizing membranes, microorganisms, and operational conditions in the MBfR (Chapters 4-6), as well as a Techno-Economic Analysis (TEA) to evaluate implementation of the technology at large scale (Chapter 7).

My first approach to address the challenges was to study a pure-H_2-based MBfR with a commercially available membrane; the goal was carboxylates and alcohols production (Chapter 4). I hypothesized that the ratio between H_2 and inorganic carbon (IC) would be a key factor in the amount and type of carboxylates and alcohols produced. Because H_2 and IC deliveries are independent in this MBfR, I could systematically

evaluate the impact of the ratio. I successfully operated the first pure-H_2-based MBfR for carboxylates and alcohols production. I obtained high production rates and titers, and I proved that the H_2:IC ratio is the key factor.

Second, I focused on improving the membranes over those used for water-treatment applications of the MBfR (Chapter 5). MBfR membranes cover a wide range of configurations and materials, from porous microfiltration membranes to non-porous dense membranes (Choerudin et al., 2021; Duyar et al., 2021; Martin and Nerenberg, 2012; Pal and Nayak, 2017; Rittmann, 2018; H.-J. Wang et al., 2018; Xiao et al., 2021). Porous membranes are easier to synthetize and provide a higher flux than non-porous membranes, but the lumen pressure needs to be close to the liquid pressure in order to avoid bubbling or counter diffusion, limiting the actual flux that can be delivered to the biofilm. Additionally, pores become water-filled and efficiency in mass transfer is reduced (Scholes et al., 2015). A dense polymer membrane needs to have a wall thick enough (usually >100 um) to be strong and durable. This results in a large diffusion distance for the gas through the dense polymer, creating mass-transfer resistance (Wu et al., 2019).

A third alternative is the combination of both, called a composite membrane (Terada et al., 2004). Composite membranes are a combination of a thin layer of dense polymer with one or two layers of porous material (Ahn et al., 2009; Chung et al., 2008, 2007b, 2007a; Martin and Nerenberg, 2012; Rittmann, 2018; Van Ginkel et al., 2008; Ziv-El and Rittmann, 2009). The most common composite membrane has two outer layers of porous material enclosing a thin layer of dense polymer, which reduces

diffusion limitation compared to dense polymer fibers; however, the two outer layers create mass-transfer resistance, particularly on the liquid side when the macropores become water-filled. My collaborators at Georgia Institute of Technology successfully synthetized several new asymmetric hollow-fiber membranes capable of holding a biofilm on the outside while minimizing mass-transfer resistance by using only one layer of porous material, on the lumen side. These membranes are based on Matrimid® and Torlon® materials. I performed mass-transfer experiments to choose the best membrane for the MBfR. One of the Matrimid® fibers had the best maximum gas delivery and the lowest selectivity between syngas components; therefore, I chose it for my syngas based-MBfRs.

I evaluated the effect of membranes in syngas-based MBfRs using conventional symmetric and the novel Matrimid® asymmetric membranes (Chapter 6). I found that the Matrimid® membrane enhanced the production rate per unit membrane area substantially, making its further development very promising. I also found that the permeability of the membrane was a key factor for microbial chain elongation (MCE).

The biofilm that forms on the outer surface of the membrane is more efficient if it is enriched with the desired microorganisms. I approached the enrichment of cultures towards syngas fermenters using the MBfR as an enrichment tool itself. I obtained enriched cultures and characterized them for syngas consumption (Chapters 6).

Large-scale facilities for syngas fermentation already are in place (Chen et al., 2018; Daniell et al., 2012). Scaling-up the MBfR for carboxylate production could improve the production rate drastically. Therefore, I examined the cost-effectiveness of

the system by performing TEA (Chapter 7). I simplified the analysis by focusing on the production of acetate. The TEA proved that the MBfR system is cost-effective, as long as efficient separation processes are available.

In summary, I successfully increased the production rate for carboxylic acids and alcohols using the MBfR by using novel high-transfer-rate membranes, enriched cultures, and optimized operational conditions in the reactor. Based on my results, I also propose *niches* of research that I consider important for exploration in the near future. These include a systematic analysis of syngas composition in fermentation, alternatives for separation of carboxylates and alcohols, and bioprospecting to find superior microorganisms for producing carboxylic acids and alcohols.

CHAPTER 2

BACKGROUND

1. Synthesis gas

Synthesis gas (or syngas) is a mixture of hydrogen, carbon monoxide and carbon dioxide that is increasingly used as a clean fuel, as well as an intermediate for biofuels and chemicals production (Henstra et al., 2007; Wender, 1996). Syngas is highly versatile in the sources for its production and the type of chemicals produced from it (Bachirou et al., 2016; Munasinghe and Khanal, 2010). Understanding syngas production, its variables, and further conversion to liquid fuels and chemicals are key to optimizing the process.

1.1.Production of synthesis gas

Currently, syngas production surpasses 6 EJ per year, equivalent to approximately 2% of primary worldwide energy consumption (El-Nagar and Ghanem, 2019). In fact, syngas and H_2 are the most used feedstocks for synthetic liquid fuels (Agrafiotis et al., 2014).

As a general principle, syngas can be derived from any hydrocarbon feedstock. The main goal is to partially oxidize the hydrocarbon to obtain H_2 and CO:

$$[2CH]_{feedstock} + O_2 \rightarrow 2CO + H_2$$

The classic source of for synthesis gas is coke, but more sustainable non-fossil alternatives have become important in the recent years (Abatzoglou and Fauteux-Lefebvre, 2016; Guerrero et al., 2020).

1.1.1. Syngas derived from fossil fuels

Fossil fuels have been the main feedstock for syngas production (Kurucz and Bencik, 2009). Even though coke was used in the early stages of the technology, natural gas reforming has been the main route of syngas production for decades (Rostrup-Nielsen, 2000). The goal of converting natural gas to syngas is to increase the energy density of the gas so that more energy is embedded in the same volume of gas (Rostrup-Nielsen, 2000).

Liquid fossil fuels also can be gasified to obtain H_2 and CO (Speight, 2019). Initially, the industry was reluctant to use this feedstock because it reduced the energy density, but they became attractive when the Fischer-Tropsch process (FTP) was commercialized (Speight, 2019). FTP allows the conversion of liquid fuels and even hydrocarbon waste to valuable organics of several natures, while avoiding impurities present in conventional processes (De Klerk, 2012). As a result, a highly enriched H_2/CO gas shifted from a direct use as a fuel to a feedstock for chemical synthesis (Reyes et al., 2003). Afterwards, syngas sources expanded to a wide variety of hydrocarbon feedstock that could be gasified at high temperature and low pressure (El-Nagar and Ghanem, 2019).

Advances in the production process include developing dozens of metallic and mineral catalysts that improve selectivity towards a desired compound, reduce the required temperature, speed up the process, and reform natural gas directly (Ereña, 2020).

1.1.2. Lignocellulosic biomass as alternative carbon source

The desire to use more sustainable alternatives has shifted away from using natural gas and petroleum-derived compounds to the gasification of lignocellulosic biomass and pyrolysis of organic waste (He et al., 2010; Santos and Alencar, 2020; Sun et al., 2019). Lignocellulosic biomass represents a large renewable feedstock for the production of biofuels. Biofuels derived from lignocellulosic biomass are referred to as second-generation biofuels, and they can be synthesized via biochemical and thermochemical platforms (Naik et al., 2010; Sims et al., 2010). Biochemical conversion of lignocellulosic biomass first involves pretreatment and then hydrolysis, followed by biological conversion of resulting sugars and alcohols (Lynd et al., 2005). Pretreatment and hydrolysis are currently major bottlenecks in making second-generation biofuels through biochemical conversion a reality (Arantes and Saddler, 2010; Yang and Wynman, 2012). Gasification is an alternative to overcome these bottlenecks, avoiding pre-treatment and making recalcitrant biomass available for conversion (Munasinghe and Khanal, 2010).

1.1.3. The use of sunlight for carbon fixation

A more recent alternative is gaining attention: as illustrated in Figure 1, solar thermochemical processing, in which zero-emissions energy (i.e., sunlight) is used to convert water and CO_2 in the atmosphere to syngas (Agrafiotis et al., 2014; Bachirou et

al., 2016). During the process, the reactants H_2O and CO_2 are reduced to H_2 and CO using a metal catalyst (Bachirou et al., 2016) and high temperature. Key advantages of the solar-thermal technology are the possibilities to manage the H_2:CO ratio, reduce CO_2 in the final product, and produce O_2 as by-product (Ermanoski et al., 2013).

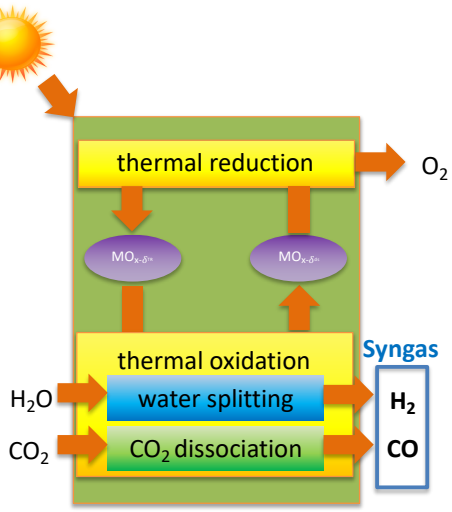

Figure 1. Solar-driven chemical reduction of CO_2 for syngas production

1.2. Uses of synthesis gas

Synthesis gas is an exceptionally versatile gas mixture. Its direct use as an energy source offers advantages over natural gas or biogas by avoiding their impurities (Liakakou et al., 2021). The high demand for liquid fuels makes the further conversion of syngas to liquid fuels more attractive than its direct use. Easier transportation, higher energy content, and a wide range of derivates are some advantages of the conversion to liquid fuels.

1.2.1. Fischer-Tropsch process

The Fischer-Tropsch process (FTP) is the most common and well-studied option for using syngas to make biofuels and chemicals. Using metallic catalysts, the FTP generate monomers by breaking complex molecular structures and then polymerizing these monomers to create longer chains (Overett et al., 2000). During FTP, the catalysts dissociate CO and then hydrogenate it, producing organic compounds and water (Santos and Alencar, 2020). FTP is a highly exothermic process, which inherently causes it to have low energy efficiency.

Several reactor configurations have been developed to reduce the FTP's energy demands and to recover the metallic catalyst from the product mixture. Each configuration has its particular benefit. The fixed-bed reactor is easily scalable, the fluidized bed reactor is relatively good at minimizing the heat loss of the exothermic reactions, and the slurry-bed reactors work best at lower temperatures (Santos and Alencar, 2020).

1.2.2. Syngas fermentation

The use of microorganisms as biocatalysts for syngas conversion presents several advantages over metallic catalysts: *e.g.*, adaptability of microorganisms to a wide range of syngas composition, operation at low temperatures, self-production of catalyst, and sustainable and environmentally friendly (Asimakopoulos et al., 2018; Henstra et al., 2007). Fermentation is carried out by anaerobic microorganisms capable of transforming H_2, CO, and CO_2 to carboxylates and alcohols (Munasinghe and Khanal, 2010). The carboxylate platform, a pairing of waste-derived syngas and carboxylates production

from syngas fermentation, is attractive due to its sustainability potential (Agler et al., 2011). Syngas fermentation is the focus of this dissertation.

2. Fundamentals of syngas fermentation

Syngas fermentation is based in the ability of microorganisms to fix inorganic carbon from the gas phase and transform it to a wide range of chemicals (Drzyzga et al., 2015). Interest in syngas fermentation surged when *Clostridium ljungdhalii* was shown to produce ethanol and acetic acid from H_2, CO_2, and CO (Klasson et al., 1993). Afterwards, several more syngas-fermenting bacteria were isolated and characterized.

2.1.Acetogenic microorganisms

Acetogenic bacteria convert CO, H_2, and CO_2 into acetic acid. Bacteria produce acetyl coenzyme A (acetyl-CoA) from small molecules, and acetyl-CoA is used as an intermediate metabolite to synthesize biomass as well as organic products, most directly acetic acid and ethanol. Production of acetic acid from H_2, CO, and CO_2 generates energy for cell synthesis, including the formation of complex molecules such as lipids and proteins, from the inorganic gas substrates (Phillips et al., 2017).

The first isolated acetogen was *Clostridium aceticum*, which produced acetic acid from H_2 and CO_2. Afterwards, more than 100 species of acetogens have been reported, with this number is continuously growing (Drake et al., 2008). Their temperature ranges extend from 5°C to 83°C, and they are able to grow in alkaline to acidic conditions. Their morphology includes rods, cocci, and spirochetes, and some tolerate anoxic conditions (Phillips et al., 2017). Important is their ability to tolerate the toxicity of CO, although that seems to vary with adaptation (Esquivel-Elizondo et al., 2018).

Syngas fermentation has mainly been studied with pure cultures of *Clostridium*, especially *C. ljungdahlii, C. carvoxidivorans*, and *C. autoethanogenum*, and it is now at commercial scale (Daniell et al., 2012; Fernández-Naveira et al., 2016; Ramió-Pujol et al., 2015a; Valgepea et al., 2017). Lately, mixed cultures are attracting attention due to their versatility for commercial scale (Lagoa-Costa et al., 2017).

2.2.Microbial chain elongation

Even though acetic acid and ethanol are valuable chemicals, upgrading them to longer acids and alcohols opens up a wide range of higher-value products. One of the most promising ways to do this upgrading is within the reactor used for syngas fermentation. Chain-elongating microorganisms are capable of producing acids and alcohols up to eight carbons from acetic acid and ethanol (Gildemyn et al., 2017; Mohammadi et al., 2011; Hanno Richter et al., 2016; Sun et al., 2018b; Zhang et al., 2013b). Recent reports even suggest that acetogens can convert H_2 and CO_2 to even longer products (Drzyzga et al., 2015; Lagoa-Costa et al., 2017).

Clostridium kluvyeri is the most known chain-elongating microorganism (Candry et al., 2020). It is a gram-positive bacterium that grows in mesophilic and strictly anaerobic conditions. The species's genome was sequenced for the first time in 2008 (Seedorf et al., 2008), but it has been used for upgrading syngas fermentation for a decade, and its discovery was in the early 1930s (Hanno Richter et al., 2016; Steinbusch et al., 2011; Weimer et al., 2015; Zhang et al., 2013b).

Most chain-elongating bacteria use reverse β-oxidation, adding two-carbon acetyl-coAs to produce butyrate (4-C) and caproate (6-C) from acetate. However, some

studies showed propionate (3-C) production from syngas, especially in thermophilic conditions (Alves et al., 2013).

Mesophilic microorganisms are well-known to carry out syngas fermentation and microbial chain elongation, but much less information is available for thermophilic microorganisms, which promise several advantages: avoiding cooling after syngas production, faster kinetics, and easier separation of products. However, the solubility of syngas is lower at thermophilic conditions (Phillips et al., 2017).

3. Reactors for syngas fermentation

The selection of reactor configuration to perform syngas fermentation has important implications for the microbial ecology of the system, as well for the production of chemicals. Several factors need to be considered when choosing a type of reactor: versatility of the microorganisms (*e.g.*, mixed or pure cultures), tolerance to toxicity, cost, and gas transfer (Asimakopoulos et al., 2018). Usually, gas is continuously supplied, but liquid can be processed in batch, semi-batch, or continuous modes (Munasinghe and Khanal, 2010). The several common reactors for syngas fermentation usually aim for a good mass transfer between gas-to-liquid.

3.1. Continuous stirred-tank reactor (CSTR)

The CSTR, illustrated in Figure 2, is the most common configuration employed for syngas fermentation. Syngas is injected continuously from the bottom of the reactor, while liquid addition supplements nutrients needed for the fermentation. Gas transfer is improved by reducing the bubble size, which increases surface area between gas and

liquid. Bubble size usually achieved by use baffled impellers that break up the bubbles and lengthen the time of the bubble in the liquid (Munasinghe and Khanal, 2010).

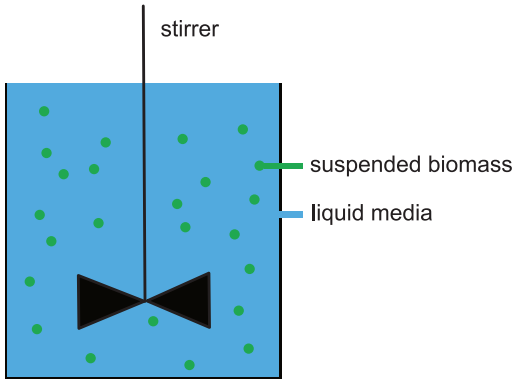

Figure 2. Continuous stirred-tank reactor

3.2.Bubble column reactor (BCR)

The BCR, Figure 3, offers a longer gas-liquid contact time than CSTRs, since its principle is bubbling the gas from the bottom of a columnar reactor. Given its columnar nature, the diameter/length ratio is a crucial parameter in BCR design (Asimakopoulos et al., 2018).

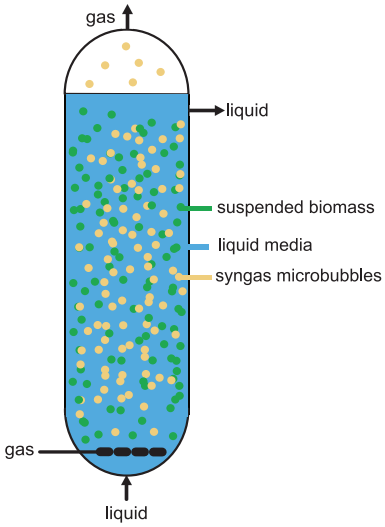

Figure 3. The bubble column reactor and its principle

The BCR has been widely studied to enhance the mass transfer between gas and liquid by increasing the area of contact between phases. Figure 4 shows the main configurations for BCRs. The cascade BCR (Figure 4- a) includes a series of vertical panels to increase the time of contact between the bubbles from the diffusor at the bottom of the tank and the liquid. BCRs with loop the liquid flow pattern is modified by sparging one section instead of the whole reactor. With the internal loop configuration (Figure 4- b), gas flow comes from inner cylinders to outer ones. In contrast, the external loop configuration (Figure 4- c) uses vertical tubes connected by horizontal sections in both ends of the reactor (Doran, 2013). The multi-shaft BCR uses horizontal panels to increase tortuosity if the gas and increase time of contact (Figure 4- d), while the BCR with static mixers aims to reduce the superficial tension between gas and liquid (Figure 4- d) (Bai, 2010). Finally, the BCR configuration as packed column aims to retain biomass with packing material, while increasing contact time between biomass and gas with bubble dispersion from the bottom (Chu et al., 2017).

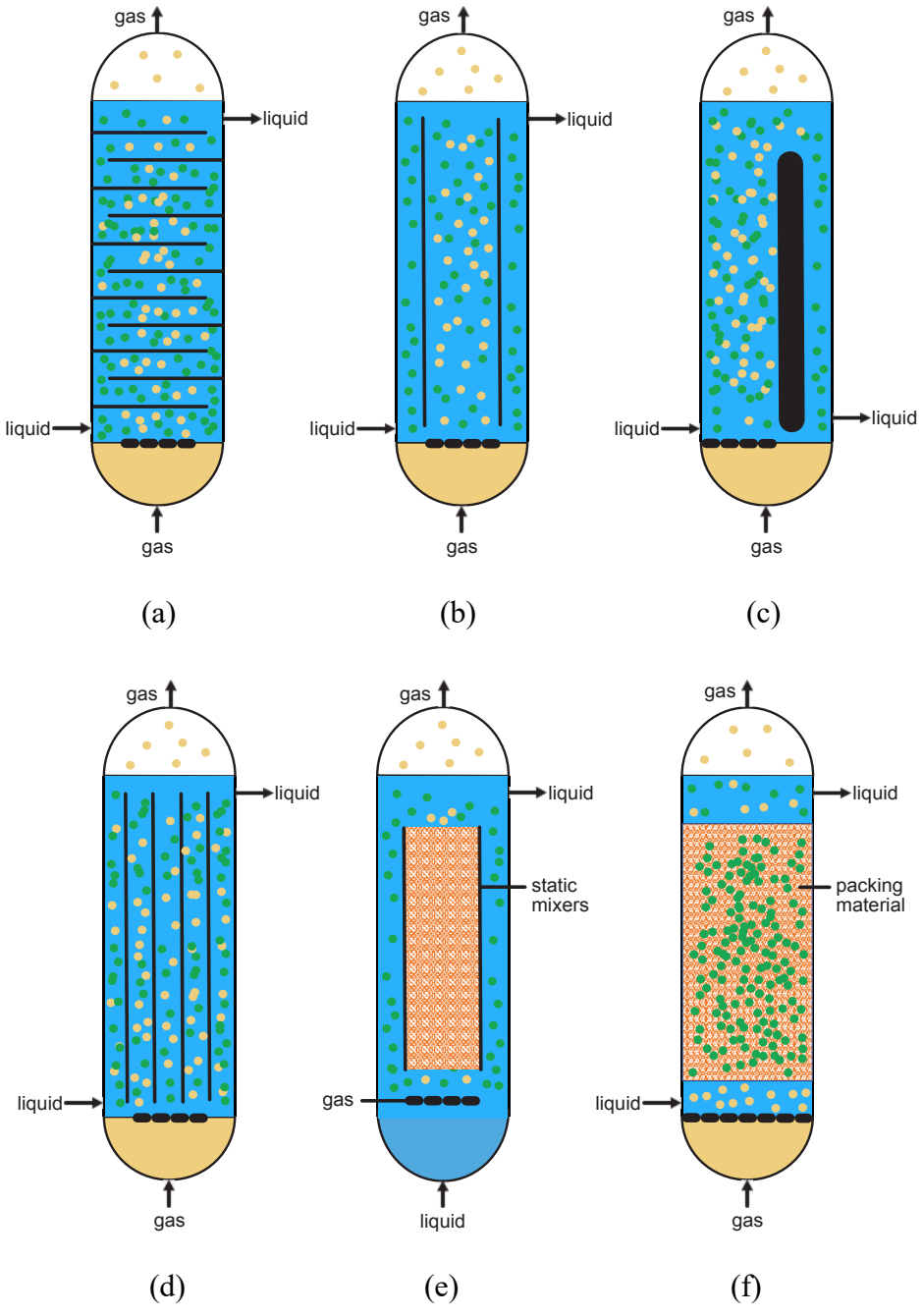

Figure 4. Types of BCRs. (a) Cascade, (b) internal loop, (c) external loop, (d) multi-shaft, (e) static mixers, (f) packed column. Yellow: gas; green: biomass, and blue: liquid medium.

3.3.Trickle-bed reactors (TBR)

The trickle-bed reactor (TBR), illustrated in Figure 5, is a column in which biofilm grows in an inert material packed in the reactor. The liquid is supplied from the top in form of "rain" that "trickles" down over the biofilm on the packing material. Syngas is supplied either co-current or countercurrent. These systems require low energy, but their efficiency is low compared to CSTR and other configurations (Bredwell et al., 1999).

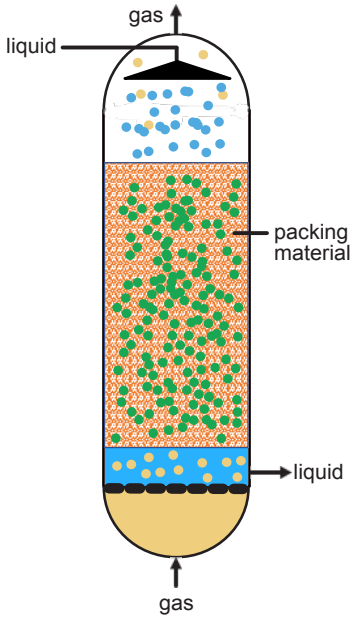

Figure 5. Trickle-bed reactor

3.4.Membrane biofilm reactor (MBfR)

Hollow-fiber membranes are an excellent alternative for supplying low-solubility gases directly to a catalyst immobilized on the membranes' surface (Rittmann, 2018). The membrane biofilm reactor (MBfR) has a microbial biofilm as the catalyst. As shown in Figure 6, the gaseous substrate is supplied to the lumen via bubble-free gas-transfer

membranes, diffuses through the membrane wall, and is utilized immediately by microorganisms growing in the outside of the membrane. Hence, the rate-limiting liquid film that forms at the gas-liquid interface in bubble systems, such as the CSTR or the gas-lift bioreactor, is eliminated and replaced by the "biofilm reaction zone," in which the substrate is consumed. When coupled with a high specific surface area of membrane surface, direct delivery can result in significant improvements in overall mass transfer coefficients: from ~100 h^{-1} with the best current bioreactor configurations to >1000 h^{-1} using the MBfR (Shen et al., 2014). This increase allows very high volumetric production rates and favorable process economics.

A corollary advantage of the MBfR is that the concentrations of the gaseous substrate that the microorganisms encounter in the membrane-associated biofilm can be significantly higher than in other bioreactor types; the outcome is faster biological kinetics. Additional advantages of the MBfR are that it can attain virtually 100% utilization efficiency for the gas and provides excellent retention of the biocatalysts, thus circumventing the need for separating solids from the product stream.

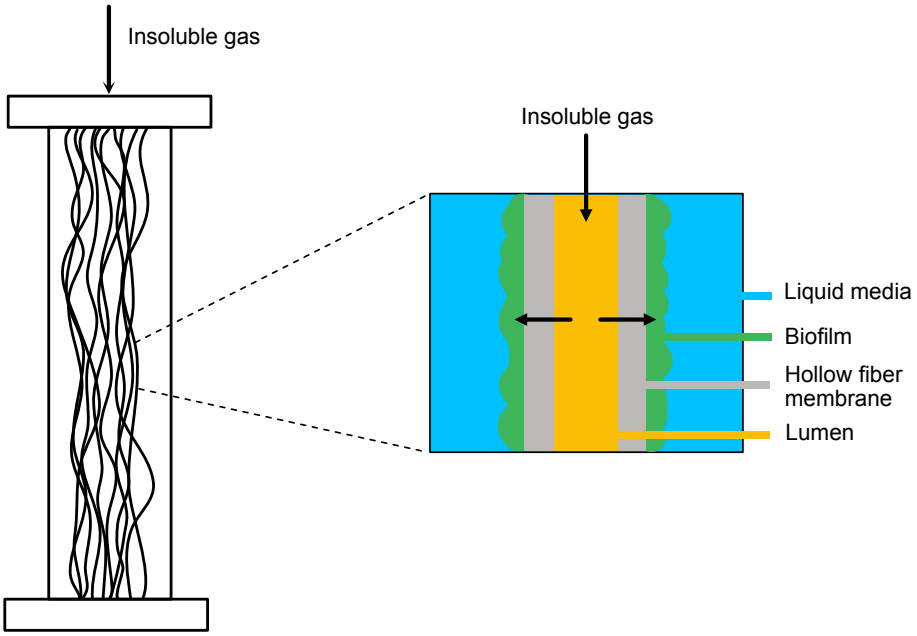

Figure 6. The membrane biofilm reactor (MBfR) and its principles.

The H_2-based MBfR is widely used for the reduction of oxidized contaminants in water, and the O_2-based MBfR has been used for oxidation of organic contaminants and nitrification (Rittmann, 2018). Variations of the MBfR have been used for syngas fermentation over the last 8 years, and their production rates far surpass other reactor configurations (Shen et al., 2018; Zhang et al., 2013b). Considering the several advantages of the MBfR and its still-limited exploration for syngas fermentation, I focus my doctoral dissertation on syngas fermentation with the MBfR.

CHAPTER 3

GLOBAL TRENDS IN SYNGAS FERMENTATION RESEARCH[1]

1. Introduction

Synthesis gas (or syngas) is a mixture of carbon dioxide (CO_2), carbon monoxide (CO), and hydrogen (H_2) that is increasingly being used as a fuel and an intermediate for biofuels and chemicals production (Henstra et al., 2007; Wender, 1996). It is a means to recycle carbon from sources such as lignocellulosic biomass, other organic wastes, natural gas, coal, and even water and CO_2 from the atmosphere (Agrafiotis et al., 2014; Wender, 1996). The high demand of liquid fuels makes conversion of syngas to fuels more attractive than its direct use as a fuel.

The Fischer-Tropsch process (FTP), which used metallic catalysts, is the most common and well-studied alternative for this conversion, but FTP is highly exothermic, which inherently causes it to have low energy efficiency (Santos and Alencar, 2020). While several reactor configurations have been developed to reduce its energy demands, FTP remains a large energy consumer (Santos and Alencar, 2020). A promising alternative to overcome FTP limitations is syngas fermentation.

[1] **Credit:** *Diana C. Calvo* – writing, conceptualization, SQ design, graphs, data analysis, edition, funding acquisition; *Hector J. Luna* – conceptualization, database standardization, data curation, graphs, data analysis, edition; *Jineth Arango* – writing, database standardization, data curation, graphs, data analysis, edition; *Cesar I. Torres* – writing, data analysis, edition; *Bruce E. Rittmann* – writing, data analysis, edition, funding acquisition.

In syngas fermentation, microorganisms are biocatalysts that convert syngas to a wide range of carboxylates and alcohols (Munasinghe and Khanal, 2010; Phillips et al., 2017). Syngas fermentation presents several advantages over FTP: self-generating catalysts, adaptability of the microorganisms to a wide range of syngas compositions, operation at low temperatures, a higher thermodynamic efficiency than FTP, and even the potential to be carbon-neutral (Agler et al., 2011; Asimakopoulos et al., 2018; Henstra et al., 2007; Molitor et al., 2017).

Syngas fermentation has been widely directed towards ethanol and acetic acid production, giving that they are easiest to produce (Phillips et al., 2017). However, upgrading them to longer-chain acids and alcohols offer advantages. To date, carboxylic acids and alcohols up to eight carbons have been produced from a wide variety of substrates using microbial chain elongation (MCE) (Candry and Ganigué, 2021; Mohammadi et al., 2011; Hanno Richter et al., 2016; Sun et al., 2018b; Zhang et al., 2013b). Some reports suggest that elongation also could be generate longer chains, fuels, and even polymers (Drzyzga et al., 2015; Han et al., 2018).

Reviews of syngas fermentation are extensive and describe fundamental concepts and their applications (Drzyzga et al., 2015; Liew et al., 2016; Mohammadi et al., 2011; Molino et al., 2016; Phillips et al., 2017; Sun et al., 2019; Yasin et al., 2015). Syngas fermentation is viewed as a promising option to direct carbon from biomass and the atmosphere to valuable products (Asimakopoulos et al., 2018; Munasinghe and Khanal, 2010).

Here, we analyze scientific publications related to syngas fermentation from the Web Of Science (WoS) database, using statistical techniques and computing technology through a bibliometric analysis, which generates qualitative and quantitative indicators of a field's status and direction (Hew, 2017; Huang et al., 2020; Zhong et al., 2016). Bibliometric analyses are widely used to identify research hotspots, research progress within groups and countries, key publications, and loci of high impact (Huang et al., 2020; Zhu et al., 2021).

In brief, we gathered data from the WoS using a designed search query (SQ). We evaluated the growth in publications and citations, charted the evolution of WoS categories, and identified the most productive authors and organizations/countries based on descriptive indicators. We also performed a deep keyword analysis to identify the prominent research *niches* and challenges. Finally, we used network analysis to link the keywords with the most productive authors and identify their specific research area. We hope our analysis will be a tool for researchers to move syngas fermentation forward in the most fruitful areas, as well as encourage collaborations between groups.

2. Methods

2.1.Design of the Search Query (SQ)

A well-designed SQ accurately and comprehensively extracts metadata from documents relevant to its topic. We created the SQ as illustrated in the Data Collection section in Figure 7. We used the WoS/Clarivate core collection database from 1900 through 2020 and included articles, reviews, proceedings papers, and book chapters. The WoS core collection included the Science Citation Index Expanded, the Conference

Proceedings Citation Index-Science, the Book Citation Index–Science, the Emerging Sources Citation Index, and the Social Sciences Citation Index. We analyzed the downloaded database from WoS using a preliminary analysis to validate the SQ, followed by a systematic review. We did the preliminary analysis using bibliometrix (Aria and Cuccurullo, 2017), and we used the application *biblioshiny* in R Studio v.1.3.1073 to visualize the database (Xie et al., 2020). For the systematic review, we reviewed each publication included in the database obtained with the SQ in order to confirm its relevance to syngas fermentation.

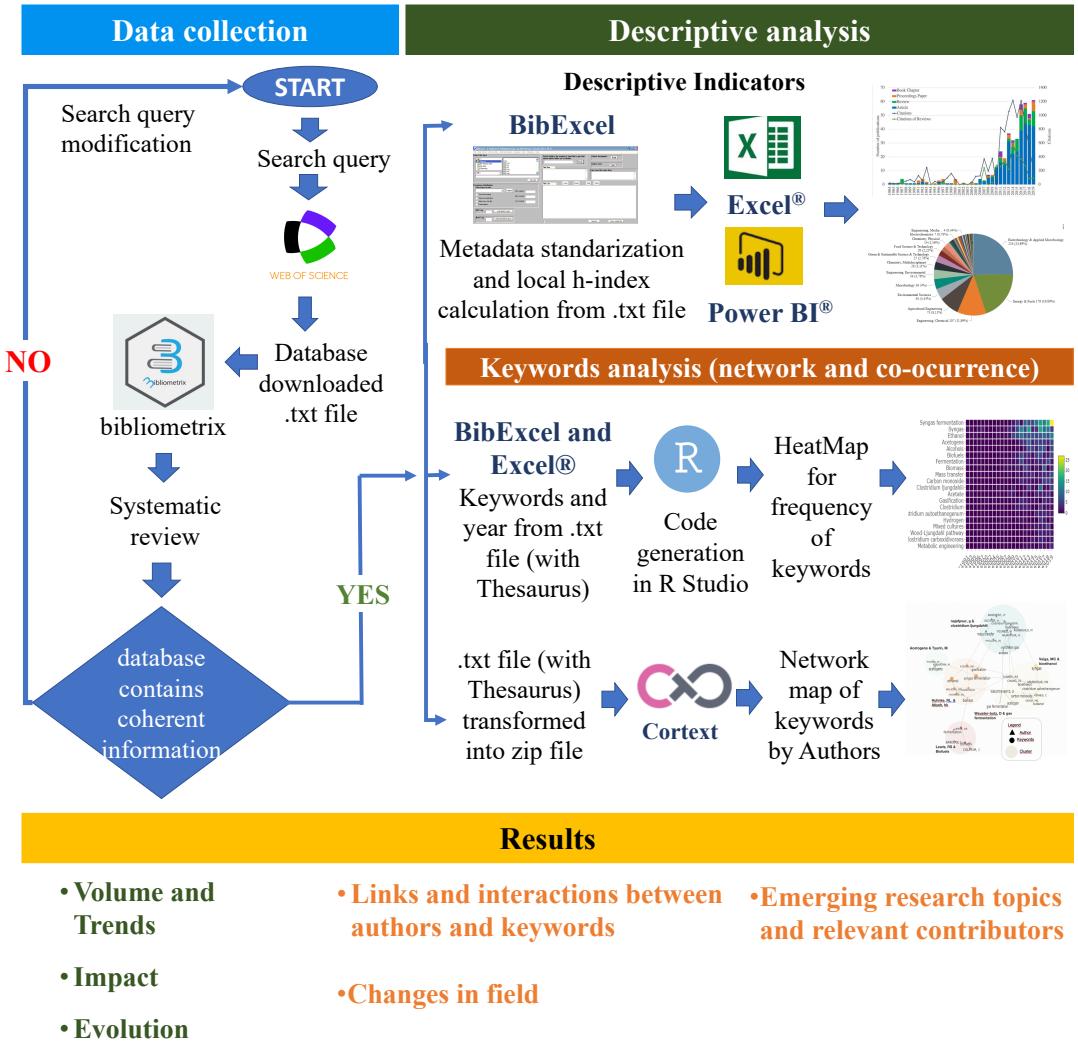

Figure 7. Flow path, logic, and methodologies used for the bibliometric analysis in syngas fermentation.

We designed our SQ by carefully evaluating well-known reviews in syngas fermentation and their references (Abubackar et al., 2012; Bertsch and Müller, 2015; Daniell et al., 2012; De Luna et al., 2019; Henstra et al., 2007; Jang et al., 2012; Latif et al., 2014; Liew et al., 2016; Lovley and Nevin, 2013; Makshina et al., 2014; Mohammadi et al., 2011; Munasinghe and Khanal, 2010; Rastogi and Shrivastava, 2017; Spirito et al.,

2014; Yang et al., 2014). We realized that using *"syngas fermentation"* as an exclusive expression in the SQ omitted documents related to the topic, since some documents do not refer to syngas fermentation directly, even when is the key topic: for example, authors used individual syngas components or "synthesis gas" instead of "syngas." Authors also often used "syngas" or "synthesis gas" and "fermentation" in no particular order. We adjusted the expression to "*(("synthesis gas" OR syngas) NEAR/5 fermentation))*." Syngas fermentation is also can be referred to as "syngas biocatalysis." Therefore, we added the expression "*(("synthesis gas" OR syngas) AND biocataly*))*."

Finally, we made sure that all documents related were included by using the syngas components in the SQ, paired with the expected products from their conversion. However, hydrogen, carbon monoxide, and carbon dioxide are very common elements coupled with conversion and the production of acids and alcohols. Also, we noticed that some authors do not mention acids or alcohols production, but the specific name of the chemical produced. Therefore, we included in the SQ *((("hydrogen and carbon" OR syngas OR "synthesis gas") NEAR/2 (use OR conversion OR from)) AND ((formate OR acet* OR propion* OR butyr* OR valer* OR capro* OR acid$ OR ethanol OR butanol OR propanol OR pentanol OR hexanol OR alcohol$ OR chemical$) NEAR/2 (production OR synthesis)))*. We used the "*" wildcard to include carboxylic acids as well as carboxylates. We made sure no other products were lost by adding longer and more complex products without seeing a difference in the number of documents in the outcome database. Additionally, it is common that syngas is converted to ethanol and other organics with metal catalysts; therefore, we modified the SQ to eliminate all entries

related to this type of process with *NOT (*cataly* OR *particle$ OR "syngas from" or "synthesis gas from"))*.

The final SQ used for the analysis was defined as: *TS=((((((("hydrogen and carbon" OR syngas OR "synthesis gas") NEAR/2 (use OR conversion OR from)) AND ((formate OR acet* OR propion* OR butyr* OR valer* OR capro* OR capryl* OR acid$ OR ethanol OR butanol OR propanol OR pentanol OR hexanol OR octanol OR alcohol$ OR chemical$) NEAR/2 (production OR synthesis))) NOT (*cataly* OR *particle$ OR "syngas from" or "synthesis gas from")) OR (("synthesis gas" OR syngas) NEAR/5 fermentation)) OR (("synthesis gas" OR syngas) AND biocataly*))*.

2.2.Data visualization

2.2.1. Descriptive analysis

We structured the database using BibExcel (Persson et al., 2009), in which we cleaned and standardized the metadata from the txt. file. Then, we used Microsoft Excel® v. 16.40. to verify the non-existence of void elements. When we identified a void element in the database, we returned to the unstructured database and modified the element in NotePad++® v. 7.8.6. Once all void elements were eliminated, we restructured the database and confirmed that all fields were valid. With the structured database confirmed, we visualized and analyzed the publications and citations over the years in Excel®, the evolution of categories using PowerBI®, and the most productive organizations/countries uploading a .zip file of the database to the CorTexT platform (https://www.cortext.net/). CortexT uses the Louvian's algorithm to clusterize information (Blondel et al., 2008). Finally, we used the software VOSviewer 1.3.16 to

study collaborations between institutions (van Eck and Waltman, 2010). VOSviewer clusterizes by similarity.

2.2.2. Keywords analysis

Heatmap timeline

We extracted the "keywords by author" and "year" fields in the unstructured database using BibExcel. Then, we created a *thesaurus* using Excel® to avoid redundancies (*e.g.,* "syngas" and "synthesis gas"). Then, we created a .txt file with the Top 20 keywords and uploaded it to R Studio v. 4.0.2. to generate a heatmap of keywords by year using the library *heatmaply.*

Network map and co-occurrence of keywords with authors

We replaced all redundant words in the clean unstructured database based on the Thesaurus. Then, we created a .zip file and uploaded it to the CorTexT platform to visualize the network map of authors and the Top 20 keywords in the field. Then, we created a VOSviewer map to analyze collaborations between authors.

3. Results

3.1.Production of documents

Figure 8 presents the year-by-year bibliographic production for syngas fermentation found in the WoS database. The figure breaks down the publications and citations by type, presents the number of publications and citations by year for each type, and shows their cumulative total value over time. The total number of publications from 1984 through 2020 was 535, and the total citations were 10,835.

We identified two key observations in the production of documents and citations. The main observation is that the field is still growing, as the slope of the cumulative production of documents shows. Also important is that the cumulative line for citations shows a classic "S" shape. Unusual is that the growth phase in citations began sooner than the growth phase of documents; this appear to be due to early review articles, which garnered many citations.

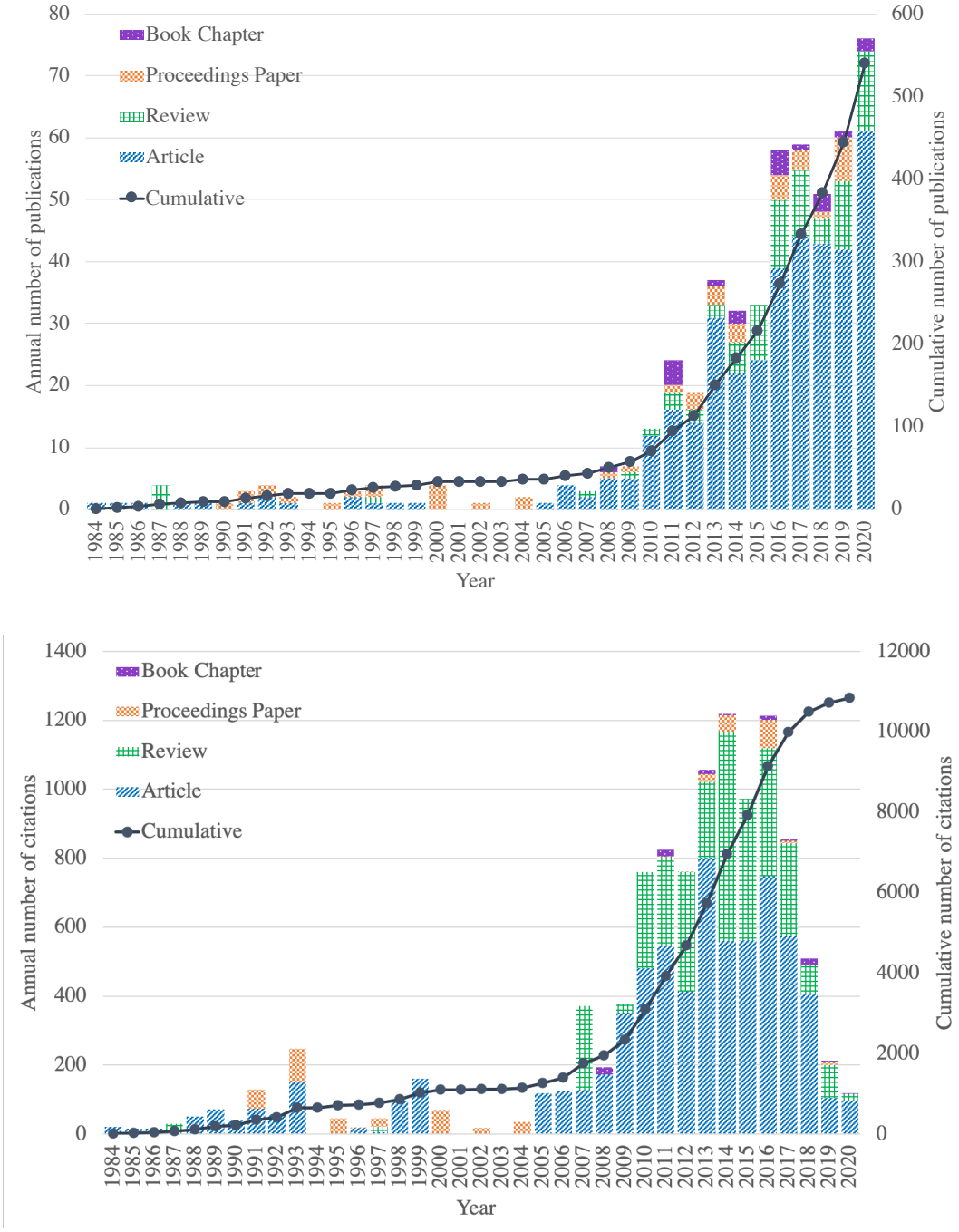

Figure 8. Annual and cumulative numbers of publications by type (top panel) and their citations (bottom panel) for syngas fermentation based on the WoS.

The field showed a "lag stage" from 1984 to 2007, a period that had 49 publications overall: 25 articles, 18 proceedings papers, and 6 reviews. Fewer than 5 documents were published annually during this period, a pattern that is usual when a new research field is in its infancy (Huang et al., 2020). What is unusual for syngas fermentation is that the lag stage lasted more than 20 years, compared to an average of 10 years for other fields that have been studied (Chen et al., 2017; Huang et al., 2020; Mallawaarachchi et al., 2020; Zhao et al., 2018). Additionally, a "dead" period occurred between 2001 and 2005, when only three proceedings papers and one article were published. Citations of publication in the lag phase are only 16.4% (1783 citations) of total citations for the field, and more than 5% occurred in the last three years (2005-2007). The key contributor in the lag period was Henstra et al. (2007), which had 263 citations. Henstra et al. (2007) reviewed the microbiology of syngas fermentation and noted a strong focus on mesophilic bacteria. Bredwell et al. (1999) was another well-cited article (170 citations) that discussed reactor design for syngas fermentation; it concluded that increasing the efficiency of gas-to-liquid mass transfer was the most important factor limiting the process. Finally, Tanner et al. (1993) (165 citations) described the isolation of *Clostridium ljungdahlii*, a well-known bacterium that produces ethanol from syngas.

From 2008, the field showed fast paced growth that continues to 2020, which showed the highest number of documents published, 76 in total. The 13-year period had 477 publications in total, a 90.6% of total publications, with an average of 37 publications per year and an average growth slope of 5.6 publications/year.

Another gauge of growing interest is the increasing number of reviews published during this period (73 in total), being the highest in 2020 as well, with 13 reviews.

Citations in the growth stage corresponded to 83.6% of the total citations, and a third were for reviews. Citations declined in the last 4 years, but part of the decline is a natural result of the publications being recent. In addition, the decline could be an indication that the field is maturing, with less opportunity to create new core knowledge. Linked with this interpretation is that based on our systematic review, articles published in the last 4 years addressed applications more than fundamentals.

The most highly cited publications in this growth period were reviews that addresses key concepts of syngas fermentation. Munasinghe and Khanal (2010) produced the most highly cited document, with 307 citations. It provides a comprehensive review of the conversion of syngas to biofuels: typical microbial catalysts used for the process and their sensitivity to factors such as pH and temperature, the advantages of converting biomass-derived syngas to biofuels, the challenges needing to be addressed (including quality of syngas, microbial catalysts suggesting the use of thermophilic microorganisms, product recovery proposing extraction, and mass-transfer), and the potential for delivering syngas via hollow-fiber membranes.

Another highly cited review was by Makshina et al. (2014) (232 citations), reviewed the chemistry for producing butadiene (a well-known precursor of polymer production) from biomass-derived feedstock. The routes for butadiene production include several relevant to syngas fermentation: Ethanol, butanol or butanediols can be obtained from syngas fermentation to later be converted to 1,3-butadiene.

A recent trend is more interest in economic and sustainability considerations. De Luna et al. (2019), which had 219 citations in less than two years, presents a deep techno-economic analysis merged with a carbon-emission analysis of possible products obtained from the electrocatalytic transformation of water and carbon dioxide. Among its products, syngas is a key chemical that can be further converted to a wide range of valuable chemicals, including acids, alcohols and polymers. Daniell et al. (2012), with 213 citations, also approached syngas fermentation from a commercial perspective, as they include economic factors along with the fundamentals needed to scale-up the process.

One key element behind the continuous growth in syngas fermentation is its versatility: It can accommodate to several a wide range if inputs and conditions, while producing a wide range of chemicals. Lovley and Nevin (2013), (217 citations) even suggested that syngas fermentation is applicable to electrobiocommodities, since the microbial communities involved in syngas fermentation could work as catalysts in systems where electricity is the energy source for the production of valuable chemicals.

3.2.Evolution of categories

Syngas fermentation is highly inter-disciplinary, which is exemplified by its publications having appeared in 48 WoS categories from 1984 to 2020. Figure 9 shows the top categories in 2007 and 2020, which spans the end of the lag stage to the end of our study period. The number of categories increased significantly over the 14 years:

from only 3 categories in 2007 to 25 categories in 2020. Thus, syngas fermentation is becoming more inter-disciplinary.

Syngas fermentation is a continually evolving field. Categories in the lag phase were closely related to fundamentals, as well as to chemical or environmental engineering. In contrast, many of the new categories in 2020 were more applied and further from chemical and environmental engineering: ecology, materials science, public health, nanoscience and nanotechnology, agricultural engineering, electrochemistry, and biophysics. The highly cited papers evolved over that period: e.g., Jang et al. (2012) using Clostridia for butanol production, Zhang et al. (2013) using membrane biofilm reactors for fatty acids production, and Haas et al. (2018) optimizing current densities for electrochemical reduction of CO_2 and H_2O to further conversion to useful chemicals.

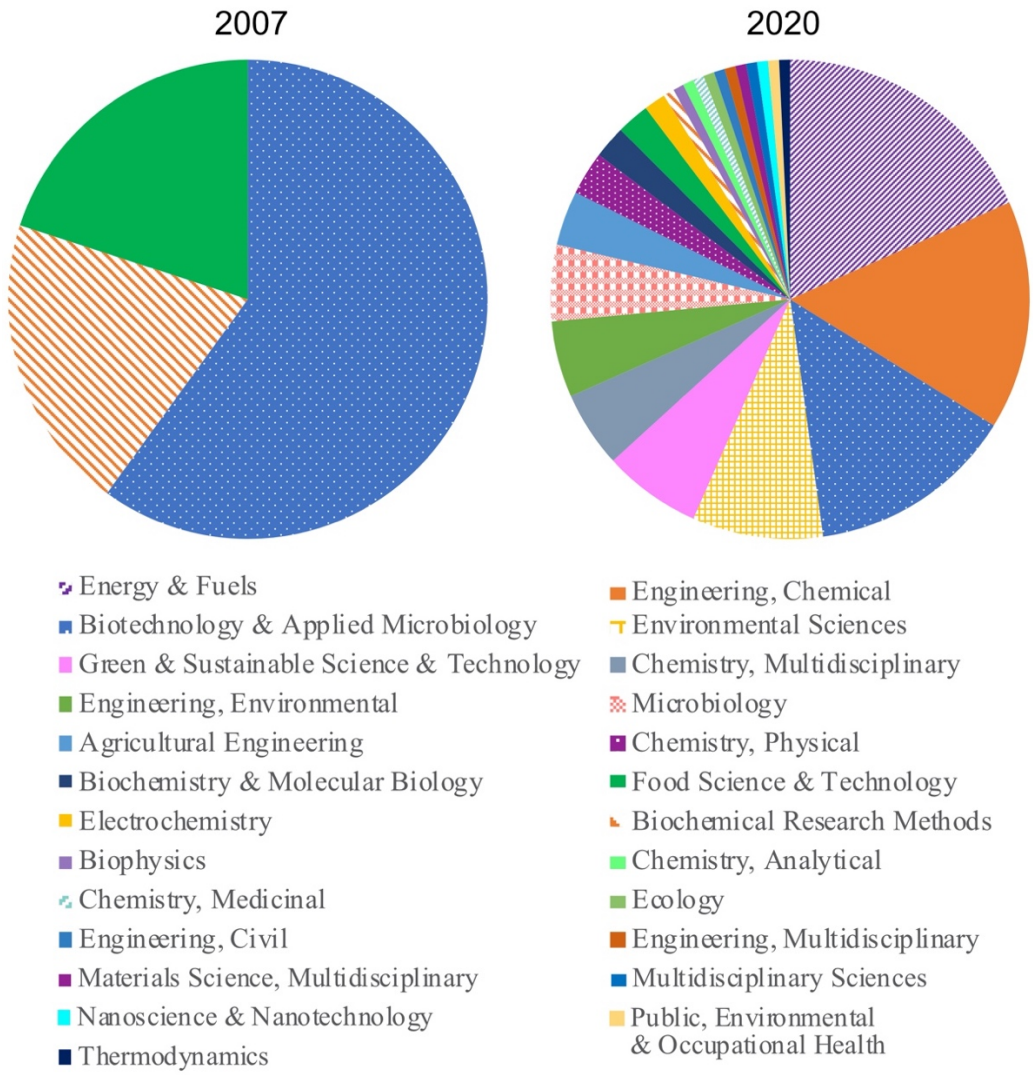

Figure 9. Growth of categories of publications on syngas fermentation from 2007 to 2020

3.3.Most influential countries and organizations

Figure 10 Panel A identifies the top contributing organizations and countries in syngas fermentation; we used a threshold of 8 or more documents, which yielded the top 22 organizations. Figure 10 Panel B complements Panel A by showing the most important collaborations between these organizations. The USA had the largest number

of productive organizations: 7 organizations with 122 publications, however, just 4 of them seem to have strong collaborations between them. Italy, Japan, Malaysia, Sweden, Russia, UK, Brazil, and France are top contributors as countries, but they had no top institutions associated to them.

Oklahoma State University had the largest number of publications (31), and its predominant theme was alcohols production (Liu et al., 2014a; Maddipati et al., 2011; Phillips et al., 2015). Oklahoma State University's collaborative network involved 3 universities in USA: Brigham Young University (12), the University of Oklahoma (11), and Iowa State University (16). The collaboration between Brigham Young University and Oklahoma State University (7 co-authored publications) focused on the effect of partial pressure of carbon monoxide in syngas fermentation, effects of nitric oxide in ethanol production, and improving gas-liquid mass transfer (Ahmed and Lewis, 2007; Devarapalli et al., 2017, 2016; Hurst and Lewis, 2010; Orgill et al., 2013). Co-authored publications (7) between Oklahoma State University and the University of Oklahoma was directed to ethanol production from syngas (Liu et al., 2014b, 2014a, 2012; Phillips et al., 2015; Sun et al., 2018a, 2018b). Iowa State University had some collaboration with Oklahoma State University (1 co-authored publication) as well as with the Technical University of Denmark (1 co-authored publication), also an active institution, with 13 publications. Iowa State University focused its work in analyzing and improving gas-liquid mass transfer for syngas fermentation (Riggs and Heindel, 2006; Shen et al., 2014; Ungerman and Heindel, 2007; Zhu et al., 2008).

Other institutions in the USA cluster were The Ohio State University (13 publications), Cornell University (15), the University of Massachusetts (9), and the National Renewable Energy Laboratory (7). The Ohio State University focused its work in using pure cultures of *Clostridium* for alcohols production (Saxena and Tanner, 2012; Wang et al., 2014), Cornell University conducted research on microbial chain elongation (Kucek et al., 2016; Perez et al., 2013; Spirito et al., 2014; Vasudevan et al., 2014), the University of Massachusetts focused on metabolic modeling (Banerjee et al., 2014; Chen et al., 2018, 2015; Chen and Henson, 2016), and the National Renewable Energy Laboratory focused on the production of biofuels in terms of its economic viability (Karatzos et al., 2017; Tan et al., 2017). Cornell University also was highly collaborative with European universities, including the University of Minho in Portugal, the University of Girona in Spain, Ghent University in Belgium, and Wageningen University in The Netherlands. Cornell also had strong collaborations with German universities that did not meet the threshold for the network map, such as Tubingen University. The University of Massachusetts also had some collaborations with Ghent University, but it mainly collaborated with the Lanzatech Inc., a company that successfully scaled up syngas fermentation as a commercial process (Chen et al., 2018).

One cluster for collaborations involved South Korean universities, including Sosang University, Hankyong University, and the Gwangju Institute of Science and Technology. Besides collaborations with Sogang University, the Gwangju Institute of Science and Technology had one co-authored publication with Oklahoma State University.

Other key institutions include the Chinese Academy of Sciences (22 publications), University of A Coruna (16) in Spain, Technical University of Munich (13) in Germany, and Tarbiat Modares University (11) in Iran, but they do not show collaborations above the threshold we used.

Using citations as a metric, the top-performing organizations roughly mirrored the top 22 by publications. The top 5 in terms of citations were Oklahoma State University (1121 citations), Cornell University (844), Wageningen University (568), University of Corona (544), and Iowa State University (456).

Figure 10 Panel B shows that networking has been modest in the field of syngas fermentation. This points to the possibility that research in syngas fermentation could be accelerated by increased collaboration among the top institutions. It may be beneficial to integrate their interests in areas such as membrane biofilm reactors, genetic modification, pure and mixed culture reactors, and MCE (Abubackar et al., 2015; Fernández-Naveira et al., 2019, 2016; Zhang et al., 2013b; Zhao et al., 2019)

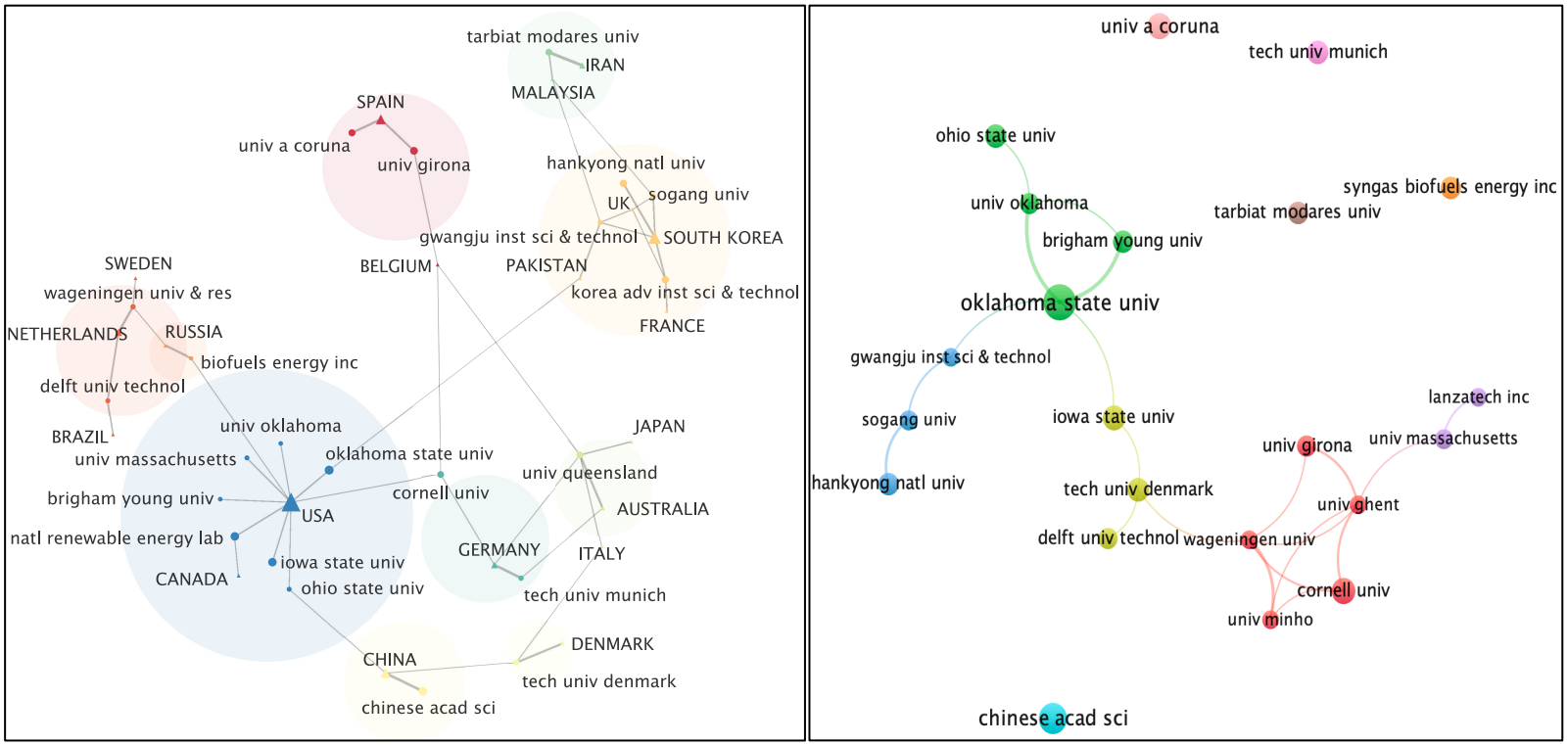

Figure 10. Panel A: Most influential organizations and their correlation with the most influential countries (threshold: 8 documents produced). Nodes identify a country with a triangle and an institution with a circle; the size of a node is proportional to the number of appearances in the search. Clusters (color-shaded circles) congregate nodes with strong topic correlation between. Every link between nodes is created by distributional proximity in the CorTexT platform. Panel B: Collaborations between institutions using VOSviewer.

3.4.Keywords analysis

3.4.1. Keywords heatmap over time

The use of keywords and their evolution over time point out research trends, challenges, and possible solutions. The heatmap in Figure 11 shows that research on products from syngas fermentation was focused more on producing "ethanol" and "biofuels" over "acetate" in the last decade. In fact, ethanol production was the main point of discussion in nine of the ten most-cited documents in syngas fermentation (Bredwell et al., 1999; Daniell et al., 2012; De Luna et al., 2019; Henstra et al., 2007; Jang et al., 2012; Lovley and Nevin, 2013; Makshina et al., 2014; Munasinghe and Khanal, 2010; Piccolo and Bezzo, 2009; Yang et al., 2014). That the world is looking for alternatives to fossil fuels explains why biofuels are an important interest. However, the usual feedstock for biofuels are sugar cane, corn starch, and seed-oil, which also are feedstock to the food system (Henstra et al., 2007; Molino et al., 2016; Munasinghe and Khanal, 2010). Feedstock alternatives that do not compete with food are residuals and by-products from agriculture, such as lignocellulosic biomass (Munasinghe and Khanal, 2010). Because biological pathways to produce ethanol from lignocellulosic biomass is technically difficult (Henstra et al., 2007), syngas is gaining interest in the context of "biomass" since lignocellulosic biomass can be gasified to syngas for conversion to biofuel (Phillips et al., 2017).

Among the components of syngas, "carbon monoxide" is a highly used keyword for two reasons: CO is toxic to microorganisms, and its low solubility in water affects process performance (Munasinghe and Khanal, 2012; Techtmann et al., 2009). H_2 also is

very insoluble in water. Therefore, "mass transfer" between the gas phase and the liquid phase is gaining recognition as one of the main challenges in syngas fermentation (Asimakopoulos et al., 2018; Mohammadi et al., 2011; Yasin et al., 2015).

Microorganisms capable of fermenting syngas have been well studied for decades, and the "Wood-Ljungdahl pathway," associated mainly with "acetogens," is the main metabolic route in the process (Spirito et al., 2014). Syngas fermentation has been carried out mainly with pure cultures of the "*Clostridium"* genus, including *"C. ljungdahlii," "C. autoethanogenum"* and *"C. carboxidivorans"* (Abubackar et al., 2016; Li et al., 2015; Martin et al., 2016; Richter et al., 2013). However, "mixed cultures" are gaining attention for their versatility in commercial processes (Liew et al., 2016). "*Clostridium"* still is the most important genus for syngas fermentation, regardless of the reactor configuration and if "chain elongation" is taking place (Calvo et al., 2021; Candry and Ganigué, 2021; Drake et al., 2008).

"Chain elongation" is a topic of increasing interest given the higher economic value of medium-chain fatty acids and alcohols over short-chain acids and alcohols, as well as the possibility to reduce separation costs given the lower solubility of longer products (Devi et al., 2021; Scarborough et al., 2018). With the current expansion of syngas fermentation in commercial scale, along with it wide range of products, "biorefineries" based on the process are becoming a hot research topic (Liakakou et al., 2021; Munasinghe and Khanal, 2010; Scarborough et al., 2018). Ways to improve biorefineries include optimizing operational conditions and employing "metabolic engineering" (Daniell et al., 2012; Ramió-Pujol et al., 2015b; Zhao et al., 2019).

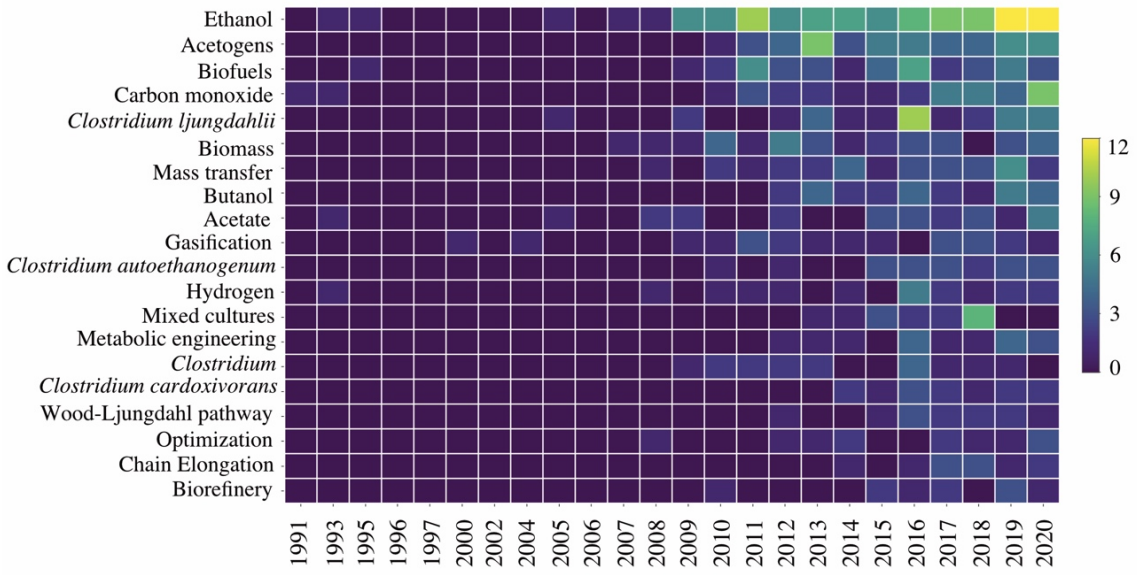

Figure 11. Heatmap timeline of the Top 20 keywords in syngas fermentation. The map excludes "syngas fermentation," "fermentation," and "syngas," since they are over-arching terms that dilute the outcomes for other keywords.

3.4.2. Network map for authors and keywords

Figure 12 is a network map representing the top keywords and their relationships with the top 23 authors (Panel A) and their collaborations (Panel B), using a threshold of 8 publications. The correlation of keywords and authors helps to understand how themes evolved within and across research teams.

The red cluster in panel A includes the main keyword in the field: "ethanol." *Clostridium* as genus appears in the cluster, joined by "gasification" and "biomass." Authors closely associated to these words included Huhnke and Atiyeh from Oklahoma State University, the most highly cited authors whose research goes towards alcohols. Other authors in the cluster are Lewis from Brigham Young University and Wilkins from Oklahoma State University. Tanner from the University of Oklahoma is part of another

cluster related to “bioethanol” and “acetogens,” although Tanner has published in a wide variety of topics. The VOSviewer graph highlights that Tanner has the largest number of collaborators among the authors from the red cluster in Panel A.

The green collaborative cluster is composed by Sousa, Stams, Yasin, Chang, Park, and Kim. The keyword analysis shows that Stams and Sousa are associated with “carbon monoxide” and “hydrogen”. Sousa also is associated with “*C. autoethanogenum,*” consistent with the author’s work with this pure culture. The publications of Stams and Sousa are related to co-cultures, isolation and microbial characterization, and the effect of the gases on the community (Arantes et al., 2020, 2018; Diender et al., 2016). Chang, Yasin, Park, and Kim are closer to “mass transfer” and “bioethanol.” Chang, Yasin, and Park focused their work on mass-transfer limitations to produce ethanol (Jang et al., 2018; Yasin et al., 2015, 2014). Additionally, Park shows a strong correlation with *“C. autoethanogenum,”* consistent with his work with the pure culture (Park et al., 2019). Ki, who focused in nanoparticles to enhance ethanol production (Kim et al., 2014), did not group with other authors in the collaborations network, while Chang, Yasin, and Park collaborated.

A closely related cluster to the green cluster is the one formed by Weuster-Botz, Najafpour, and Younesi. Weuster-Botz is associatd with “gas” and “acetate,” consistent with the author’s focus in acetate production (Groher and Weuster-Botz, 2016; Kantzow et al., 2015; Straub et al., 2014), while Najafpour and Younesi are associated with “*C. ljungdahlii,*” consistent with the line of work for the two authors (Mohammadi et al.,

2012). Najafpour and Younesi show a strong and exclusive collaboration network between them, while Weuster-Botz does not collaborate with any other top 23 author.

The blue cluster shows that Angenent and Ritcher are closely related through "chain elongation," "biorefinery," and "*C. ljungdahlii*," while Colprim and Baneras are closely related to "mixed culture," the "Wood-Ljungdahlii pathway," and "*C. carboxidivorans."* Angenent and Ritcher have a wide range of research topics in syngas fermentation, but their collaborative work with *C. ljungdahlii* and chain elongation from acetate and ethanol is prevalent (Cavalcante et al., 2017; Perez et al., 2013; H. Richter et al., 2016; Hanno Richter et al., 2016; Richter et al., 2013). Colprim and Baneras are exclusive collaborators, and their work emphasizes biofuel production and *C. carboxidivorans* use for syngas fermentation (Ramí O-Pujol et al., 2018; Ramió-Pujol et al., 2015a, 2015b).

Kennes, Veiga, and Abubackar from the University A Coruna are associated with "biofuel," "butanol," and "*C. autoethanogenum.*" They collaborate exclusively among themselves, and their work is known for its pure-culture applications (Abubackar et al., 2015; Arslan et al., 2019; Fernández-Naveira et al., 2016; Lagoa-Costa et al., 2017). Similarly, Tyurin and Kiriukhin are exclusive collaborators clustered with "acetogens," consistent with their most cited work focused in metabolic engineering of acetogens to either potentiate or inhibit acetate production (Berzin et al., 2013; V. Berzin et al., 2012; Vel Berzin et al., 2012; Yasin et al., 2015, 2014).

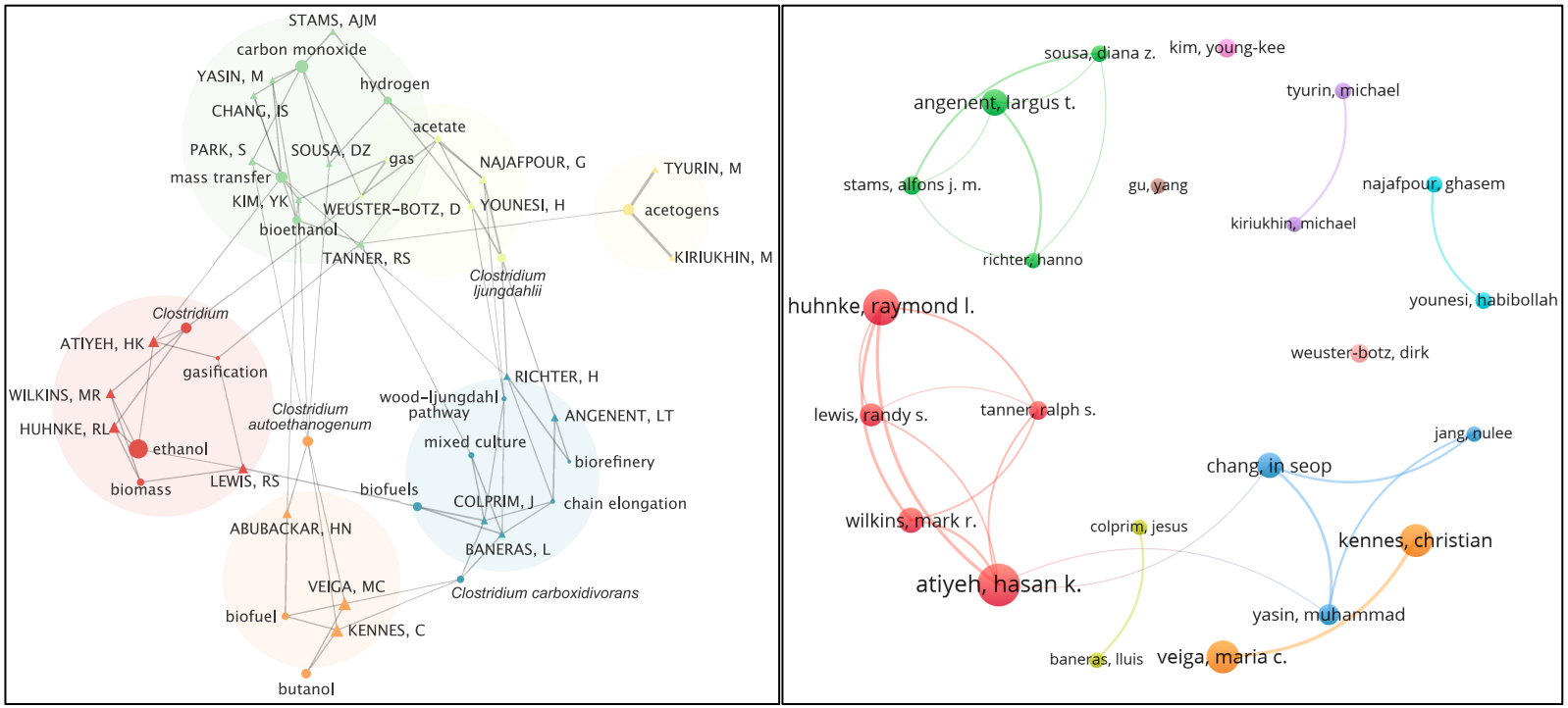

Figure 12. Panel A: Most influential authors and their correlation with the top 23 keywords (threshold: 8 documents produced). Nodes identify an author with a triangle and a keyword with a circle; the size of a node is proportional to the number of appearances in the search. Clusters (color-shaded circles) congregate nodes with strong topic correlation between them. Every link between nodes is created by distributional proximity in the CorTexT platform. Panel B: Collaborations between authors using VOSviewer.

4. Conclusion

A bibliometric analysis for syngas fermentation shows major growth in the field from 2008 through 2020: an average of 37 articles per year with an increase rate of 5.6 articles/year; a total of 10,835 citations, and an increase in research categories from 3 in 2007 to 25 in 2020. Historically, research in syngas fermentation emphasized alcohol production and pure cultures, but mixed cultures, other products, and genetic engineering have begun to emerge as promising new avenues. Although the field of syngas is highly inter-disciplinary, collaboration across disciplines and research groups has been modest, with research clusters focused on tightly defined topics. The analysis identifies mass transfer as a major research hurdle that is being addressed by a large cluster of researchers.

CHAPTER 4

CARBOXYLATES AND ALCOHOLS PRODUCTION IN AN AUTOTROPHIC HYDROGEN-BASED MEMBRANE BIOFILM REACTOR[2]

1. Introduction

Carboxylates and alcohols are important industrial feedstock and also are biofuel precursors (Agler et al., 2011; Phillips et al., 2017; Steinbusch et al., 2008). Furthermore, generating products with more than two carbons (>2CP) is even more promising. Longer products are more reliable biofuel precursors (Chen and Ni, 2016; T. I.M. Grootscholten et al., 2013a), are easier to separate from aqueous phase because of their low solubility (Xu et al., 2015), and have higher economic value (T. I.M. Grootscholten et al., 2013a).

Syngas fermentation is a biological alternative to produce alcohols and carboxylic acids from waste materials (Fernández-Naveira et al., 2019; Henstra et al., 2007; Liu et al., 2014a, 2012). These products can be elongated through microbial chain elongation (MCE), creating renewable chemicals and biofuels (Spirito et al., 2014).

Microbial communities can produce carboxylates and alcohols from inorganic carbon (IC) sources, such as CO_2, using hydrogen gas (H_2) as an electron donor (Asimakopoulos et al., 2018). The communities include acetogens and chain-elongating

[2] This chapter is published in an altered format in as: Calvo, D. C., Ontiveros-Valencia, A., Krajmalnik-Brown, R., Torres, C. I., & Rittmann, B. E. (2021). Carboxylates and alcohols production in an autotrophic hydrogen-based membrane biofilm reactor. Biotechnology and Bioengineering, 1–10. https://doi.org/10.1002/bit.27745

bacteria as the key microbial mediators (Esquivel-Elizondo et al., 2017; Latif et al., 2014). Optimizing carboxylates and alcohols production with these communities has faced two main obstacles. First, autotrophic acetogens use H_2 as electron donor, but H_2 has very low water-solubility: i.e., a Henry's constant of $7.7x10^{-6}$ $mol.m^{-3}.Pa^{-1}$, compared to $3.4x10^{-4}$ $mol.m^{-3}.Pa^{-1}$ for CO_2 (Sander, 2015). Second, anaerobic autotrophs are slow growers, making biomass retention a crucial element for process stability and high carboxylate yields (Rittmann and McCarty, 2020; H.-J. Wang et al., 2018). The membrane biofilm reactor (MBfR) overcomes both obstacles, because it delivers the H_2 gas directly to a biofilm that grows on the outer surface of a hollow-fiber gas-transfer membrane and it is capable to retain slow growing microorganisms (Martin and Nerenberg, 2012; Rittmann, 2018).

The MBfR has been widely used to achieve microbial reduction of a broad spectrum of oxidized water pollutants (Lai et al., 2016; Martin and Nerenberg, 2012; Van Ginkel et al., 2010; Zhou et al., 2014), but its application as a production system is relatively new. Ten recent studies (Chen and Ni, 2016; Shen et al., 2018, 2014; H.-J. Wang et al., 2018; H. J. Wang et al., 2018; Y. Q. Wang et al., 2017, 2018; Yasin et al., 2014; Zhang et al., 2013b, 2013a) demonstrated the production of carboxylates in MBfRs from mixtures of H_2, CO, and CO_2, at different concentrations. We compiled these studies in Table 6, where half of the studies used a H_2/CO_2 gas mixture. Among these, Chen & Ni (2016) modeled MBfR performance in regard to its capacity to ferment H_2/CO_2 to acetate, butyrate, and caproate when delivering different gas compositions through the membranes and with a spectrum of hydraulic retention times (HRTs). The

studies mentioned above did not test pure H_2 supplementation through the membranes, and they did not separate the delivery of the electron donor from the delivery of the carbon source, which are hallmarks of our work.

Three metrics of MBfR-performance are the production rate per unit area, the product titer, and the presence of acetate and ethanol (two carbon products) versus >2CP. Production rate and titer have been related to mass-transfer aspects, such as membrane porosity when advective membranes are used, and higher rates and titers were associated with smaller pore sizes (H.-J. Wang et al., 2018). Carboxylates longer than 2 carbons usually were more important in reactors with longer hydraulic retention times (HRT > 1 d) (Chen and Ni, 2016; Y. Q. Wang et al., 2017; Zhang et al., 2013b) and mesophilic temperatures (lower than 35°C) (H.-J. Wang et al., 2018; Y. Q. Wang et al., 2017), and *Clostridium* was the main bacteria reported in mesophilic MBfRs (Shen et al., 2018; H.-J. Wang et al., 2018; Zhang et al., 2013b, 2013a).

Given that the carbon in >2CP is more reduced than two carbon products, we hypothesize that the H_2:IC mole ratio (from now on H_2:IC ratio) will control the length of carboxylates and alcohols produced. A higher H_2:IC ratio will lead to longer, more reduced carbon chains. The H_2:IC ratio can be increased in three ways: (1) increasing the H_2 pressure, which controls the H_2-delivery capacity (Tang et al., 2012), (2) decreasing the IC concentration in the influent, and (3) increasing the HRT. However, these changes should have different impacts on the carboxylate production rate and carboxylate titers. Increasing H_2 pressure should increase the overall rate and titer, but production will shift to >2CPs when IC becomes limiting. Increasing the input

concentration of IC should increase the overall products titer, as long as H_2 is not limiting and there is not competition from methanogenesis. Increasing the HRT should lower the overall production rate per unit volume of the reactor but increase the overall titer.

Here, we systematically evaluate the production rate and product distribution for a H_2-based MBfR in which we independently changed the H_2 pressure, influent IC concentration, and HRT. We relate those factors to the overall production rate, the distribution of carbon in the products, and the microbial ecology of the biofilm.

2. Methods

2.1.Experimental set-up

We adapted the MBfR described by Ziv-El et al. (2012) and illustrated in Figure 13. Briefly, the MBfR consisted of two glass tubes connected with tubing and fittings and sealed with caps, all of them of polytetrafluoroethylene (PTFE) to avoid oxygen intrusion and adsorption of metabolites. Two three-way valves (Hamilton Company, Reno, NV) were located as shown for sample collection. The 70-mL system was maintained at 25°C and completely mixed using a high recirculation rate (80 mL/min) obtained with a peristaltic pump (Master Flex, model 7520-40, Cole-Parmer Instrument Company, U.S.A.).

We used composite hollow-fiber membranes with a non-porous layer of urethane polymers between two layers of polyethylene (Mitsubishi-Rayon®, MHF200TL, Japan). The membrane thickness was ~50 μm with an outer diameter of 280 μm. We put 50 fibers with a length of 25 cm in one of the two glass tubes (main bundle), and 10 fibers with the same length in the second glass tube (coupon bundle for fiber samples), giving a

total fiber surface area of 108 cm^2 and a specific surface area for the reactor of 188 m^2/m^3. The fibers in the main bundle were connected to a 100% H_2 supply from both ends, while the coupon fibers were connected from one end to the supply and sealed on the other end with a knot.

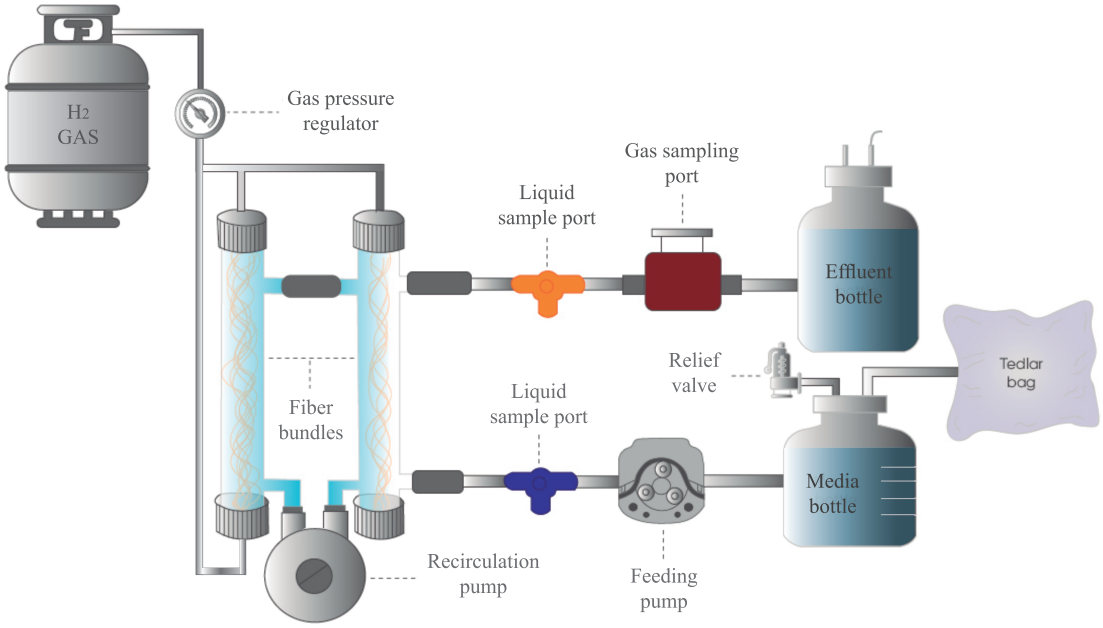

Figure 13. Schematic of the MBfR experimental set-up

We fed the MBfR with an anaerobic mineral medium (Delgado et al., 2012) held in a feed reservoir having a 100%-CO_2 headspace and we added 10 mM of 2-bromoethanesulfonate (BES) as a methanogenesis inhibitor. The $NaHCO_3$ concentration was adjusted between 10 mM and 120 mM to control the influent IC concentration and Na_2S x 9 H_2O was 0.02 mM during the whole experiment. A Tedlar® bag containing

100% CO_2 was connected to the medium bottle's headspace. The pH of the medium was adjusted to 7.5-8.0 by adding HCl or NaOH.

We inoculated the MBfR with 10 mL of wasted activated sludge from a local wastewater treatment plant and allowed the biomass to attach to the fibers for three days in batch mode and with 2 psig (~1.15 atm total pressure) of UHP H_2 in the membranes and 30 mM of HCO_3^- in the liquid. After three days, we replaced the medium inside the reactor every two days for 20 days to replenish nutrients but allow the biofilm to accumulate. The influent medium was fed with a peristaltic pump (Master Flex, model 7520-20, Cole-Parmer Instrument Company, U.S.A.) through PTFE tubing.

After the batch phase of 3 days and the semi-batch phase of ~20 days, the system was operated continuously for 390 d through three series of changes to one operating parameter. The first series (segment A) had a constant IC influent concentration of 64 mM and an HRT of 24 ± 1.06 h, and we stepwise increased the H_2 pressure from 2 psig (~ 1.15 atm absolute pressure) to 30 psig (~ 3 atm) from day 1 to day 197. The second series (segment B) kept the H_2 pressure constant at 20 psig (~1.4 atm) and the HRT at 24 ± 0.72 h, and we stepwise increased the influent IC concentration from 44 mM to 154 mM over days 198 to 303. Finally, the third series (segment C) increased the HRT from 11.1 h to 50.4 h over days 304 to 390 while keeping the H_2 pressure at 20 psig (~ 1.4 atm) and the influent IC at 64 mM. Each condition was maintained for at least 15 days, which allowed the concentrations of all solute to come to steady state, defined as less than ±20% differences in carboxylates concentration for 5 consecutive days.

2.2.Sampling

2.2.1. Liquid samples

We collected 3-mL liquid samples daily from the influent and effluent sampling ports using a sterile syringe and then filtered it through a 0.2-μm PTFE membrane filter (Whatman Inc., Haverhill, MA).

2.2.2. Gas samples

We installed a 20-mL serum bottle with two open ends close to the effluent port as a gas-sampling port. Headspace accumulated in the bottle, and each day we measured the headspace volume and took a 300-μL gas sample using a gastight syringe (Hamilton Company, Reno, NV). After sampling, we reset the gas-sampling port by sparging pure N_2.

2.2.3. Biofilm samples

We cut a ~10-cm piece from one fiber of the coupon bundle using sterile scissors four times during the experiment: At a low H_2 pressure (4 psig or ~1.3 atm absolute), at the highest H_2 pressure (30 psig or ~3 atm absolute) (segment A), at the highest IC concentration (154 mM) (segment B), and at the longest HRT (50.4 h) (segment C). We opened the system under a continuous UHP N_2 flow through the cap to avoid O_2 intrusion. We immediately placed the fiber sample into sterile anaerobic medium and knotted the remaining coupon fiber. We then vortexed the fiber sample for 30 min to dislodge the biomass, removed the fiber, and centrifuged the liquid at 13200 rpm to form a biomass pellet (micro-centrifuge 5415 D, Eppendorf, Hauppauge, NY). The supernatant was discarded, and the pellet was stored at -80°C for DNA extraction.

2.2.4. Chemical Analysis

We measured the concentrations of carboxylic acids and alcohols by High Performance Liquid Chromatography (HPLC, LC-20AT, Shimadzu) using a photodiode array and a refractive index detector. The HPLC was equipped with an Aminex HPX-87H (Bio-Rad) column maintained at 50°C, with 2.5 mM H_2SO_4 as eluent at a flow rate of 0.6 mL/min until 29 min, ramped to 0.8 mL/min for 1 min, and then run for additional 60 min. We built calibration curves for acetate, ethanol, propionate, propanol, butyrate, butanol, valerate, pentanol, caproate, and hexanol from 0.1 mM to 100 mM, along with calibration curves for heptanoate and octanoate from 0.1 mM to 5 mM. The minimum detection limit, as determined by Joshi et al. (2021), was ≤0.04 mM for carboxylates and ≤0.1 mM for alcohols. We determined the IC concentration in the liquid samples with an Ion Chromatograph (Dionex ICS-2000) having an AS16 column and AG16 pre-column using 1.5 ml/min of KOH as eluent.

We determined gas composition (H_2, CO_2, and CH_4) with a gas chromatograph (Shimadzu, GC-2010, Columbia, MD) equipped with a Thermal Conductivity Detector and a fused-silica capillary column (Carboxen 1010 PLOT, Supelco, Bellefonte, PA), using 7 mL/min Ar as the carrier gas. The chromatograph was kept at 80°C for 3 min and then ramped to 155°C over 1.5 min. The inlet temperature was 150°C, the detector temperature was 220°C, and the electric current was 41 mA.

2.3.DNA Extraction, sequencing, and downstream analysis

We slowly thawed the biomass pellets harvested from coupon fibers in an ice rack and extracted the DNA by using a PowerSoil DNA isolation kit (MoBio laboratories,

Inc., Carlsbad, CA). We assessed the DNA quantity and quality by using a spectrophotometer at 260 nm and 280 nm (Nanodrop ND-1000, Nanodrop Technologies, USA).

The DNA was sent to the Microbiome Analysis Laboratory at Arizona State University (Arizona, USA) for 16S rRNA barcode amplicon sequencing. Triplicate PCR amplifications were performed and targeted the V4 region of the 16S rRNA gene with primer set 515f/806r designed by Caporaso et al. (2011) and following the protocol by the Earth Microbiome Project (EMP) (http://www.earthmicrobiome.org/emp-standard-protocols/). DNA samples were analyzed by a MiSeq Illumina sequencer with the Illumina chemistry version 2 (2x150 paired-end). Raw sequences were submitted to the NCBI Sequence Read Archive under Project ID PRJNA666643.

We analyzed the 16S rRNA gene sequences using the Quantitative Insights into Microbial Ecology software package, QIIME version 2.1 (Bolyen et al., 2019). 16S rRNA gene sequences were clustered into OTUs (Operational Taxonomic Units) according to the Greengenes database using an identity threshold of 97% by using the UCLUST algorithm. Representative sequences for each OTU were aligned with the Greengenes core reference alignment 57 by using PYNAST. The taxonomy of the OTU representative sequences was classified by RDP CLASSIFIER v.2.2 (Caporaso et al., 2012). After alignment of the sequences, we constructed the OTU table and removed singletons. Finally, the OTU table was rarefied to 39,008 sequences, which was the minimum number of sequences obtained among all samples.

2.4.H_2:IC ratio

We calculated the H_2:IC ratio by dividing the actual H_2-delivery flux delivered to the reactor (HDF, in mmol H_2/m^2-d) by the IC surface loading (ICSL, mmol C/m^2-d). HDF was computed with:

$$HDF = \Sigma \eta_i C_i (V/HRTxA)$$

where η_i is the conversion of the mmol of the product to its H_2 equivalent, C_i is the concentration of measured product *i* (mmol/L), *V* is the volume of the reactor (L), *HRT* is the hydraulic retention time (d), and *A* is the surface area of the hollow fiber membranes (m^2). The H_2 equivalency of each product is shown in Table 1. ICSL was calculated as:

$$ICSL = [IC]V/(HRTxA)$$

where *[IC]* is the influent IC concentration.

The influent IC concentration was calculated by adding the IC from the $NaHCO_3$ (10 to 120 mM $NaHCO_3$, which has 1 mol C/1 mol $NaHCO_3$) and the IC from the 100% CO_2 headspace. For CO_2 from the headspace, we determined the molar concentration (or density) of CO_2 in gas phase using the ideal gas law $(n/V)_{gas}$:

$$(n/V)_{gas} = P/RT$$

where P is the pressure in the headspace (1 atm), R is the ideal gas constant (0.082 atm.L/mol.K), and T is the temperature (298 K) of the system: $(n/V)_{gas}$ = 0.041 mol/L_{gas}. We then calculated the $CO_{2(aq)}$ concentration in the liquid $(n/V)_{liquid}$ by Henry's law:

$$(n/V)_{liquid} = (n/V)_{gas} x H_{cc}$$

where Hcc is the Henry's constant for CO_2 at the P and T of the system (0.82 mol_{liquid}/mol_{gas} (Sander, 2015)). The value of $(n/V)_{liquid}$ was 0.034 mol/L_{liquid}. At the pH

of the medium (~7.6), all the base added in $NaHCO_3$ was present in HCO_3^-. Thus, the total IC concentration was the sum of $(n/V)_{liquid}$ plus the added $NaHCO_3$: e.g., 0.034 + 0.01 = 0.044 M for addition of 10 mM $NaHCO_3$ and 0.034 + 0.1 = 0.134 M for addition of 100 mM $NaHCO_3$.

2.5.Carbon balance

We calculated the carbon balance of the reactor by dividing each output by *[IC]* after converting the mmol of each product to its mol C equivalent χ_I, as shown in Table 1. If the sum of the measured output values did not equal the input *[IC]*, we calculate an "unknown" concentration by difference.

Table 1. H_2 and C equivalents for each compound present in the effluent

Compound	e^- eq/mol	η_i mol H_2/mol	χ_i mol C/mol	η_i / χ_i mol H_2/mol C
Acetate	8	4	2	2
Ethanol	12	6	2	3
Propionate	14	7	3	2.3
Butyrate	20	10	4	2.5
Butanol	24	12	4	3
Valerate	26	13	5	2.6
Caproate	32	16	6	2.7
Octanoate	44	22	8	2.7
Unknown	-	-	-	3
HCO_3^-	0	0	1	0
H_2	2	1	0	-
CO	2	1	1	1
CO_2	0	0	1	0

3. Results & Discussion

3.1.Concentrations and rates of carboxylates and alcohols for each condition

The effects of the different operational parameters are presented in Figure 14. The top panel presents the effluent concentrations as carbon (mM C), while the bottom panel presents the concentrations in electron equivalents (me^- eq/L). The trends are similar, but the impacts of forming carboxylates longer than two carbons via MCE are accentuated using me^- eq/L, because the carbon in them is more reduced than in acetate. Alcohol production followed the same trend, which is accentuated when viewing the results in me^- eq/L, since alcohols are more reduced than acids with the same number of carbons.

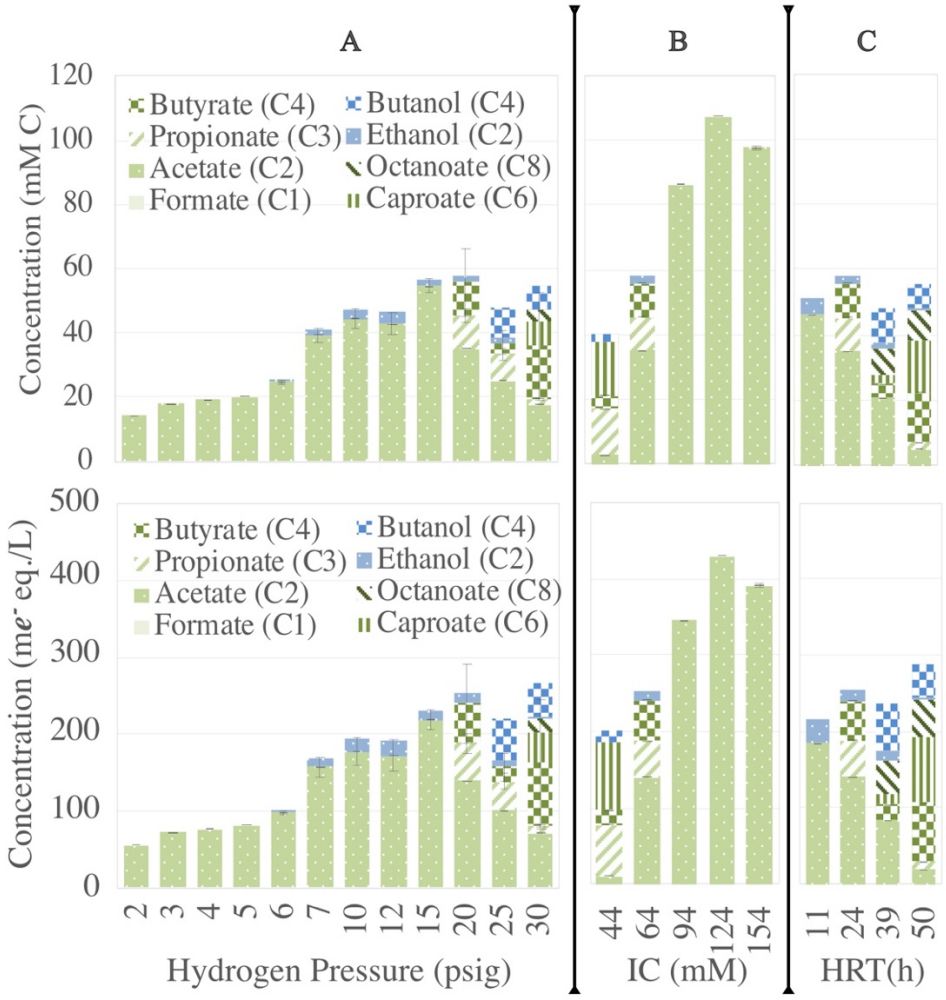

Figure 14. Effect of H_2 pressure (Segment A; IC = 64 mM; HRT = 23.4 ± 0.6), IC concentration (Segment B; H_2 P= 20 psig; HRT = 23.7 ± 1.1), and HRT (Segment C; H_2 P= 20 psig; IC = 64 mM) on the concentration of carboxylates and alcohols produced, expressed in mM C (top panel) and me^- eq/L (bottom panel). Valerate concentrations were non-detectable under any conditions. Trace amounts of formate were detected at the first condition and may have been introduced with the inoculum.

In segment A (increases of the H_2-delivery capacity), the only detected products had two carbons when the H_2 pressure was lower than 15 psig (~2.0 atm absolute). The acetate concentration increased up to 54.6 ± 9.9 mM C (218 ± 40 me^- eq/L) as the H_2 pressure was stepwise increased from 2 psig (1.1 atm) to 15 psig (2.0 atm); a low concentration of ethanol also was detected, and it reached a maximum of 3.5 ± 0.8 mM C (20.8 ± 4.7 me^- eq/L) at 12 psig (1.8 atm). The acetate and ethanol concentrations declined for higher H_2 pressures, but >2CPs, up to octanoate (C8), were generated, clear evidence of MCE. Expressed as mM C, the production of carboxylates and alcohols increased with higher H_2 pressure and delivery capacity when two-carbon-products were the only metabolites present in the system, but slightly decreased when MCE was occurring. In MBfR studies, Chen and Ni (2016) demonstrated that higher availability of H_2 by means of augmenting H_2 to the syngas supply led to increasing amounts of butyrate and caproate. Skidmore et al. (2013) also demonstrated the importance of H_2 pressure for the efficiency of syngas fermentation in experiments in completely mixed reactors.

In segment B (increases of the input IC concentration), overall production increased with higher input concentration of IC up to 124 mM, but this increase was accompanied by a loss of >2CP production. The highest acetate concentration achieved was 107.3 ± 8.5 mM C (429.2 ± 34.2 me^- eq/L), with IC of 124 mM C, which corresponded to the highest rate achieved, 741 ± 59 mmol C m^{-2} d^{-1}. Previous results also suggested that IC limitation promoted MCE (Arslan et al., 2012).

Finally, shortening the HRT (segment C) promoted the exclusive production of acetate, since the IC input loading was greater with shorter HRT. This finding agrees

with results from a thermophilic-MBfR that achieved a high acetate concentration at a HRT equal to 1 day (Y. Q. Wang et al., 2017). Chen & Ni (2016) also reported that short HRTs allowed more acetate to be produced in syngas-fermenting MBfRs, while increasing the HRT promoted butyrate and caproate formation. In general, longer retention periods in anaerobic microbiomes promoted the accumulation of short-chain carboxylates and MCE up to octanoate, regardless of the configuration of the system (Agler et al., 2012; T. I M Grootscholten et al., 2013; T. I.M. Grootscholten et al., 2013b; Joshi et al., 2021; Spirito et al., 2018, 2014). Our observed trends support that the production of >2CPs was favored by a high H_2:IC ratio, but suppressed by a low ratio.

Some patterns observed in this study are reinforced by the results of other MBfR studies. The maximum concentration of acetate was obtained when other metabolites were zero or negligible, same as Shen et al. (2018) with the highest reported acetate concentration as 27.9 g/L (930 mM C). Similarly, long HRTs promoted MCE, with the longest carboxylate reported being 8-C octanoate (up to 0.77 g/L), which was achieved in batch mode at 35ºC (Zhang et al., 2013b). Table 6 summarizes carboxylate production for MBfR systems in the literature.

3.2.Inorganic carbon limitation promoted chain elongation

We performed a carbon balance in the MBfR for all operational conditions, accounting for how much carbon was converted to each metabolite and how efficient the system was at converting IC to carboxylates. Figure 15 relates the carbon balance of the H_2-based MBfR to the H_2:IC ratio. When the H_2 pressure was stepwise increased, keeping the other variables constant (segment A), the H_2:IC ratio increased up to 2.7 mol

H_2/mol C (with a H_2 pressure of 30 psig or 3.0 atm absolute). For the lower H_2:IC ratio values (low H_2 pressures), H_2 limitation constrained the ability of biofilm's microbial community to reduce carbon to produce carboxylates, and acetate was the only detected metabolite. This trend was also suggested by H. J. Wang et al. (2018b). When the H_2:IC ratio was higher than 2.0 mol H_2/mol C, with a H_2 pressure over 15 psig, the product distribution shifted to propionate (C3) and butyrate (C4), comprised 17.3 ± 1.4% and 17.4 ± 4.1% of available carbon. At a H_2 gas pressure of 30 psig (H_2:IC of 2.7 mol H_2/mol C), 6% ± 0.2% of carbon was routed to octanoate (C8), 12 ± 0.3% to caproate, with 43 ± 1% to the C3-C4 organic products. With the higher H_2:IC ratios, at least 97% of the influent IC fed was reduced, and the MBfR had fully shifted from H_2 limitation to IC limitation.

IC concentration was reduced from 64 to 44 mM at a constant H_2 pressure of 20 psig (2.3 atm) and a HRT of 23.7 ± 1.1 h (the start of segment B). This increased the H_2:IC ratio to 2.8 mol H_2/mol C, and about 95% of input IC was converted to C3-C8 organic products. Afterwards, H_2:IC ratio was decreased by stepwise increasing IC concentration. Similarly to low H_2:IC ratios when H_2 pressure was low, acetate again became the only metabolite produced.

When the HRT was stepwise increased, keeping the other variables constant (segment C), the H_2:IC ratio increased by having a constant flux of H_2 with decreasing IC loadings. While acetate was the exclusive product for the lowest H_2;IC ratio (an HRT of 11.1 h), increasing the H_2:IC ratio lead to MCE. When H_2:IC ratio was higher than 2.0 mol H_2/mol C, the products included carboxylates from C2 to C8. Carbon limitation

favored metabolism that invested the electrons from H_2 in longer and more reduced >2CPs.

Unknown products were less than 20% for all cases except the highest IC concentration studied. Less than 20% unattributed carbon is typical for anaerobic systems, and it comes from generation of biomass and soluble microbial products (SMP) (Rittmann and McCarty, 2020). For the highest IC concentration, acetate production decreased even with IC available, which could indicate inhibition due to the high IC concentration in the medium (Li et al., 2016). This inhibition could have increased SMP produced by the biofilm.

Figure 15 also shows that the real H_2:IC ratio never exceeded the Maximum H_2:IC ratio based on the maximum H_2-delivery flux (Tang et al., 2012) and the ICSL. During the early stages in segment A, the H_2 delivery was significantly lower than the maximum H_2 delivery rate. Considering that the MBfR delivers H_2 on-demand based on the biofilm's metabolic need, this might indicate that the biofilm was still growing and being stablished during this time. For segment B, the highest IC input in the last experiment has a ratio approaching 1.7 mol H_2/mol C, which clearly signifies that H_2 delivery was rate limiting. All maximum H_2:IC ratios were larger than 2.0 mol H_2/mol C, and the highest maximum ratio was 10 mol H_2/mol C. A high maximum H_2:IC ratio means that IC clearly was rate limiting. Because actual H_2 delivery is on-demand, H_2 was not wasted for the high ratios.

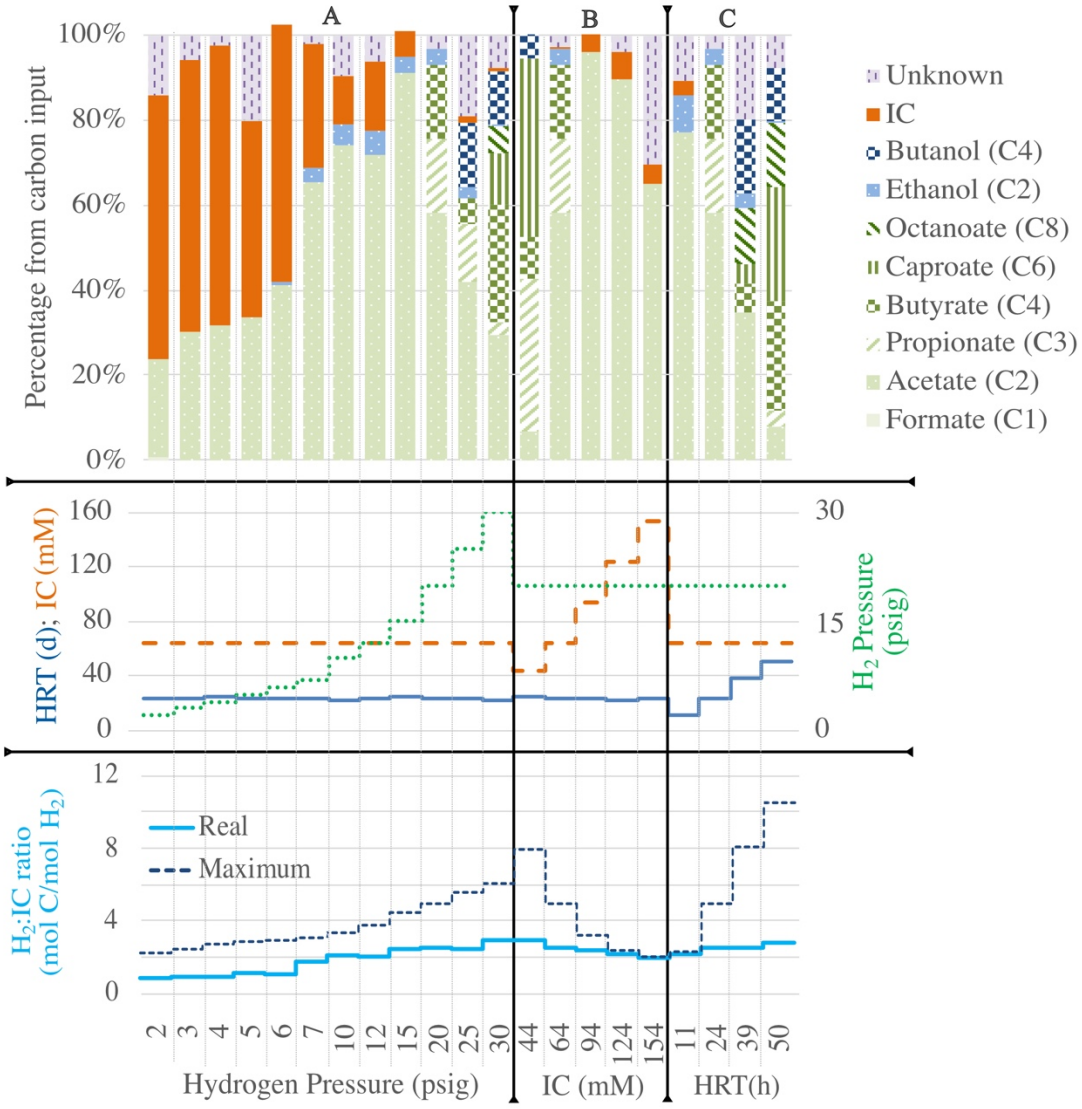

Figure 15. Distribution of carbon in the MBfR and its relation with the H_2:IC mole ratio, which was determined by the IC loading and the H_2 delivery. The Real H_2:IC ratio was computed from the electron equivalents in the measured products divided the input rate of IC. The Maximum H_2:IC ratio was computed as the H_2-delivery capacity (Tang et al., 2012) divided by the input rate of IC. Methane was detected in trace amounts only for the first pressure tested in A.

3.3.Microbial Ecology of Biofilm

As shown in Figure 16, the most abundant phylotypes in the microbial communities were associated with microbes able to perform acetogenesis and MCE. When the H_2:IC ratio was less than 2.0 mol H_2/mol C, phylotypes most similar to the Eubacteriaceae family were dominant, and up to 50% of the community was represented by phylotypes closely related to *Acetobacterium*, a well-known H_2-oxidizing and IC-reducing genus (Balch et al., 1977). The *Acetobacterium*-related phylotype was still abundant when the H_2:IC ratio was greater than 2.0 mol H_2/mol C, but its percentage was smaller. Besides *Acetobacterium*, chain-elongating bacteria has been metagenomically identified in the Eubacteriaceae family, although they were not isolated (Candry and Ganigué, 2021). A phylotype most closely related to Tissierellaceae, was also abundant in all conditions. Tissierellaceae was reported to produce either acetate or other short-chain carboxylates (Coma et al., 2016).

As the H_2:IC ratio increased, the relative abundances of phylotypes similar to chain-elongating bacteria augmented: specifically, phylotypes similar to families from the order Bacteroidales (Candry and Ganigué, 2021; Coma et al., 2016) and phylotypes similar to the family Alcaligenaceae (Han et al., 2018). Phylotypes most similar to Thermoanaerobacteriales and Erysipelotrichaceae, which are reported as chain-elongating microorganisms (Coma et al., 2016; Spirito et al., 2014), were present for high H_2:IC ratios, although less abundant. Phylotypes most similar to Rhodobacteraceae, an alkalophilic chain-elongating family, were present when the IC concentration was the highest, with a H_2:IC ratio of 1.8 (Coma et al., 2016). Present in all samples were

phylotypes most similar to Rhodocyclaceae, which dominated chain-elongating communities in previous studies (Kucek et al., 2016; Spirito et al., 2018). Some genera, such as *Dechloromonas* are able to use BES as electron acceptor, given the similar chemical structure with usual electron acceptors such as nitrate (Steinbusch et al., 2011).

Microbes in the Families such as Desulfomicrobiaceae and Methanobacteriaceae families are undesired, since they divert H_2 for sulfate reduction and methanogenesis, respectively. Phylotypes related to these two families, were present in the sample for day 32 (Low H_2 P; Low H_2:IC), an early stage of the biofilm, although, they have been found as competitors in chain-elongation systems (Candry and Ganigué, 2021; Kucek et al., 2016).

Most phylotypes found in the system correspond to the order Firmicutes, which includes all known caproate-producing strains reported so far (Candry and Ganigué, 2021). It also includes *Clostridium*, which is a key family for acetogenesis, as well as for chain elongation (Drake et al., 2008). Further research is needed to identify key players in chain elongation processes.

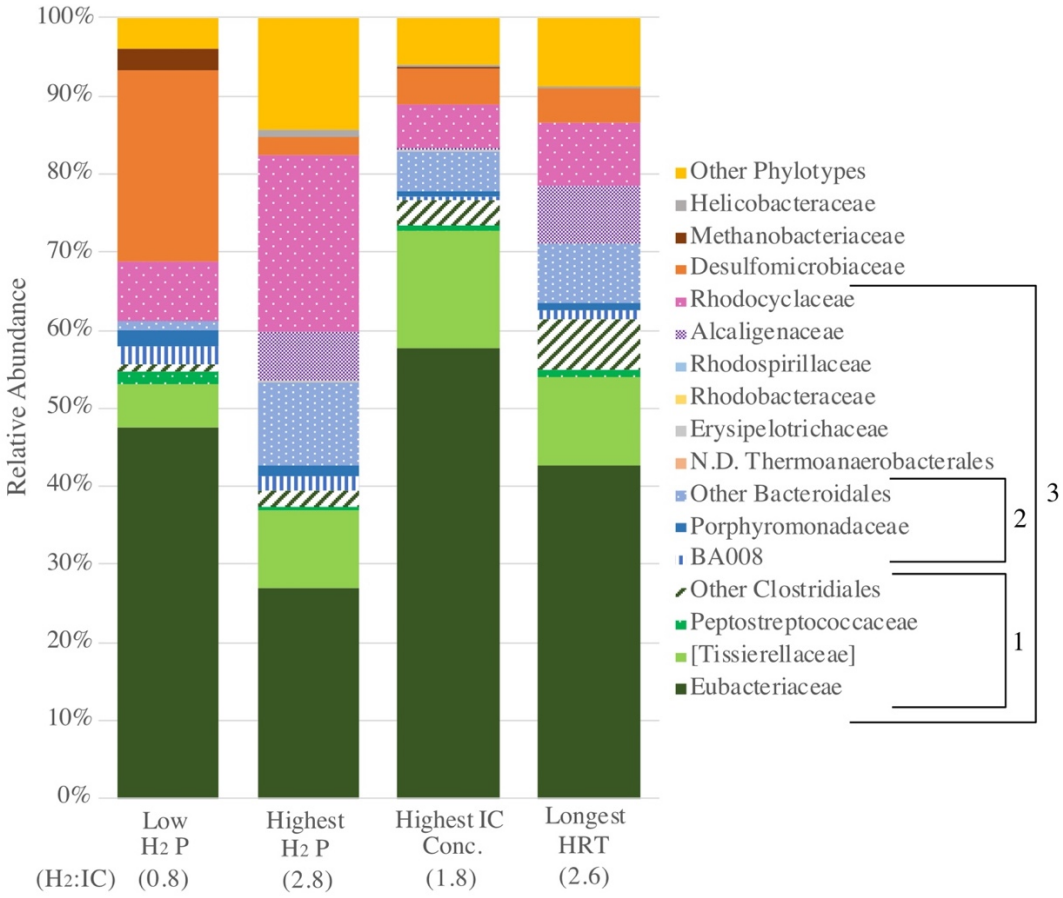

Figure 16. Relative abundance at the family level in the microbial communities when operating the MBfR. Group 1. Clostridiales; Group 2. Bacteroidales; Group 3. Phylotypes reported as acetogens/microbial-chain-elongating bacteria. The H_2:IC ratio is in mol H_2/mol C.

4. Conclusions

We used a H_2-MBfR to control the H_2:IC ratio by adjusting the H_2-delivery capacity with the H_2 pressure or the IC loading rate via its influent bulk liquid concentration or the HRT. We documented that the H_2:IC ratio directly influenced the production rate of carboxylates, alcohols, and the MCE process. When the H_2:IC ratio was less than 2.0 mol H_2/mol C, the system produced only two carbon products, at a rate up to 741 ± 59 mmol C/m^2-d for acetate and 73 ± 17 mmol C/m^2-d for ethanol. When the H_2:IC ratio was greater than 2.0 mol H_2/mol C, the MBfR also produced >2CP, particularly caproate (84 ± 16 mmol C/m^2-d) and octanoate (28 ± 4 mmol C/m^2-d). The biofilm's microbial community reflected the changes in H_2:IC ratio and organic products: phylotypes related to chain-elongating families became more abundant when the ratio was low, and phylotypes related to acetogens declined proportionally. These results show that the MBfR is a versatile tool that can be used either for maximizing the rate of acetate production (low H_2:IC ratio) or for emphasizing formation of >2CP (high H_2:IC ratio).

CHAPTER 5

SYNTHESIS AND MASS TRANSFER EVALUATION OF A NOVEL MATRIMID® SYMMETRIC HOLLOW FIBER FOR SYNGAS AND ITS COMPONENTS[3]

1. Introduction

Synthetic gas (syngas), composed of hydrogen (H_2), carbon dioxide (CO_2), and carbon monoxide (CO) gases, is a product of biomass gasification and an excellent source to produce valuable chemicals biologically (Molino et al., 2016). Yet, the effective use of these gases by microorganisms is hindered by their low solubility in water (Phillips et al., 2017). Bubble-free hollow-fiber membranes, through which gas is delivered from the lumen or inside of the membrane, have been used in several studies to deliver low-permeability gases, including syngas, to microbial cultures at a higher rate than typical achievable by sparging (Rittmann, 2018; Xiao et al., 2021; Zhang et al., 2013a; Zhao et al., 2013b).

When a biofilm accumulates on the outer (shell) side of the hollow-fiber membrane, it is a membrane biofilm reactor (MBfR). The gas diffuses across the membrane wall and is consumed by bacteria in the biofilm, which can convert it to useful products that can be separated from the medium. High conversion rates are possible in

[3] **Credit:** *Diana C. Calvo* – writing, conceptualization, $H_2/CO/CO_2$ permeance experiments, graphs, data analysis, edition, funding acquisition; *Hye-Youn Jang* – membrane synthesis, preliminary permeance experiments; *Ryan Lively* – conceptualization, membrane synthesis, data analysis; *Cesar I. Torres* – writing, data analysis, edition; *Bruce E. Rittmann* – conceptualization, writing, data analysis, edition, funding acquisition.

MBfRs, as long as the membrane can deliver the gas at a rate the meets the demand from the microorganisms (Rittmann, 2018). Thus, high-flux membranes are needed for MBfR applications.

An added challenge occurs when mixed gases are delivered, and syngas is a prime example of a mixed gas in which all the components are utilized by the biofilm microorganisms (Esquivel-Elizondo et al., 2017; Shen et al., 2018). As each gas must diffuse through the membrane wall at a rate that is stoichiometrically related to the diffusion rates of the other gases, it is crucial to know the mass-transport kinetics of each gas. One important aspect of mass transfer in a mixed-gas setting is the selectivity of the membrane between gases ($\propto$). Selectivity affects relative mass-transfer rates and changes in gas composition in the membrane's lumen.

Used membranes for MBfR applications cover a wide range of configurations and materials. Common membranes include a simple one-layer of dense polymer fibers or symmetric composite fibers that have two layers of macroporous materials material "sandwiching" a thin dense layer (Rittmann, 2018), as shown in the left and center graphics Figure 17. A dense-polymer membrane needs to have a wall thick enough to be strong and durable. This results in a large diffusion distance for the gas through the dense polymer. Symmetric composite fibers reduce resistance by thinning the dense polymer and using the two porous layers for structural integrity. The symmetric membrane has greatly reduced mass-transport resistance in the thin dense layer, and mass-transport resistance in the microporous layers is minimal as long as the macropores are gas-filled. However, water in an MBfR will fill the macropores of the exterior layer

and increase mass-transport resistance there. While the extra mass-transport resistances have proven acceptable for the modest mass-transfer rates needed in water treatment (Martin and Nerenberg, 2012; Ontiveros-Valencia et al., 2014; Zhao et al., 2013b), it is unsatisfactory for high-rate bioproduction applications.

An asymmetric composite fiber, illustrated in the right image of Figure 17, offers advantages over the dense and symmetric membranes. Like the symmetric membrane, it has a thin dense polymer layer (the skin-layer) that minimizes mass-transport resistance from the membrane material. Unlike the symmetric membrane, it has only one macroporous layer, on the lumen side of the hollow fiber. This avoids water-filling on the porous layer. Also, the dense layer can be thinner than is typical in symmetric composites (Pesek and Koros, 1994).

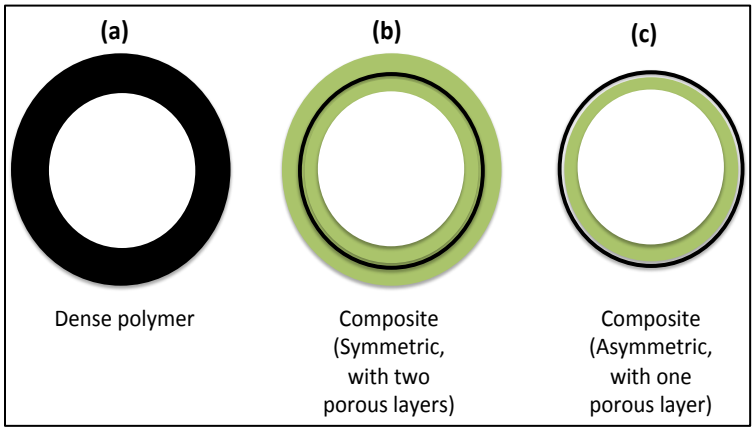

Figure 17. Schematic showing the different layers in three different types of hollow-fiber membranes: (a) dense polymer, (b) symmetric composite, and (c) asymmetric composite. The black lines represent a dense polymer, while green represents a macroporous polymer layer.

In this work, colleagues at the Georgia Institute of Technology synthetized several asymmetric layers using Matrimid® and Torlon® polymers. This created a high-flux/low-selectivity membrane. Following screening tests, I selected the best asymmetric membrane for each polymer (one for Matrimid® and one for Torlon®) and compared their permeance and selectivity with a commercially available symmetric composite membrane for the syngas components and a synthesized syngas.

2. Methods

2.1. Synthesis of asymmetric membranes

A "dry-wet" solution-processing technique was modified as shown in Figure 18 (Kosuri and Koros, 2008; Pesek and Koros, 1994). The polymeric dope solution for the fiber spinning was made by mixing polymer into the solvent and non-solvents mixtures, followed by mixing on a heated roller maintained at 50°C for 3-7 days. Dope solution was transferred into a syringe pump, heated to 50°C, and kept undisturbed at that temperature overnight to degas the dope solution. The polymeric solution was extruded through a spinneret into the air gap ("dry") and then into the water quench bath ("wet") where phase separation occurs. These phase-separated fibers were collected on a take-up drum. The residual solvents corresponding to the dope and bore fluids were removed from the fiber. The fibers were soaked in a deionized (DI) water for 3-5 days, with daily exchange of fresh DI water. The absorbed water was removed from the fiber by exchanging three successive 30-min methanol baths, followed by three successive 30-min hexane baths. To remove the hexane, the fibers were dried at room temperature for 1 hour, followed by heating the fibers under vacuum at 120°C overnight.

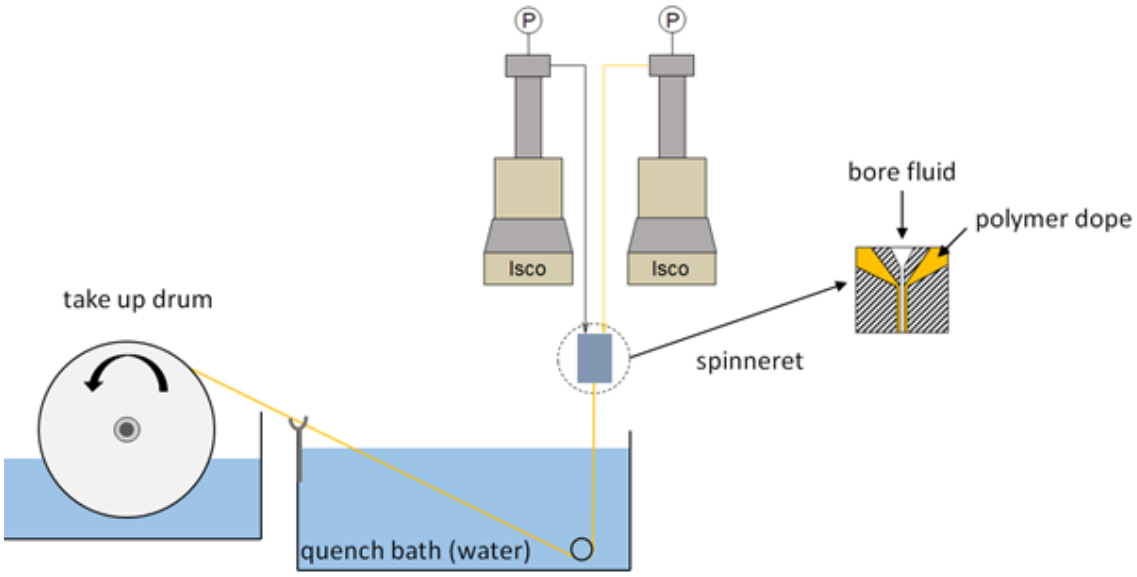

Figure 18. Schematic of the experimental set up for spinning asymmetric hollow fiber membranes.

After several adjustments for tuning the membranes, the Georgia Tech team made seven sets of Matrimid® fibers and two sets of Torlon® fibers. Table 2 summarizes the parameters for the Matrimid® and Torlon® fibers. Synthesis of Matrimid® fibers aimed to have a high flux, while synthesis of Torlon® fibers aimed to avoid defects in the fibers. Synthesis of the hollow-fiber membranes was conducted 2 times with different polymer solution batches for each membrane set.

Table 2. Adjustments to the dry-wet method for fibers produced for this study

Parameter	Matrimid®	Torlon®
Dope Composition [wt%]	26.2 Matrimid® 53 NMP 5.9 THF 14.9 EtOH	34 Torlon® 47.2 NMP 11.8 THF 7 EtOH
Bore Fluid Composition [wt%]	95 NMP 5 Water	80 NMP 20 Water
Dope/Bore Flow Rates [ml/hr]	300/10	180/60
Air Gap [cm]	(1) 6; **(2,6,7) 8**; (3)12.5; (4)17.5	23
Take Up Drum Rate [m/min]	20	3.2
Dope/Quench Bath Temp [C]	(5) 25/40; (6) 35/40;**(1-4) 40/40**; (7) 45/40	Defect free (8): 30/25 Macro-void (9): 50/45

2.2.Preliminary gas-permeation tests

Gas permeation for He and N_2 was tested at the Georgia Institute of Technology for each set of membranes using a reliable and fast method before I did mass transport studies for syngas components. He and N_2 are commonly used gases to gauge membrane permeation (Scholes and Ghosh, 2017). They used an isobaric permeation system with temperature controlled at 35ºC, as described in Liu et al. (2020). The inner side of the membrane was slowly pressurized to 100 psig, allowing the system to come to steady state by holding the conditions for one day for He and two days for N_2. Afterwards, the flow rate on the outer layer was measured using a soap bubble flowmeter (Bubble-O-Meter), and the permeation flow rate was recorded ($m^3 \cdot m^{-2} \cdot d^{-1}$) when the value was stable for two hours.

I used the flow rate to calculate the permeance of the fibers:

$$\frac{P}{l} = \frac{\dot{n}}{A_m . \Delta P}$$

where P/l is the permeance (mol.m^{-2}.s^{-1}.Pa^{-1}), $\dot{n}$ is the molar flow rate (mol.s^{-1}), A_m is surface area of membrane (m^2), and ΔP is the difference between inner partial and outer partial pressure of the gas (Pa). I calculated permeance in GPU, which is equivalent to 3.35 x 10^{-10} mol.m^{-2}.s^{-1}.Pa^{-1} (L. Wang et al., 2017). When permeance is calculated for a gas mixture being delivered through the membrane, each permeance is calculated using that gas's partial pressure (e.g., 40% H_2 in 1 atm= 0.4 atm)

I also calculated the selectivity of the membrane ($\propto$) by dividing the permeance of He by the permeance of N_2 for the initial characterization and dividing the H_2 permeance by the permeance of CO or CO_2 when I evaluated syngas components.

2.3.Syngas permeation tests

2.3.1. Set-up

Based on the preliminary tests with He and N_2, I selected the highest flux/lowest selectivity membrane for each material used (i.e., Matrimid® and Torlon®) and compared it to a commonly used commercial composite membrane (Mitsubishi-Rayon MHF200TL®, Japan).- I determined gas-gas permeance using the setup in Figure 19 for a synthetized syngas mixture of 40% H_2, 30%CO and 30% CO_2, as well as for pure H_2, CO, and CO_2. I fitted a 280-mL glass bottle with 14-cm-long hollow-fiber membranes that spanned across the bottle: eighteen for asymmetric Matrimid®, five for asymmetric Torlon®, and fifty for the symmetric composite. I sealed both ends of the fiber with a crimped rubber septum prior to the experiment. The bottle and fiber were purged with

UHP N_2 gas and sealed before each run. Afterwards, I purged the membranes with the gas to study (synthetic mixture, UHP H_2, UHP CO or UHP CO_2) at the evaluation pressure I used for 10 min, purged the bottle again with UHP N_2 at high flow, and then delivered the test gas from both ends on the fibers to start the experiment. I inserted a needle into the bottle stopper and attached a PTFE valve (Hamilton, Reno, NV), which was closed except when I collected gas samples. I inserted a frictionless gas syringe to ensure the system was at a constant ambient pressure and to measure gas volume added from gas diffusion through the fiber. The size of the syringe varied depending on the pressure evaluated.

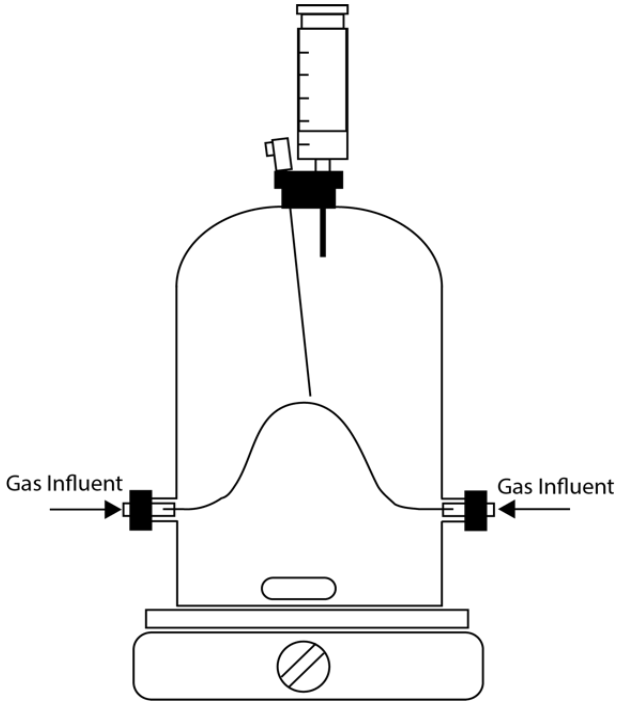

Figure 19. Experimental design for determining H_2, CO, and CO_2 permeances across a hollow-fiber membrane

I calculated the gas-volume-addition rate by plotting the volume in the frictionless syringe over a period of time from the start of the run. The result was a linear increase in volume after a lag phase of less than 0.1 min. I calculated the volumetric flow as the slope of the linear fit after the lag phase and later converted it to molar flow using ideal gas law.

2.3.2. Gas composition

I took a 300-µL sample with a gas-tight 500-µL syringe (Hamilton, Reno, NV) from the top of the reactor. I took a sample when the frictionless syringe had at least 5 mL of increased volume; thus, the frequency of sampling varied depending on the volumetric flow.

I determined the gas composition (H_2, CO, CO_2, and N_2) with a gas chromatograph (Shimadzu, GC-2010, Columbia, MD) equipped with a Thermal Conductivity Detector and a fused-silica capillary column (Carboxen 1010 PLOT, Supelco, Bellefonte, PA), using 7 mL/min Ar as the carrier gas. The temperature profile of the column was 35°C for 3.5 minutes, then an increase of 10°C every minute for 10.5 minutes. The temperature of the injection port and detector was 180°C. The detector temperature was 220°C, and the electric current was 41 mA. Detection limits were 0.05% for H_2 and CO and 0.2% for CO_2.

3. Results & Discussion

3.1.Selection of membrane

Table 3 shows the permeance (*P/l*) for He and N_2 for each set of membranes, as well as the selectivity (α) between the two gases. As the dope temperature increased, He and N_2 permeances declined, and the He/N_2 selectivity increased, from 2.4 to 17.5. Volatile components, such as THF and ethanol in the polymer solution, evaporate quickly at high dope temperature, which leads to the higher skin layer quality on the asymmetric membranes overall. The evaporation of the solvents happens in the air gap, where the polymer-extrusion from the spinneret goes to be quenched in the water bath. While changes in He/N_2 selectivity were negligible with changes in the air-gap, both He and N_2 permeance gradually decreased with an air-gap increase. Thus, the skin layer became thicker with bigger air gaps, and the overall resistance of the membrane increased.

For my MBfR application, I aim for a membrane with high permeance, but low selectivity, in order to deliver gas to the biofilm in the fastest way possible, but without selecting strongly for any of the gases. Therefore, the Matrimid® membrane #3 was the best choice for my purposes and further evaluation. I also further evaluated one Torlon® fiber, membrane #8.

Table 3. Gas permeances and He/N_2 selectivities of the synthesized hollow-fiber membranes

	Matrimid®						**Torlon®**	
Set number	1	2	**3**	4	5	6	7	8
Air gap (cm)	6	8	**8**	12.5	8	17.5	23	23
Dope/Quench	40/40	25/40	**35/40**	40/40	45/40	40/40	30/25	50/45
$\frac{\mathbb{P}}{\ell}_{\mathbf{He}}$ **[GPU]**	158.5	140	**910**	112	80.2	86.7	26	0.287
$\frac{\mathbb{P}}{\ell}_{\mathbf{N_2}}$ **[GPU]**	11	7.2	**375**	7.9	4.6	6.2	0.114	0.0485
$\alpha_{\mathbf{He/N_2}}$	14.1	20	**2.4**	14.1	17.5	14.1	231	5.92

3.2. Permeance comparison between membranes for the pure gases

Figure 20 shows the permeance results for both membranes at different pressures. The permeance of the asymmetric Matrimid® membrane was 90- to 1600-fold greater than the permeance for the symmetric Mitsubishi-Rayon® composite membrane for H_2, 75- to 210-fold greater for CO, and 400- to 3100-fold greater for CO_2. I ran pressures up to 30 psig for Torlon® for 24 hours (data not shown) but did not see any significant change in volume on the frictionless syringe. Therefore, the permeance of the Torlon® membrane was negligible.

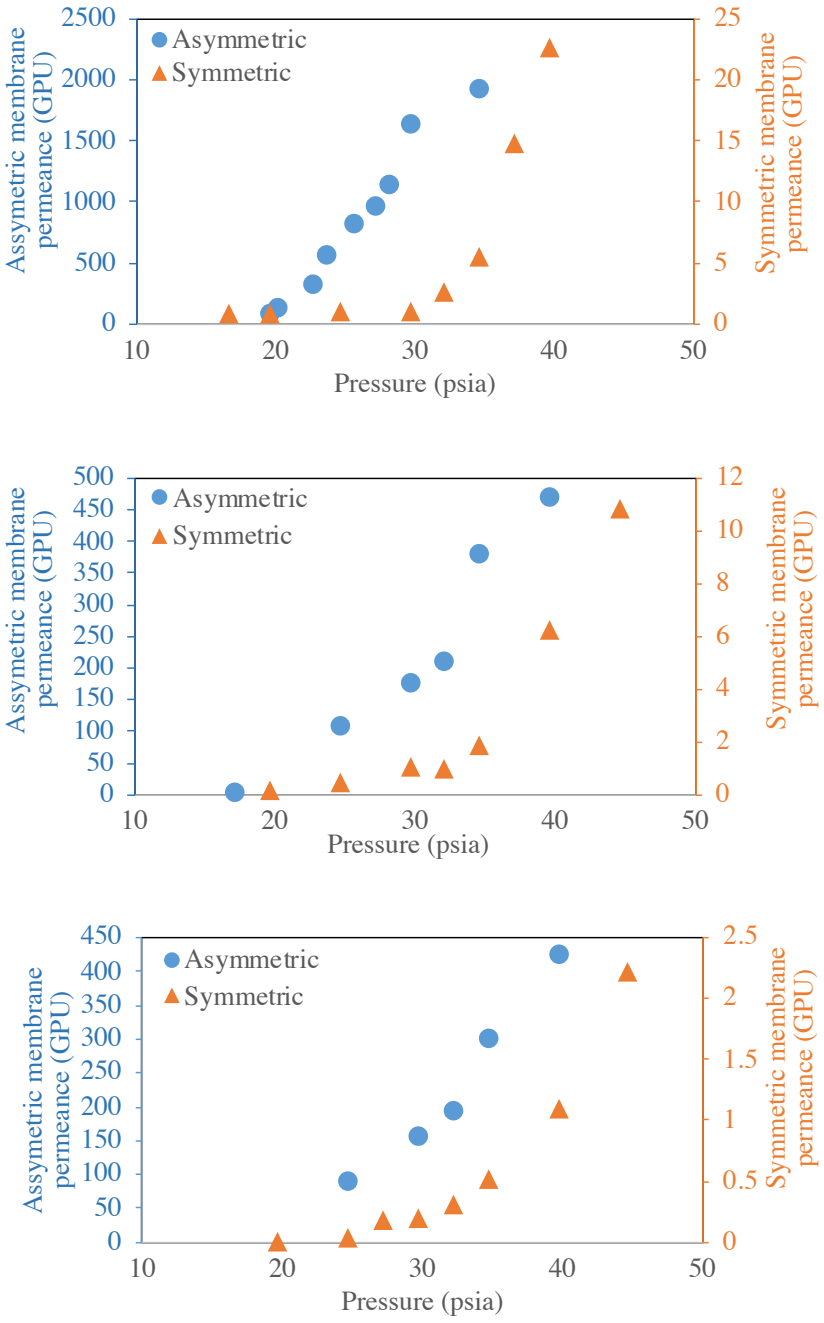

Figure 20. Comparison of asymmetric and symmetric membrane permeances for pure gases: H_2 (Top), CO (middle), and CO_2 (Bottom). Note that scales for the vertical axes differ, and the range is much greater for the asymmetric membranes.

3.3. Permeance comparison between membranes for syngas mixture

Figure 21 shows permeances in GPU for each component when a syngas mixture was delivered to the membranes. The trends are similar than pure gases, but permeance values are lower for all gases in most cases, which can be explained by the fact that gases are "competing" inside the fiber.

The Matrimid® permeance was 30- to 490-fold greater than the permeance for the symmetric Mitsubishi-Rayon® composite membrane for H_2, between 60- and 980-fold greater for CO, and 210- to 700-fold greater for CO_2. The difference of permeance between membranes for H_2, although still large, is smaller than the difference between the membranes for CO and CO_2. Consequently, the selectivities, expressed as the H_2:CO:CO_2 permeances normalized by H_2 permeance, were 1:0.94:0.78 for the asymmetric Matrimid® fiber, compared to 1:0.48:0.11 for the symmetric Mitsubishi-Rayon® membrane. Therefore, the asymmetric Matrimid® should be superior to the Mitsubishi-Rayon® membrane for high-rate syngas fermentation in an MBfR, since it has much greater permeance and does not impose severe selectivity.

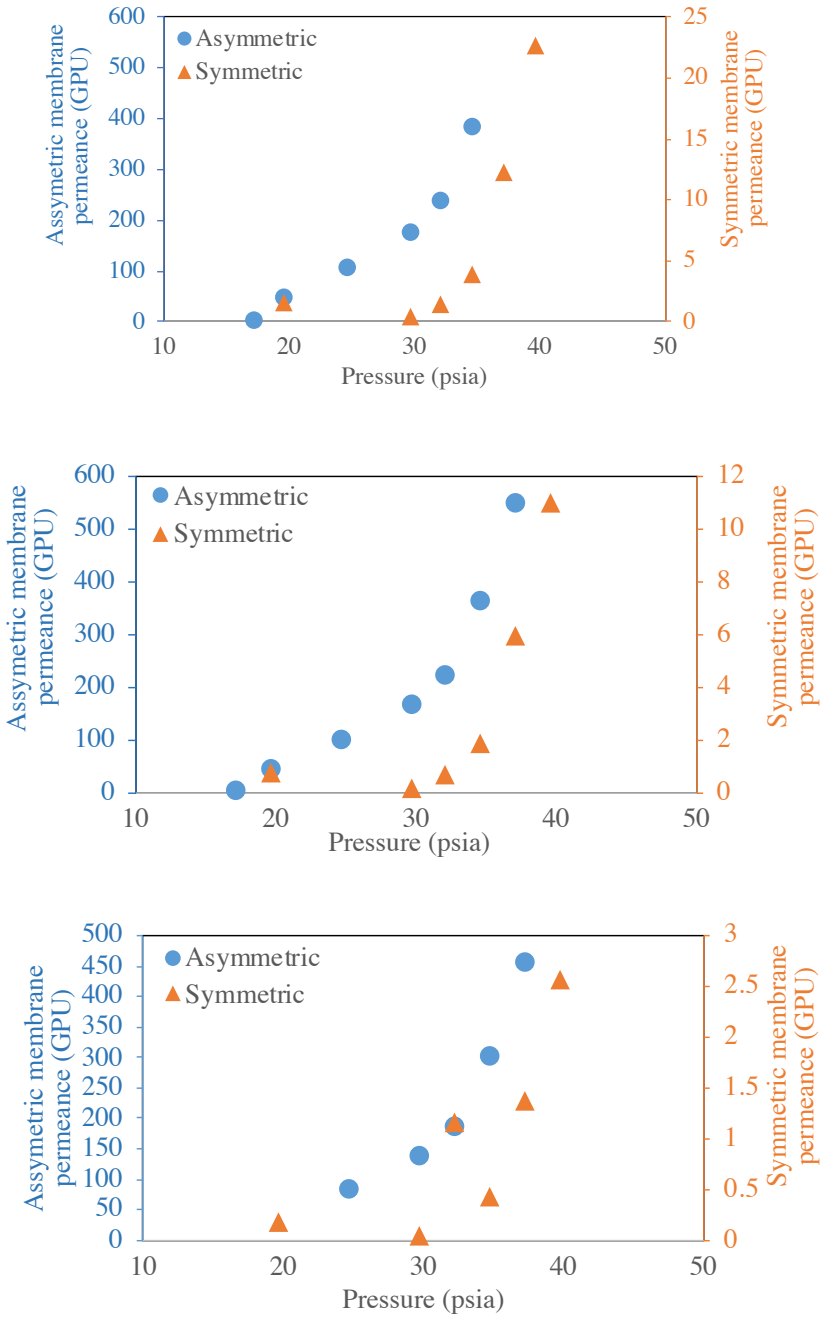

Figure 21. Comparison of asymmetric and symmetric membrane permeance for syngas mixture: H_2 (Top), CO (middle) and CO_2 (Bottom). The syngas was composed of 40%H_2, 30% CO, and 30% CO_2. Note that the vertical axes have different scales.

4. Conclusion

My Georgia Tech collaborators successfully synthetized an asymmetric composite Matrimid® hollow-fiber membrane that had far superior mass transfer properties compared to commercially available symmetric composite membranes. The Matrimid® membrane had permeances from 30- to 700-fold greater than the symmetric membrane for the syngas components. It also has much lower selectivity among the syngas components. Thus, the asymmetric membrane should enable high fluxes of H_2, CO, and CO_2 without imposing strong selectivity against any gas component. These characteristics make the asymmetric Matrimid® fiber a promising option to create high productivity MBfR for converting syngas to valuable organic acids and alcohols.

CHAPTER 6

MEMBRANE EFFECTS ON CARBOXYLATES PRODUCTION IN AN AUTOTROPHIC SYNGAS-BASED MEMBRANE BIOFILM REACTOR[4]

1. Introduction

As I described in Chapters 3, 4, and 5, two main challenges in syngas fermentation are mass-transfer limitation from gas to liquid and biomass retention. From 2013, researchers have used the Membrane Biofilm Reactor (MBfR) to overcome both obstacles (Zhang et al., 2013a, 2013b). Ten studies used the MBfR for autotrophic carboxylates and alcohols production to date (Chen and Ni, 2016; Shen et al., 2018, 2014; H.-J. Wang et al., 2018; H. J. Wang et al., 2018; Y. Q. Wang et al., 2017, 2018; Yasin et al., 2014; Zhang et al., 2013b, 2013a), and they reported that operational parameters such as hydraulic retention time (HRT), temperature, and membrane-pore size had direct effects on production rates, concentrations achieved, and product chain length. My results in Chapter 4 show that the H_2:Inorganic Carbon (IC) ratio determined the organic product length when only H_2 was the exclusive electron donor and was delivered by the membrane, while the production rate directly depended of the rate of gas delivery.

Because syngas is a mixture of CO, H_2, and CO_2, the delivery rate (or flux) of each gas will depend on its own characteristics, membrane characteristics, and also on the

[4] **Credit**: *Diana C. Calvo* – writing, conceptualization, methods development, installation, sequencing data processing, data analysis, funding acquisition. *Cesar I. Torres* - Writing, conceptualization, data analysis, supervision. Bruce E. Rittmann - Writing, conceptualization, data analysis, funding acquisition,

proportion of each gas in the lumen. Each gas has its own permeance with a particular membrane, and the factor was explored in Chapter 5. In brief, the asymmetric Matrimid® membrane has a permeance between 30- and 700- fold greater than the symmetric commercial membrane for syngas and its components. Therefore, the asymmetric fiber has the potential to deliver much larger volumes of gas to the biofilm.

When a mixture of gases is delivered by a membrane, selectivity is a key parameter, since it helps determine the actual gas composition in the lumen and the relative delivery rates. Chapter 5 presented a detailed analysis of selectivity, which is usually reported as the ratio of permeances, or Permeance gas 1/Permeance gas 2. From Chapter 5, I calculated the permeance ratio among the three components. When normalized by the CO_2 permeance, the permeance ratios are 1.3:1.2:1.0 for the asymmetric Matrimid® fiber and 9.1:4.4:1.0 for the symmetric Mitsubishi-Rayon® membrane. While analyzing biotic experiments that can use more than one gas for one purpose, it is important to account for the selectivities and how the differ for the symmetric membrane versus the asymmetric membrane. Based on permeances, the asymmetric fiber favors delivery of all gases, while the symmetric fiber is highly selective towards H_2.

Considering the importance of the H_2:IC ratio for carboxylates and alcohols production in Chapter 4, it is crucial to estimate the maximum flux of each component, considering not only selectivity, but also the partial pressure of each gas in the mixture and the total surface area in the reactor to know the actual H_2:IC ratio in the system.

Another important factor to consider with delivering syngas is that H_2 and CO act as electron donors, while CO and CO_2 provide IC. For the donors, flux must be framed in terms of e^- equivalents. For the IC source, flux must be frame in terms of C equivalents. When comparing all three components of syngas, I used the ratio between total fluxes of e^- eq and mol C as the analog to the H_2:IC ratio for pure H_2-MBfRs.

Here, I hypothesize that the membrane's gas flux ratio between e^- equivalents and IC (i.e. e^-:C ratio) plays a key role in syngas fermentation, because the electrons and C are delivered through the same fiber. A high e^-:C ratio should lead to C limitation, which will promote chain elongation. In contrast, a low e^-:C ratio should lead to shorter carboxylic acids. Production rates will increase when the membrane allows a higher delivery capacity for both gases.

In this chapter, I evaluate the production rate and product distribution for a commercially available membrane that favors electron donor over carbon source versus the specially synthetized high-rate asymmetric membrane that delivers all components with less selectivity in a syngas-based MBfRs. I analyzed the overall production rate, the distribution of carbon in the products, and the microbial ecology of the biofilms.

2. Materials and Methods

2.1.Experimental set-up

I used a set-up similar to that of the H_2-based MBfR in Chapter 4, published in Calvo et al. (2021). The main difference was that I delivered synthetic syngas (40% H_2: 30% CO_2: 30% CO) instead of pure H_2. I ran several preliminary experiments to determine if the system's fibers should be closed-end, intermittently flushed, or

continuously flushed. To avoid non-steady state conditions, I decided to set-up a continuously flushed MBfR, as shown in Figure 22. The syngas was fed to the membranes from the top of the MBfR with a constant pressure of 5 psig (1.34 atm absolute pressure) and exhausted at atmospheric pressure (1 atm) at the bottom of the MBfR.

I used the two types of membranes described in Chapter 5: a commercial symmetric composite hollow-fiber membrane with relatively low delivery capacity, but high selectivity towards H_2 (Mitsubishi-Rayon®, MHF200TL, Japan) and a specially synthetized asymmetric composite hollow-fiber membrane with high delivery capacity and low selectivity among the syngas components (Matrimid®). I operated two reactors with 60 symmetric membranes and another two reactors with 2 asymmetric membranes. I used only 2 fibers for Matrimid® because of its exceptionally fast gas-transfer kinetics (Chapter 5).

I fed an MBfR with an anaerobic mineral medium (Delgado et al., 2012) held in a feed reservoir having a 100%-CO_2 headspace. I also added to the feed medium 10 mM of 2-bromoethanesulfonate (BES) as a methanogenesis inhibitor (Joshi et al., 2021), 10 mM $NaHCO_3^-$ as pH buffer, and 0.02 mM of Na_2S as a reducing agent. The pH of the medium was adjusted to 7.0-7.5 by adding HCl. I connected a Tedlar® bag containing 100% N_2 to the medium bottle's headspace to maintain anaerobic conditions in the feed medium.

I inoculated the MBfR and accumulated biofilm as described in Calvo et al. (2021). All reactors had a 39-h HRT and were run for approximately 270 days. All data

are presented for steady state, which was achieved when carboxylates production did not vary by more than 10% over 10 days.

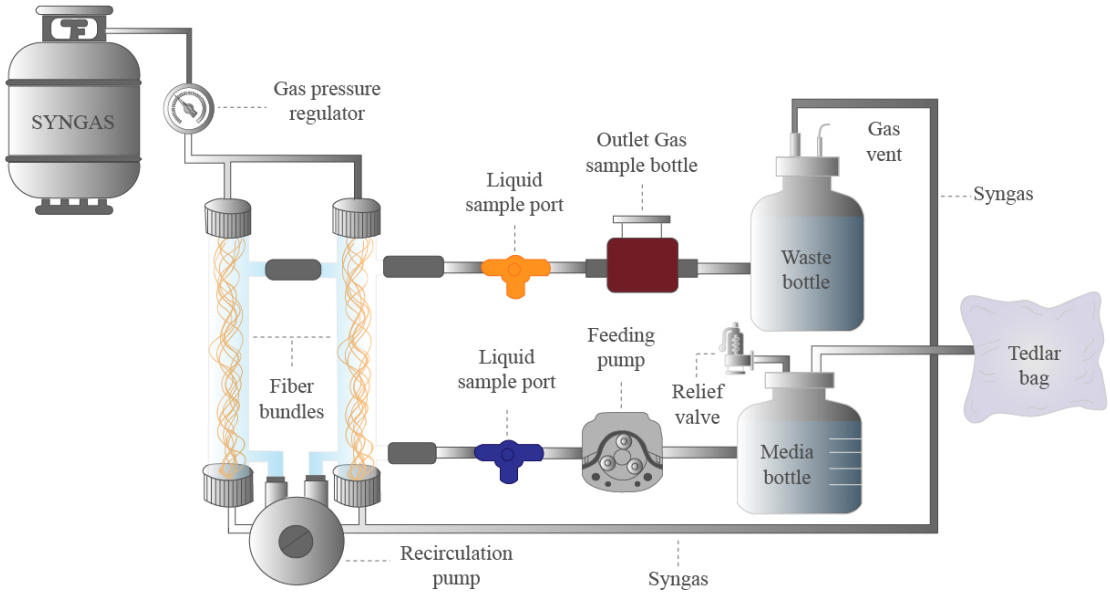

Figure 22. Schematic of the experimental set-up of a syngas-based MBfR

2.2.Sampling

2.2.1. Liquid and gas samples

I took liquid and gas samples as described in Calvo et al. (2021).

2.2.2. Biofilm samples

I took a biofilm sample for each reactor once the MBfR reached steady state. To avoid O_2 exposure, I opened the system under a continuous UHP N_2 flow through the cap. I then scraped one membrane's surface with a razor blade while avoiding the membrane and immediately washed biofilm from the blade in sterile anaerobic medium. I then centrifuged (micro-centrifuge 5415 D, Eppendorf, Hauppauge, NY) the liquid at

13200 rpm to form a biomass pellet. The supernatant was discarded, and the pellet was stored at -80°C for DNA extraction.

2.3.Chemical Analysis

I measured the concentrations of carboxylic acids and alcohols as described in Calvo et al. (2021). I measured pH with a pH Benchtop Meter (Thermo Scientific, #9142BN) and determined gas composition (H_2, CO, CO_2, and CH_4) with a gas chromatograph (Shimadzu, GC-2010, Columbia, MD) as described in Chapter 5.

2.4.DNA Extraction, sequencing, and downstream analysis

I extracted, sequenced, and analyzed the DNA pellets as described in Calvo et al., (2021).

2.5.Calculation of gas delivery ratio between membranes

In Chapter 5, I calculated the flux of the syngas components in mol·s^{-1}·m^{-2} for the two types of fibers when a mixture of 40% H_2, 30% CO and 30% CO_2 was delivered. I converted each specific flux to e^- eq·s^{-1}·m^{-2} and calculated a total flux of electron equivalents for each membrane:

$$\text{E Flux}\ (e^- \text{eq.} \cdot \text{s}^{-1} \cdot \text{m}^{-2}) = \sum_i \text{Flux}_i\ (\text{mol}_i \cdot \cdot \text{s}^{-1} \cdot \text{m}^{-2}) \cdot \beta_i$$

where *i* is syngas component H_2 or CO, and β_i is the e^- equivalent per mol of the component *i*.

Similarly, I calculated the flux in mol C·s^{-1}·m^{-2} for each membrane:

$$\text{C Flux}\ (\text{mol C} \cdot \text{s}^{-1} \cdot \text{m}^{-2}) = \sum_i \text{Flux}_i\ (\text{mol}_i \cdot \cdot \text{s}^{-1} \cdot \text{m}^{-2}) \cdot \chi_i$$

where i is the syngas component CO or CO_2, and χ_i is the mol C per mol of the component i. β_i and χ_i values are shown in Table 4.

Table 4. Equivalencies for E and C Flux for each component

Compound	β_i e^- eq/mol	χ_i mol C/mol
H_2	2	0
CO	2	1
CO_2	0	1

With the calculation of e^- and C fluxes, I estimated the e^-:C ratio for each membrane:

$$e^-\text{: C ratio} = \frac{\text{E Flux}}{\text{C Flux}}$$

For this chapter, I used the same pressure in all MBfRs, but the surface area was different depending on the type of fiber used. Therefore, I considered the difference in surface area to estimate the delivery capacity of electrons and IC in the reactor:

$$DC_{e-eq} = \text{E Flux } (e^-\text{eq.} \cdot \text{s}^{-1} \cdot \text{m}^{-2}) \cdot \text{A}_j$$

$$DC_{mol\ C} = \text{C Flux } (\text{mol C.} \cdot \text{s}^{-1} \cdot \text{m}^{-2}) \cdot \text{A}_j$$

where j is the type of membrane.

Finally, I estimated the delivery capacity ratio between the membranes by dividing the delivery capacity of the asymmetric fiber by the symmetric fiber, for electrons and carbon:

$$DC_{e^-eq\ membrane\ ratio} = \frac{DC_{e^-eq\ M_1}}{DC_{e^-eq\ M_2}}$$

$$DC_{C\ eq\ membrane\ ratio} = \frac{DC_{mol\ C\ M_1}}{DC_{mol\ C\ M_2}}$$

where M_1 is the asymmetric fiber and M_2 is the symmetric fiber.

3. Results & Discussion

3.1.Concentrations and rates of carboxylates for each membrane

Figure 23 shows the effects of the type of membrane on the carboxylates and alcohols titers achieved during steady-state operation with the syngas MBfRs. Table 5 shows the electron equivalents and carbon content of each detected product. The delivery-capacity ratio of electron equivalents and moles of C at 5 psig (1.34 atm) were 1.6 e^- eq./ e^- eq. and 4.2 mol C/mol C, where the ratio is for the asymmetric membrane normalized to the symmetric membrane. Therefore, the asymmetric membrane had delivery capacities that were 1.6-fold higher than the symmetric membrane reactor for electron equivalents, but 4.2-fold higher for C.

The asymmetric fiber gave total titers that were 1.5-fold greater than for the symmetric fiber in terms of electron equivalents, while the titers were about 2-fold greater for the symmetric fiber in terms of C equivalents. This supports that the delivery of electron equivalents was the rate-limiting factor for the asymmetric fiber, while carbon was not limiting. This explanation is consistent with the observation of only C1 and C2 products with the asymmetric fiber. In contrast, I observed products up to 8 carbons with the symmetric fiber. This difference corresponds to the principles of Chapter 4, where IC limitation promoted microbial chain elongation (MCE).

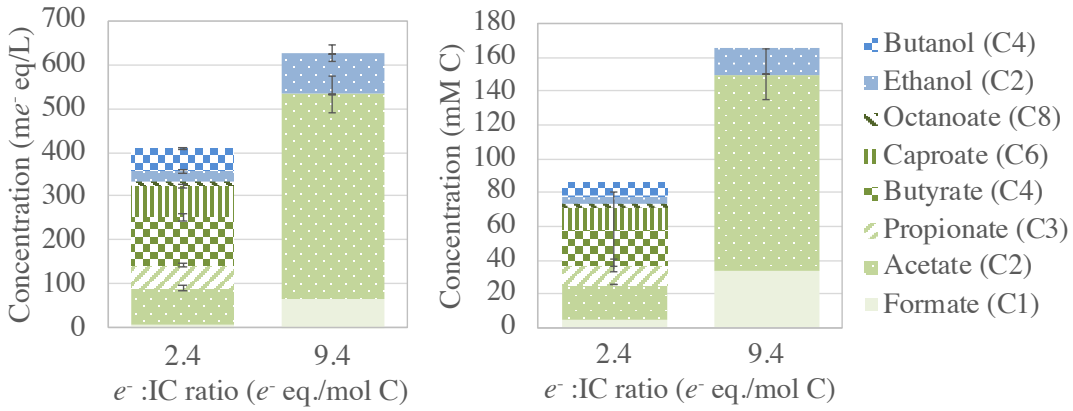

Figure 23. Carboxylates and alcohols concentrations (left panel in me^- eq./L and right panel in mM C) for symmetric membranes (left bar) and asymmetric membranes (right bar) in syngas-fed MBfRs at steady state. The steady states were for 26 days of continuous operation with HRT 39.15 ± 0.61, P=5 psig, T=35°C, and a gas mixture of 40% H_2, 30% CO and 30% CO_2

That the symmetric membrane led to MCE can be explained by its higher e^-:C ratio. The measured value of e^-:C ratio as 2.4 e^- eq./mol C for the asymmetric membrane is lower than the 4:1 ratio stoichiometrically needed for acetate production. This corroborates that carbon is highly available in the asymmetric fiber, having a higher production due to the permeance of the fiber, but limiting the products to formate, acetate, and ethanol. The 4:1 mole ratio (equivalent to a H_2:C ratio of 2:1) is what I found in Chapter 4 as the threshold for MCE. Thus, the asymmetric fiber did not promote MCE. In contrast, the measured e^-:C equivalents ratio for the symmetric membrane was 9.4, which is well above the ratio need to promote MCE. Thus, producing from syngas carboxylates up to 8 carbons is consistent with the results in Chapter 4, where MCE was evident for H_2:IC mole ratio of 2 to 1.

Table 5. Electron equivalents and carbon content of products observed in the MBfRs

Compound	β_i e- eq/mol	χ_i mol C/mol	β_i / χ_i e- eq/mol C
Acetate	8	2	4.0
Ethanol	12	2	6.0
Propionate	14	3	4.7
Butyrate	20	4	5.0
Butanol	24	4	6.0
Valerate	26	5	5.2
Caproate	32	6	5.3
Octanoate	44	8	5.5

The highest acetate titer achieved with the asymmetric fiber was 3.5 g/L, compared to 42 g/L of acetate as the highest value reported in literature (Y. Q. Wang et al., 2017). However, the production rate with the asymmetric fiber was 253 $g \cdot m^{-2} \cdot d^{-1}$, which surpasses the highest production rate by area reported up to now, 107 $g \cdot m^{-2} \cdot d^{-1}$ using 60% of H_2 and 40% of CO_2 (Y. Q. Wang et al., 2017). It also is greater than the maximum areal rates in Chapter 4 using H_2 (24 $g \cdot m^{-2} \cdot d^{-1}$). My MBfR had only two asymmetric membranes, and increasing the number of fibers (and thus the specific surface area) should increase the titer approximately proportionally. For example, the MBfR with the symmetric membrane had 60 fibers, and 60 asymmetric fibers should yield a titer of 105 g/L. For comparison, all reported rates and titers can be found in Table 6.

Table 6. MBfRs for carboxylates production reported to date

H_2:CO:CO_2:N_2	Vol (L)	HRT (d)	Gas P (atm)	Type	pH	T (℃)	SA (m^2)	Product	Max. Conc. ($g \cdot L^{-1}$)	Max. Px Rate ($g \cdot m^{-2} \cdot d^{-1}$)	Reference
60:0:40:0	0.24	n.a.	0.4	Batch	6 ±0.2	35±1	0.11	Acetate Butyrate Caproate Caprylate	7.40 1.80 0.98 0.42	n.a.	Zhang et al., 2013b
60:0:40:0	0.32	n.a.	0.987	Batch	4.65±0.1	35±1	0.28	Acetate	12.50	n.a.	Zhang et al., 2013a
60:0:40:0	0.32	9	1.987	Continuous	4.65±0.1	35±2	0.28	Acetate	3.30	0.42	Zhang et al., 2013a
5:20:15:60	8	n.a.	1.021	Batch	6	37	1.4	Ethanol Acetate	15.00 8.20	n.a. n.a.	Shen et al., 2014
5:20:15:60	8	n.r.	1.021	Semi-batch	4.5-5.5	37	1.4	Ethanol Acetate	23.93 5.00	2.80 3.40	Shen et al., 2014
0:100:0:0	0.5	n.a.	n.r.	Batch	5.5-7.0	37	0.014	Acetate	1.98	n.a.	Yasin et al., 2014
60:0:40:0	0.24	n.a.	0.4	Batch	6	35	0.11	Acetate Butyrate Caproate	8.3 6.0 3.3	n.a.	Chen and Ni, 2016
60:0:40:0	0.32	n.a.	n.r.	Batch	6	55	0.023	Acetate	42.4	n.a.	Y. Q. Wang et al., 2017
60:0:40:0	0.32	2.5	n.r.	Continuous	6	55	0.023	Acetate Butyrate	19.3 0.09	107.41 0.50	Y. Q. Wang et al., 2017
60:0:40:0	0.32	n.a.	n.r.	Batch	6	25	0.023	Acetate Butyrate Caproate Ethanol Butanol	30 15.7 5.7 0.2 0.8	n.a.	Y. Q. Wang et al., 2018
60:0:40:0	0.32	n.a.	0.4	Batch	4.5	35	0.023	Acetate	16.9	n.a.	H. J. Wang et al., 2018

H_2:CO:CO_2:N_2	Vol (L)	HRT (d)	Gas P (atm)	Type	pH	T (℃)	SA (m^2)	Product	Max. Conc. ($g \cdot L^{-1}$)	Max. Px Rate ($g \cdot m^{-2} \cdot d^{-1}$)	Reference
60:0:40:0	0.32	9	H_2: 0.4 CO_2: 0.6	Continuous	4.5	35	0.023	Acetate Ethanol	1 4.2	1.55 6.49	H. J. Wang et al., 2018
60:0:40:0	0.32	9	H_2: 0.2 CO_2: 0.3	Continuous	4.5	35	0.023	Acetate Ethanol	7.4 0.6	11.44 0.93	H. J. Wang et al., 2018
60:40:0:0	0.39	n.a.	0.1-0.15	Sequential batch	6	35	0.1	Acetate Butyrate Caproate Caprylate	4.22 1.35 0.88 0.52	n.a.	Shen et al., 2018
60:40:0:0	0.39	1.5	0.1-0.15	Continuous	6	55	0.1	Acetate	19.44	50.54	Shen et al., 2018
60:40:0:0	0.39	1.5	0.1-0.15	Continuous	6	55	0.24	Acetate	27.9	30.23	Shen et al., 2018
60:40:0:0*	0.42	n.a.	0.099	Semi-batch	6	35	0.016	Acetate Butyrate Caproate	10.2 13.5 3.5	n.a.	H.-J. Wang et al., 2018
60:40:0:0**	0.42	n.a.	0.099	Semi-batch	6	35	0.016	Acetate Butyrate	29.4 0.6	n.a.	H.-J. Wang et al., 2018
60:40:0:0	0.42	5.5	0.099	Continuous	6	35	0.016	Acetate Butyrate Caproate Ethanol	3.3 1.1 0.77 0.11	15.75 5.25 3.68 0.53	H.-J. Wang et al., 2018
100:0:0:0	0.07	0.93	1.36	Continuous	7.2	20	0.013	Acetate	3.21	24.16	Calvo et al., 2021
100:0:0:0	0.07	2.04	1.36	Continuous	7.2	20	0.013	Acetate Ethanol Propionate Butyrate Butanol Caproate Octanoate	0.142 0.055 0.057 0.33 0.13 0.31 0.21	0.49 0.19 0.20 1.13 0.47 1.06 0.73	Calvo et al., 2021
40:30:30:0	0.07	1.62	1.36	Continuous	7.0	35	4.7E-4	Acetate	0.625	253	This chapter

n.r.: Not reported; n.a.: Not applicable. *Pore size: 0.01-0.05 μm;**Pore size: 8-10 μm

3.2.Microbial Ecology of Biofilm

The microbial ecology in the MBfR biofilms was consistent with the performance results. Figure 24 shows that phylotypes related with acetogenic families were the most abundant for the asymmetric membrane, whereas families capable of MCE were most abundant with the symmetric membrane. For the MBfR with the asymmetric membranes, the most abundant family was Eubacteriaceae (56% of total reads). When I zoom into the Eubacteriaceae family sequences, 71% correspond to *Acetobacterium*, a well-known acetogenic genus (Balch et al., 1977). For the MBfR with the symmetric membrane, the most abundant family was Clostridiaceae (32%), which includes phylotypes capable of acetogenesis and MCE. Ruminococcaceae, which has been identified as a key family for MCE (Angenent et al., 2016; Candry and Ganigué, 2021), also was more abundant (2.3%) for the symmetric membrane.

Another noteworthy difference was that the biofilm on the symmetric membrane contained a sizable fraction (20% of total reads) of Methanobacteriaceae, a well-known H_2-oxidizing methanogen. If the goal is to generate carboxylic acids, production of methane is an undesired diversion of electron equivalents from H_2. The inhibition of methanogenesis by CO has been widely studied (Esquivel-Elizondo et al., 2018), and the limitation of the symmetric fiber for delivering CO could have helped methanogens establish themselves it the biofilm. In contrast, the asymmetric fiber delivers more CO actively, which could have played a role in the absence of methanogens in the biofilm.

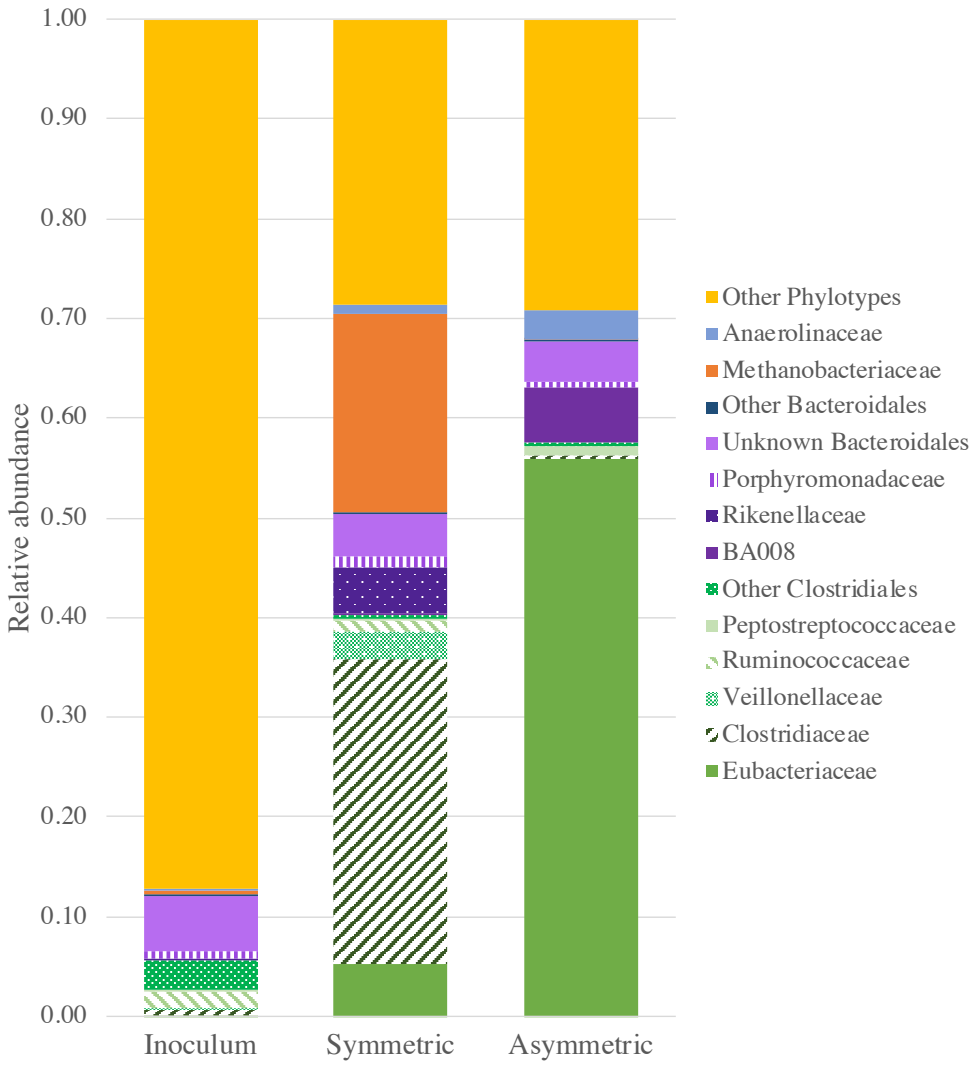

Figure 24. Relative abundance of phylotypes observed in the syngas-based MBfRs at family level. Green tones are phylotypes related with the order Clostridiales, purple tones are phylotypes related with the order Bacteroidales

4. Conclusion

Membrane properties had profound effects on the performance of MBfRs fed synthetic syngas. On the one hand, the very high permeance of the asymmetric Matrimid® membrane led to exceptionally high areal production rates of formate and acetate. The areal productivity of acetate was by far the highest ever reported: 253 $g \cdot m^{-2} \cdot d^{-1}$. On the other hand, the greater selectivity of the symmetric membrane towards electrons favored microbial chain elongation to carboxylates up to 8 carbons. Thus, a membrane should be chosen so that it is compatible with the desired products and syngas composition. Additionally, the total surface area inside the system, as well as the syngas composition, are key parameters to manage the e^-:C ratio. The syngas composition could be modified to match with membrane properties. For example, MCE should be favored when using the asymmetric membrane if the syngas composition were less than 18 % H_2.

Similar to Chapter 4, the e^- :C ratio played an important role in precluding or allowing MCE. Consistent with the threshold found in Chapter 4 – MCE with a ratio > 4:1 e-eq/mol C -- the asymmetric fiber (2.4 ratio) did not produce any acid longer than 2 carbons, while the symmetric fiber (9.4 ratio) produced carboxylates up to octanoate and alcohols up to butanol.

Using the specially produced asymmetric fiber, I can obtain more than double areal production rate over any rate reported so far. Promising lines of future research are to evaluate how to achieve very high volumetric rates by increasing the membrane area while maintaining a high per-area production rate and adjusting the syngas composition to enable MCE.

CHAPTER 7

TECHNO-ECONOMIC ASSESSMENT OF SYNGAS FERMENTATION IN A MEMBRANE BIOFILM REACTOR[5]

1. Introduction

The increase of carbon dioxide (CO_2) in the atmosphere demands sustainable industrial processes that have neutral or negative carbon balances. One way to achieve this is with carbon recycling. Syngas production is a well-known alternative for recycling carbon by either capturing CO_2 and water from the atmosphere or by utilizing lignocellulosic biomass, creating a mixture of hydrogen (H_2), carbon monoxide (CO), and CO_2. Although syngas is already considered an alternative fuel, further conversion to liquid organic products, such as carboxylic acid and alcohols, can be even more economically attractive (Mohammadi et al., 2011).

The classic Fisher-Tropsch process (FT) has been studied for decades and uses metallic catalysts to convert syngas to liquid fuels and chemical precursors (Santos and Alencar, 2020). Several operational requirements -- such as high temperature, high pressure, and the use of metals -- makes the FT process economically unattractive (Asimakopoulos et al., 2018). Furthermore, while promising developments are occurring

[5] **Credit:** *Diana C. Calvo* – writing, conceptualization, engineering parameters, data analysis, graphs, edition, funding acquisition; *Robert Stirling* – writing, economic parameters, TEA model, data analysis, graphs, edition; *Ellen Stechel* – conceptualization, funding acquisition*; Ivan Ermanoski* – conceptualization; *Cesar I. Torres* – writing, data analysis, edition; *Bruce E. Rittmann* – conceptualization, writing, data analysis, edition, funding acquisition.

in biomass gasification to small-scale FT, the technical risks are still high and, commercialization is uncertain (Frilund et al., 2021). Additionally, a main weakness of the Fischer-Tropsch process is the large scales typically required for commercialization -- often 30,000+ bbl/day for gas-to-liquid and 80,000+ bbl/day for coal-to-liquid (De Klerk, 2012).

Biological systems have advantages that can reduce the cost of syngas conversion to valuable products and make the process attractive for commercial uses: low temperature, low pressure, and the abilities of microorganisms to tolerate impurities and to ferment a wide range of syngas compositions (Bengelsdorf et al., 2013). Currently, one facility, operated by LanzaTech (www.lanzatech.com), is successfully producing ethanol from syngas fermentation, but attempts from INEOS Bio (www.ineos.com) and Coskata (www.coskataenergy.com) were unsuccessful and shut down. Daniell et al. (2012) indicated that syngas fermentation could be profitable, but the biggest bottleneck is mass-transfer limitation due to the low solubilities of CO and H_2. According to our bibliometric analysis (Chapter 4) in syngas fermentation, mass transfer is a main limitation in the process and has been investigated by several teams in the field.

One strategy to overcome mass-transfer limitations with a low-solubility gas is the membrane biofilm reactor (MBfR), in which microorganisms grow as a biofilm on the outside of hollow-fiber membranes that deliver a gaseous substrate directly to the biofilm (Rittmann, 2018). The biofilm can be used to remove contaminants, recover metals, or produce chemicals (Calvo et al., 2021; Zhou et al., 2014). The MBfR has been successfully applied to improve production rates of carboxylic acids and alcohols using

syngas fermentation, and it has achieved higher production rates than other reactor configurations (Y. Q. Wang et al., 2017). However, the membranes add capital costs that create a trade-off with higher production rates.

Considering the success of MBfRs for overcoming mass-transfer limitations of low-solubility gaseous substrates, we present a techno-economic assessment (TEA) of acetate production in an integrated process of syngas fermentation in a MBfR followed by a separation process using extraction.

2. Methods and system description

2.1.Production Scale

A core goal of the analysis was to scan the opportunity space for fermentation techniques that could pair well with smaller-scale syngas production facilities. Because we wanted to explore scaling down the process to small modules without sacrificing scale-up economy while taking advantage of the versatility of microorganisms to work reactors of any scale, we decided to fix our syngas consumption to 100 bbl/day (0.16 m^3/day), which translates to roughly 5000 Gasoline Gallon Equivalent (GGE)/day (18,900 Gasoline Liters Equivalents/day). With an enthalpy of combustion (ΔH_c) of acetic acid of -75 kJ/mol, this translates to a nameplate capacity of ~14,000 metric tons per year (U.S. Secretary of Commerce, 2018).

2.2.Syngas source

We do not examine the source of the syngas feedstock, but instead treat it as a fungible commodity provided at a cost of $1/kmol. This cost assumption was based on

de Medeiros et al (2020), who interpreted techno-economic studies of shale gas and biomass conversion (de Medeiros et al., 2020; Martinez-Gomez et al., 2017; Yao et al., 2018).

2.3.System description

2.3.1. Membrane Biofilm Reactor

In an MBfR, syngas diffuses through hollow-fiber membranes submerged in an aqueous solution. Microorganisms accumulated as a biofilm on the exterior of the membrane convert the syngas to desired bioproducts, including acetic acid. The membranes can be geometrically packed within the reactor to achieve high volumetric mass transfer rates of the feed gases without off-gassing. The production rate of the reactor normalized by membrane area ($g \cdot m^{-2} \cdot d^{-1}$) is a key performance parameter of the system's overall cost effectiveness. We calculated the threshold value with our TEA model, but we used as an initial value the acetate-production rate obtained in our laboratory-scale syngas-based MBfR: 253 $g \cdot m^{-2} \cdot d^{-1}$ (Chapter 6). We approximated the value to 250 $g \cdot m^{-2} \cdot d^{-1}$.

We estimated the costs of anMBfR unit by using top-down metrics for capital expenses (CapEx) per surface area based on a previous well-detailed TEA analysis for the MBfR (Evans et al., 2013). We scaled down the costs by using the "Rule of Six-Tenths" (AACE®, 2018): for two (i and ii) scenarios:

$$\mathrm{CapEx_{ii}} = \mathrm{CapEx_{Ai}} \left[\frac{\mathrm{Capacity_{ii}}}{\mathrm{Capacity_{i}}} \right]^{\mathrm{e}}$$

with $0.5 < e < 0.85$ and e typically close to 0.6, which we used. Expenses of the MBfRwere taken from Evans et al. (2013) and adjusted to 2021 dollars with current

CEPCI data ("Chemical Engineering Plant Cost Index," 2021), yielded the following predictive formulas:

$$Total\ Installed\ Cost = \$15000A^{0.590}$$

$$Total\ Operating\ Expenses = \$260A^{0.619}$$

where A is the total surface area of membranes in the MBfR (m^2).

2.3.2. Product extraction

As with many biologically driven chemical conversions, the product often is a combination of many bioproducts in varying proportions that can be tuned by adjusting feed composition, pressure, temperature, and microorganisms. In this case, we assumed the simplest product mix: only acetic acid (HAc). HAc was chosen to build a robust foundation for further work that will analyze complex product compositions. Choosing HAc as the only product presents two main challenges that the MBfR shares with other front-end approaches that produce a broth containing a mixture of dilute (<30% w/w) C1-C6 bioproducts: 1) concentrating very dilute products to highly concentrated feedstocks (>99% for industrial customers), and 2) the bioproducts' tendencies to form azeotropes with water (Aghapour Aktij et al., 2020; Atasoy et al., 2018). Practically, choosing HAc as the only product creates a "worst-case scenario," because, among the likely products, HAc has the lowest market price and is challenging to separate.

Producing a saleable product often requires multistage extraction, separation, and purification steps that are costly in capital and energy requirements. Separation processes reported for carboxylic acids include distillation, gas stripping, precipitation, adsorption, solvent extraction, pressure-driven membrane separation (nanofiltration), forward

osmosis, reverse osmosis, membrane distillation, electrodialysis, pervaporation, and perstraction (Aghapour Aktij et al., 2020; Atasoy et al., 2018; López-Garzón and Straathof, 2014; Murali et al., 2017; Nayak et al., 2015; Pal and Nayak, 2017; Petersen et al., 2018).

Although acetic acid and water do not form an azeotrope, acetic acid has volatility that is problematic for simple distillation. Furthermore, separating dilute HAc (NBP 118°C) from water require vaporization of large amounts of water. The commonly used techniques in industry to avoid these challenges are multi-effect distillation (MED), azeotropic distillation using an entrainer, or a hybrid liquid-liquid-extraction (solvent extraction using different solvents) followed by distillation. A comparative TEA (Li et al., 2014) among the alternatives showed that the fraction of total annual costs (CapEx + OpEx) attributable to direct distillation were 57% for MED, 80% for azeotropic distillation with vinyl acetate, 35.4% for azeotropic distillation with isobutyl acetate, 31% for solvent extraction with ethyl acetate, and 19% for solvent extraction with MTBE (methyl tert-butyl ether) (Li et al., 2014). While MTBE-solvent extraction presented the lowest-cost option, MTBE itself is a challenging groundwater pollutant, as it is resistant to biodegradation and travels quickly with the groundwater (Li et al., 2014). Since ethyl acetate (EA) has shown a favorable partition coefficient to extract acetic acid from corn stover fermentation (Aghazadeh et al., 2016), we chose to use an ethyl-acetate extraction for acetic acid after the MBfR syngas fermentation.

We modeled the chosen extraction system using Aspen Plus v10 and based on operational units described by Seader et al. (2011). The detail of flows for each unit is shown in Figure 25.

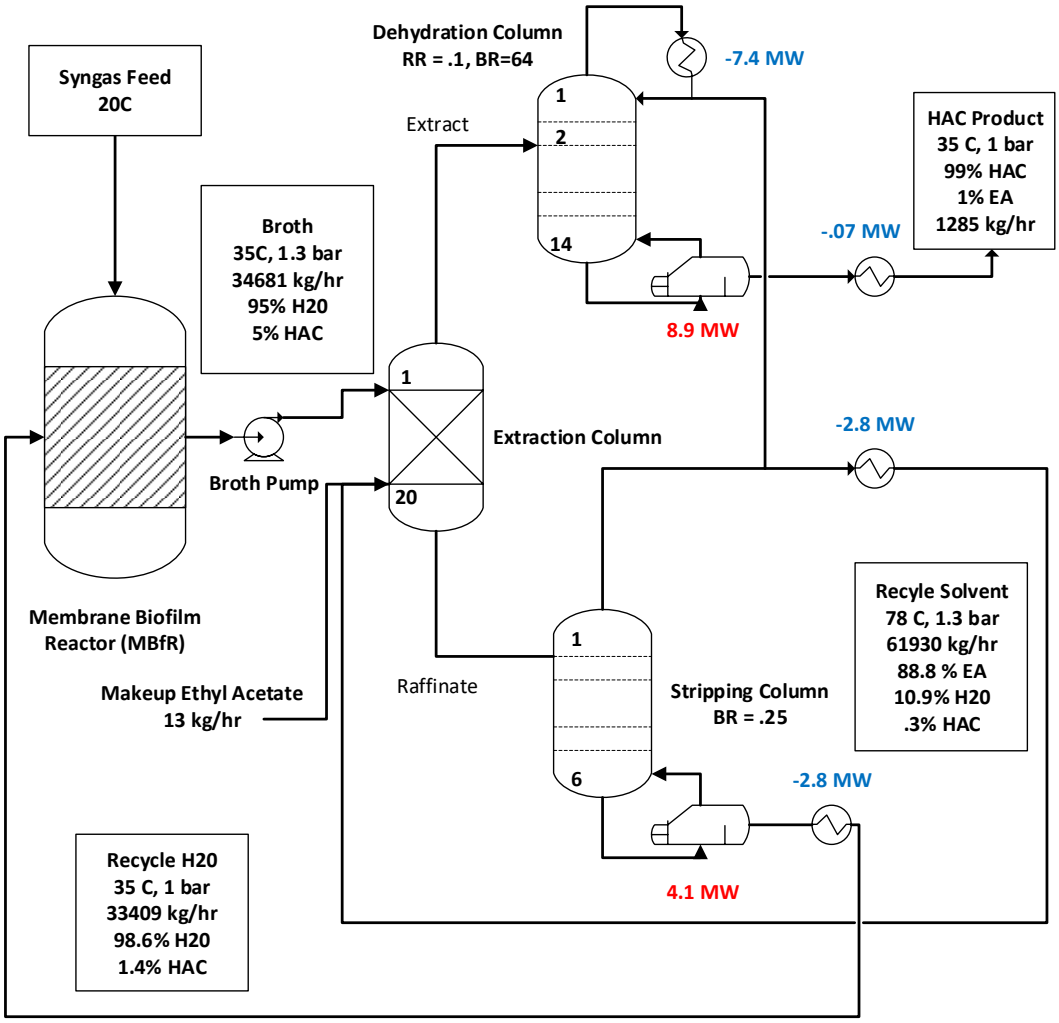

Figure 25. Aspen Plus model for acetic acid extraction with ethyl acetate

We used the non-random two-liquid activity-coefficient model within the Hayden O'Connell framework (NRTL-HOC) to account for acetic acid dimerization in a vapor phase (George Hayden and O'Connell, 1975). The activity coefficients used are listed

were provided by the Aspen APV100 database. The extraction column was modeled using the rigorous counter-current "Extract" model. The distillation columns were modeled using the rigorous "RadFrac" model and equilibrium calculations.

We assumed a 5% HAc concentration in the broth coming from the MBfR, based on the maximum concentration reported for acetate production by syngas fermentation (Y. Q. Wang et al., 2017). This broth is continuously removed from the MBfR and pressurized to 1.3 bar, which was chosen as the operating pressure for all components in the system for energy efficiency reasons, primarily linked to the largest energy consumer -- the dehydration column. The mostly aqueous broth is mixed in a contact extractor ("Extraction Column") with a recycled solvent stream consisting of mostly EA. The lower-density, solvent-rich extract stream contains 91% of the HAc. The higher-density, water-rich raffinate stream contains 9% of the HAc. The 91% extraction efficiency is lower than the typical 99.8% extraction efficiency achieved because our 5% HAc content in the feed is much lower than the 20-30% concentration typically modeled (Chien et al., 2004; Lee and Kim, 2018; Li et al., 2014; Seader et al., 2011).

The extract is sent to a 14-stage distillation column with 99% HAc as the bottom product. The EA-rich distillate is sent to a decanter along with the stripping column where the two liquid phases are separated by gravity. The raffinate from the extraction column is sent to a 6-stage stripping column to remove the vast majority of EA from the product. The water product contains some HAc and insignificant fractions of ethyl acetate (<1 ppb). This product is recycled to the MBfR.

The cost of equipment was estimated by importing the Aspen Plus simulation data into Aspen Capital Cost Estimator (ACCE). Unless specified otherwise, default values for Aspen Plus simulations and ACCE were used. The mathematic models were mapped to equipment lists, *e.g.,* Radfrac maps to shell and tube condenser, condenser accumulator vessel, reflux pump, U-tube kettle reboiler, and a trayed single diameter columns with 2' tray spacing. We included installation, construction and contingency for capital cost estimation using accepted values for additions to existing fluid processing plants (Peters and Timmerhaus, 2014). The separation equipment ends up being oversized by about 1-2% due to recycling of produced HAc back to the bioreactor.

Utility costs for the operation were estimated based on the amounts of cooling water and medium-pressure steam required. Utility assumptions are shown in Table 7. Costs per unit were sourced from Khan and Adewuyi (2019) and validated with US Energy Information Administration statistics (www.eia.gov). The steam requirements were estimated based on the two distillation towers' reboiler needs. The cooling water requirements are based on the dehydration tower's condenser power and those of the three stream cooling heat exchangers. Electrical requirements in this model are minimal, as they are only represented by the broth and reflux pumps. Actual requirements for instrumentation, controls, and auxiliary pumps are likely minimal compared to the total utility bill.

2.4.Assumptions for TEA

Table 7 summarizes the assumptions made for the TEA model considering the scale, syngas source. and the system configuration.

Table 7. Assumptions for the MBfR TEA model

Parameter	Value	Unit	*Note or Reference*
Plant Location	USA		*
Scale of Production	5000	GGE/d	*
Acetic Acid Mass Fraction of Broth	5%	%w/w	(Y. Q. Wang et al., 2017)
Acetic Acid Productivity (MBfR)	250	$g/m^2/d$	**
MBfR Syngas to Product Mass Efficiency	100%		*
Market Price of Acetic Acid	745	$/tonne	(Kelley, 2018)
Market Price of Ethyl Acetate	960	$/tonne	(Petersen et al., 2018)
Cost of Syngas Feed	1.00	$/kmol	(de Medeiros et al., 2020)
Cost of Electricity	0.07	$/kWh	*
Cost of Cooling Water (20C)	120	$/MMGal	(Khan and Adewuyi, 2019)
Cooling Water Temperature - Inlet	20	°C	ASPEN Plus Default
Cooling Water Temperature - Outlet	25	°C	ASPEN Plus Default
Cooling Water Minimum Approach Temp.	5	°C	Aspen Plus Default
Cost of Medium Pressure Steam	3.72	$/klb	(Khan and Adewuyi, 2019)
MP Steam Temperature - Inlet (Vapor)	175	°C	Aspen Plus Default
MP Steam Temperature - Outlet (Liquid)	174	°C	Aspen Plus Default
MP Steam Minimum Approach Temp.	10	°C	Aspen Plus Default
Operator Annual Wage	51,500	$/year	(U.S. Bureau of Labor Statistics, n.d.)
Operators	2	per shift	*
General & Administrative Overhead (as % of Wages & Supervision)	50%		*
Supervisory Rate	25%		*
Required Return on Capital Employed	10%		*
Project Life	20	Years	*
Salvage Value	0%		*
Shifts per Day	3		*
Uptime (Plant Availability)	95%		*
Maintenance (as % of ISBL)	5%	% ISBL	*, (Peters and Timmerhaus, 2014)

* Indicates a primary assumption that is discussed in the text.
** From Chapter 6.

3. Results & Discussion

Considering a 5,000 GGE/day (18,900 GLE/day) target capacity, we estimated that 122,000 m^2 of membrane-surface area are needed, giving a total installed cost of $15,083,000 and annual operations cost of $364,000. The discretization of these values is shown in Table 8.

Table 8. Parametric cost estimates for MBfR subprocess

Scenario Capital Expenses	**Calculated**
Equipment Installed Cost	$5,915,000
Civil and Construction Cost	$447,000
Piping and Mechanical Installed Cost	$307,000
Electric and I&C Installed Cost	$962,000
Subtotal Direct Cost	$7,631,000
Permit Fees and Sales Taxes	$916,000
Bond and Insurance	$229,000
Subtotal A	$8,775,000
General Conditions	$878,000
Contractor Overhead and Profit	$1,316,000
Subtotal B	$10,969,000
Contingency	$2,742,000
Subtotal C	$13,712,000
Engineering Design Services	$1,371,000
Total Installed Cost	$15,083,000
Scenario Operating Expenses	
Electricity	$272,000
Nutrients	$13,000
Stirring	$40,000
Membrane Replacement	$39,000
Annual Operation Cost	$364,000

For the extraction subprocess, we estimated a total capital investment of $4,221,000, detailed in Table 9. Capital and Operating expenses were totaled for all the subsystems. Labor costs were estimated based on two operators and three shifts using Bureau of Labor Statistics wages. The Required Return on Capital Employed (RROCE) technique is a commonly used technique to determine a minimum viable price when profit margins for an industry or product are uncertain. In this case, the operator of the plant is expected to achieve a profit equal to of 10% of total capital employed (including working capital). This is higher than the current 6.6% weighted average cost of capital (WACC) for the basic chemical industry. The increment was based on our judgment that a novel process requires a higher-than-usual ROI. The life of the project was assumed to be 20 years with no salvage value. Itemization for the entire process is in Supplementary Information - Table 10.

Summing capital and operating costs, the overall cost of HAc production is $716/MT, compared to its market price of $745/MT. While the cost-to-price difference suggests that the system is feasible, cost and price are close, which means that modest increases in costs or declines in market price could alter the comparison. It is important to note that this analysis already factors in a sizable charge for the cost of capital.

Table 9. Parametric cost estimates for extraction subprocess

Purchased Equipment	**Purchased Cost**
Stripping Column	
U-Tube Kettle Reboiler	$27,300
Trayed Single Diameter Tower	$73,300
Dehydration Column	
Condenser - Shell and Tube	$38,900
Condenser Accumulator	$21,500
U-Tube Kettle Reboiler	$69,200
Reflux Pump	$8,800
Trayed Single Diameter Tower	$218,400
Heat Exchangers	
Shell and Tube HX - Product Acetic Acid	$8,800
Shell and Tube HX - Recycle Solvent	$27,600
Shell and Tube HX - Recycle Broth	$22,100
Extraction Column - Single Diameter Trayed Tower	$190,000
Decanter - Recycle Solvent	$23,600
Broth Pump	$5,600
	$735,100
Direct Costs	**Cost Value ($)**
Purchased Equipment Delivered	$735,000
Purchased Equipment Installation	$345,000
Instrumentation	$265,000
Piping	$500,000
Electrical	$81,000
Buildings	$132,000
Yard Improvements	$74,000
Service Facilities	$515,000
Total Direct Plant Cost	$2,647,000
Indirect Costs	
Engineering Design and Supervision	$243,000
Construction	$301,000
Legal Expenses	$29,000
Contractor's Fee	$162,000
Contingency	$323,000
Total Indirect Plant Cost	$1,058,000
Fixed Capital Investment	$3,705,000
Working Capital	$654,000
Total Capital Investment	$4,359,000

The cost distribution is shown in Figure 26. We assume labor, maintenance, and overhead are applied based on fraction of total capital contribution. The extraction cost was 42% of the total system cost, while the MBfR was about 48% and the syngas feed about 10%. The first conclusion from the distribution is that alternative ways to separate the product from its broth could yield tremendous cost savings, as separation has a large share of costs. A second conclusion is that increasing the areal production rate of the MBfR can decrease the cost by reducing the amount of membrane and MBfR size. A lower cost of syngas might be possible, depending on the source and if the installation is co-located with the MBfR. However, the syngas source contributes only 10% of the total cost. Restricting the syngas sources to those with favorable LCA's would likely increase its feedstock cost.

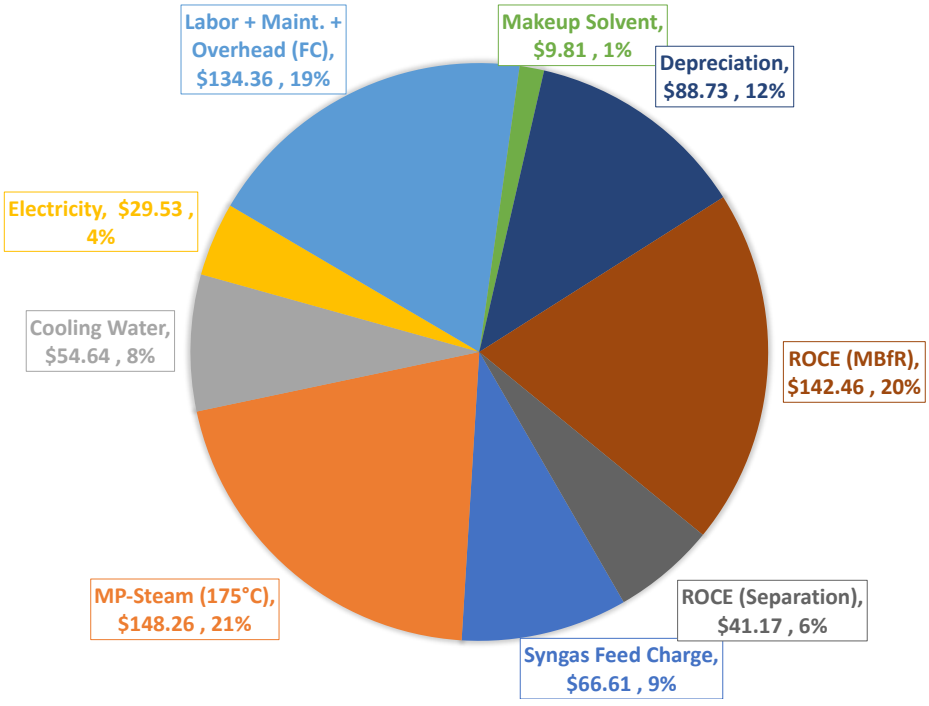

Figure 26. Cost distribution ($/MT HAc) from the TEA simulation of syngas conversion to acetic acid using the MBfR followed by ethyl acetate extraction.

Figure 27 amplifies on the cost-reduction strategies with a tornado chart. We present the change in the total cost of production of HAc in $/metric ton for a variation of ±25% in one of the most relevant model parameters. As suggested by Figure 26, the most-important parameter is the production rate by area; therefore, efforts should be directed towards increasing the areal production rate. The parameter with the second highest impact in the cost is the MBfR-fermentation CapEx in $/m^2, which is related to areal production rate. The cost of MP-Steam is closely associated with the extraction system, and it has a strong impact in the cost of production as well.

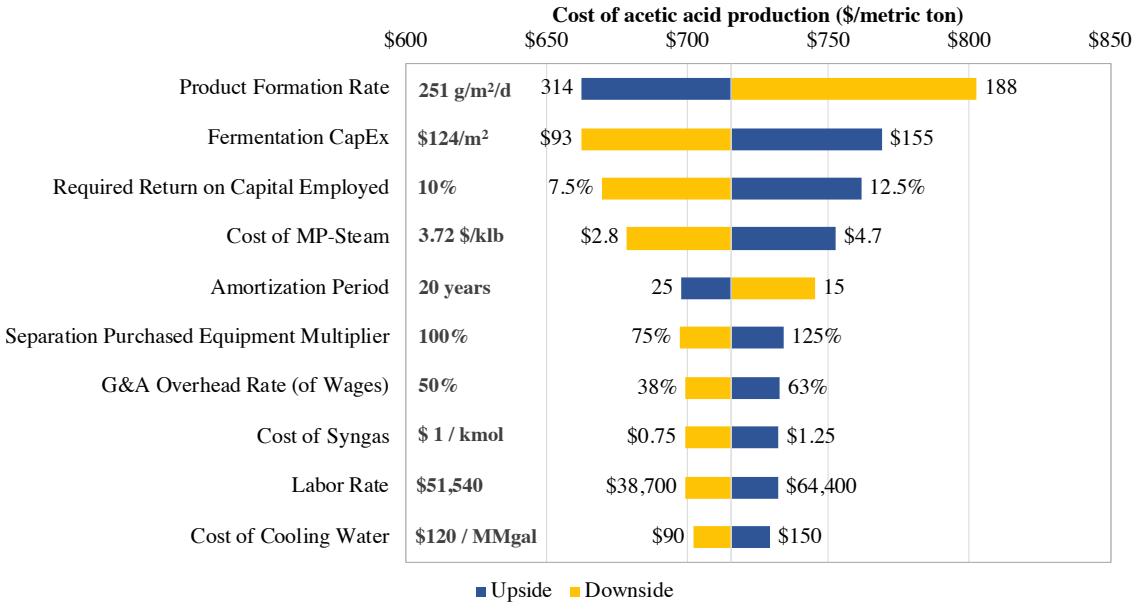

Figure 27. Tornado chart for the total cost of production of acetic acid ($/metric ton)

4. Conclusion

Techno-economic analysis for an MBfR coupled with ethyl-acetate extraction showed that the cost of acetic acid production (including ROI) is slightly lower than the current market price for acetic acid in the USA. This supports that the process has potential to create value in its mature phase. Greater per-area productivity in the MBfR and more cost-effective separation have the largest potential for lowered costs and make the system more economically attractive.

5. Supplementary Information

Table 10. Total cost estimation sheet

PLANT STATISTICS		
Feed	Syngas	
Analysis Date	Jun-20	
Location	USA	
Nameplate	11,144	MT / Yr
Operating Rate	95%	
Throughput	10,587	MT / Yr
Products	Acetic Acid (99%)	

CAPITAL COST	$	% of Plant
ISBL (Inside Battery Limits)	$9,688,864	94.3%
OSBL (Outside Battery Limits)	$589,000	5.7%
Total Plant Capital	$10,277,864	**100.0%**
Other Project Costs (Contingency, EPC)	$8,510,629	82.8%
Total Project Investment	$18,788,493	**182.8%**
Working Capital	$654,000	6.4%
Total Capital Employed	**$19,442,493**	**189.2%**

PRODUCTION COST SUMMARY						$ Per MT Product	$ Per Ton Product	Annual Cost (USD Millions)
			Units per MT Product	*Price ($ / Unit)*				
CONSUMABLES								
	Syngas	kmol	66.6	$	1.00	67	60	0.71
	Ethyl Acetate	MT	0.01		960	9.81	8.90	0.10
TOTAL RAW MATERIALS						*76*	69	*0.81*
UTILITIES	Electricity	kWh	422	$	0.07	29.5	26.8	0.31
	Cooling Water	MMGal	0.455	$	120	54.6	49.6	0.58
	MP Steam (175C)	kLb	39.9	$	3.72	148.3	134.5	1.57
TOTAL UTILITIES						*232.44*	210.86	*2.46*
TOTAL VARIABLE COST						**308.85**	**280.19**	**3.27**

				$ Per MT Product	$ Per Ton Product	Annual Cost (USD Millions)
Labor and Maintenance	Labor and Supervision	$ 463,860		43.81	39.75	0.46
	Maintenance (Material)	5% of ISBL		45.76	41.51	0.48
	Overhead	50% of Labor + Super. + Maint.		44.79	40.63	0.23
TOTAL FIXED COSTS				**134.36**	**121.89**	**1.42**
TOTAL CASH COSTS				**443.22**	**402.08**	**4.69**
Depreciation @	5.0%	for OSBL + OPC		42.98	38.99	0.45
	5.0%	for ISBL		45.76	41.51	0.48
Total Depreciation				*88.74*	*80.50*	*0.94*
COST OF PRODUCTION				**531.95**	**482.58**	**5.63**
Required Return on Capital Employed (including Working Capita			10.0%	183.65	166.60	1.94
COST OF PRODUCTION + ROCE				**715.60**	**649.18**	**7.58**

CHAPTER 8

SUMMARY

Syngas, a mixture of H_2, CO, and CO_2, already is widely used as a non-fossil fuel and a building block for a variety of chemicals using the Fischer-Tropsch process. Recently, syngas fermentation has attracted attention as a more sustainable way for conversion of syngas to chemical, since its biocatalysts are self-generating, are resilient, and can work with a wide range of syngas compositions. However, syngas fermentation has technical and economic limitations. This dissertation contributes to with the understanding of syngas fermentation and helps to overcome the limitations.

This dissertation started with a bibliometric analysis showing the on-going bloom of syngas fermentation as a research field and for applications (Chapter 3). Even though I found strong collaborations between some authors, network cluster analysis showed high potential of more collaboration if strong teams were to join forces and link related fields. Through keywords analysis, I identified that mass transfer is the biggest challenge for syngas fermentation. To address this challenge directly, I chose to evaluate the MBfR as the focus of my research.

I first ran MBfRs with pure H_2 gas from the gas phase and inorganic carbon (HCO_3^-) in liquid phase (Chapter 4). I found that the H_2:IC ratio was the key factor to control the overall production rate of organic compounds and their length. A low H_2:IC ratio (< 2 mol H_2/mol C) increased productivity of acetate, but a high H_2:IC ratio (> 2

mol H_2/mol C) led to chain elongation of carboxylates up to 8 carbons and alcohols up to four carbons.

Giving the importance of the membrane in the system, I partnered with the Georgia Institute of Technology, who synthetized a novel asymmetric membrane that dramatically improved mass transfer rates. Comparing the performance of the best asymmetric membrane for syngas fermentation with a commercial symmetric membrane (Chapter 5), I found that the novel asymmetric membrane far surpassed the commercial symmetric membrane for mass-transfer kinetics, by at least two orders of magnitude for all syngas components. Additionally, the low selectivity of our Matrimid® between syngas components, makes the fiber ideal for biological processes such as syngas fermentation.

I next compared the membranes' performance in biotic experiments using MBfRs using a synthetic syngas feed with the asymmetric and symmetric membranes (Chapter 6). The high permeance of the asymmetric membrane enabled high productivity of C1-C2 products, and I achieved a production rate by area of 253 $g.m^{-2}.d^{-1}$ for acetate, the highest reported to date. Similar to the H_2-based MBfR, I found that the key parameter is the H_2:C ratio. Since the membrane delivered both H_2 and C, selectivity drives the type of carboxylates and alcohols produced, and the low selectivity of the asymmetric membrane favored acetogenesis over microbial chain elongation.

I partnered with Robert Stirling to create a techno-economic analysis (Chapter 6) of the MBfR using my achieved rate from Chapter 5. My findings, based solely of producing acetate, were that the MBfR system should be profitable, since the market

price of acetate is $745, while the production cost was estimated at $716. A sensitivity analysis showed that the most important parameter affecting cost was the areal production rate in the MBfR. Therefore, efforts should be focused on increasing it. Another major cost factor in the TEA was the separation process, emphasizing the importance to look for alternatives to avoid its high costs.

My dissertation involved several innovations that lead to better understanding of syngas fermentation: I performed the first bibliometric analysis in the field, I ran the first pure-H_2 autotrophic reactor for production of carboxylic acids and alcohols, I evaluated a novel asymmetric fiber with very high permeance, I obtained the highest production rate by area in a syngas-fermenting MBfR, and I enabled the first TEA for syngas fermentation using an MBfR. These innovations offer promise for making syngas fermentation technically and economically feasible as a means to displace the Fischer-Tropsch process.

CHAPTER 9

FUTURE WORK

The variety of feedstock able to produce syngas has several advantages in terms of carbon recovery and minimizing greenhouse-gas emissions. However, the wide range of sources also makes syngas composition quite variable. As I demonstrated here, the H_2:C ratio is a key factor in the process; consequently, syngas composition should have a strong impact on operating conditions and performance. Therefore, I suggest exploring syngas fermentation in MBfRs using a wide range of syngas compositions.

My syngas MBfR experiments were operated with open-end membranes to avoid changes in composition inside the membrane. However, open-end operation could waste syngas. Closed-end or restricted-end operation minimizes loss of syngas, but it also can lead to changes in gas composition in the membrane lumen, particularly when membrane selectivity among components is high. I suggest addressing this issue by investigating techniques such as gas recirculation or periodic flushing to reduce wasting syngas.

The TEA concluded that the areal production rate is the most important factor to improve for a better cost-effectiveness of the syngas-based MBfR. I explored new asymmetric membranes, which offer great promise. The “other side of the coin” is improving microbial kinetics could further improve production rate, such as by using higher temperature. I suggest enriching for microorganisms that produce carboxylates and alcohols at high temperatures. Thermophilic and hyper-thermophilic bacteria are prime candidates.

The syngas-based MBfR has documented potential to create carboxylates and alcohols up to eight carbons, which have higher economic value and are easier to separate. While some researchers have explored several operational parameters, the result is usually a mixture of several products, making separation hard, even with long products. I suggest a systematic study of how to select a specific long product in the syngas-based MBfR.

Finally, I suggest integrating the syngas-based MBfR with the generation of the syngas. An especially promising partnership is with solar-thermal production of syngas from reduction of CO_2 and H_2O. On the one hand, solar-thermal production offers the possibility for tailoring the syngas composition to optimize the performance of the MBfR. On the other hand, using atmospheric CO_2 and solar energy is a means to totally replace fossil feedstock for fuels and chemicals.

REFERENCES

AACE®, 2018. Skills and knowledge of cost engineering, Sixth Edit. ed. AACE International.

Abatzoglou, N., Fauteux-Lefebvre, C., 2016. Review of catalytic syngas production through steam or dry reforming and partial oxidation of studied liquid compounds. Wiley Interdiscip. Rev. Energy Environ. 5, 169–187. https://doi.org/10.1002/wene.167

Abubackar, H.N., Bengelsdorf, F.R., Dürre, P., Veiga, M.C., Kennes, C., 2016. Improved operating strategy for continuous fermentation of carbon monoxide to fuel-ethanol by clostridia. Appl. Energy 169, 210–217. https://doi.org/10.1016/j.apenergy.2016.02.021

Abubackar, H.N., Veiga, M.C., Kennes, C., 2015. Carbon monoxide fermentation to ethanol by *Clostridium autoethanogenum* in a bioreactor with no accumulation of acetic acid. Bioresour. Technol. 186, 122–127. https://doi.org/10.1016/j.biortech.2015.02.113

Abubackar, H.N., Veiga, M.C., Kennes, C., 2012. Biological conversion of carbon monoxide to ethanol: Effect of pH, gas pressure, reducing agent and yeast extract. Bioresour. Technol. 114, 518–522. https://doi.org/10.1016/j.biortech.2012.03.027

Aghapour Aktij, S., Zirehpour, A., Mollahosseini, A., Taherzadeh, M.J., Tiraferri, A., Rahimpour, A., 2020. Feasibility of membrane processes for the recovery and purification of bio-based volatile fatty acids: A comprehensive review. J. Ind. Eng. Chem. 81, 24–40. https://doi.org/10.1016/j.jiec.2019.09.009

Aghazadeh, M., Ladisch, M.R., Engelberth, A.S., 2016. Acetic acid removal from corn stover hydrolysate using ethyl acetate and the impact on *Saccharomyces cerevisiae* bioethanol fermentation. Biotechnol. Prog. 32, 929–937. https://doi.org/10.1002/btpr.2282

Agler, M.T., Spirito, C.M., Usack, J.G., Werner, J.J., Angenent, L.T., 2012. Chain elongation with reactor microbiomes: upgrading dilute ethanol to medium-chain carboxylates. Energy Environ. Sci. 5, 8189. https://doi.org/10.1039/c2ee22101b

Agler, M.T., Wrenn, B.A., Zinder, S.H., Angenent, L.T., 2011. Waste to bioproduct conversion with undefined mixed cultures: The carboxylate platform. Trends Biotechnol. 29, 70–78. https://doi.org/10.1016/j.tibtech.2010.11.006

Agrafiotis, C., Roeb, M., Sattler, C., 2015. A review on solar thermal syngas production via redox pair-based water/carbon dioxide splitting thermochemical cycles. Renew.

Sustain. Energy Rev. 42, 254–285. https://doi.org/10.1016/j.rser.2014.09.039

Agrafiotis, C., Von Storch, H., Roeb, M., Sattler, C., 2014. Solar thermal reforming of methane feedstocks for hydrogen and syngas production - A review. Renew. Sustain. Energy Rev. 29, 656–682. https://doi.org/10.1016/j.rser.2013.08.050

Ahmed, A., Lewis, R.S., 2007. Fermentation of Biomass-Generated Synthesis Gas: Effects of Nitric Oxide. Biotechnol. Bioeng. 97, 1080–1086. https://doi.org/https://doi.org/10.1002/bit.21305

Ahn, C.H., Oh, H., Ki, D., Van Ginkel, S.W., Rittmann, B.E., Park, J., 2009. Bacterial biofilm-community selection during autohydrogenotrophic reduction of nitrate and perchlorate in ion-exchange brine. Appl. Microbiol. Biotechnol. 81, 1169–1177. https://doi.org/10.1007/s00253-008-1797-3

Alonso, D.M., Bond, J.Q., Dumesic, J.A., 2010. Catalytic conversion of biomass to biofuels. Green Chem. 12, 1493–1513. https://doi.org/10.1039/c004654j

Alves, J.I., Stams, A.J.M., Plugge, C.M., Madalena Alves, M., Sousa, D.Z., 2013. Enrichment of anaerobic syngas-converting bacteria from thermophilic bioreactor sludge. FEMS Microbiol. Ecol. 86, 590–597. https://doi.org/10.1111/1574-6941.12185

Andrei, V., Reuillard, B., Reisner, E., 2020. Bias-free solar syngas production by integrating a molecular cobalt catalyst with perovskite–BiVO4 tandems. Nat. Mater. 19, 189–194. https://doi.org/10.1038/s41563-019-0501-6

Angenent, L.T., Richter, H., Buckel, W., Spirito, C.M., Steinbusch, K.J.J., Plugge, C.M., Strik, D.P.B.T.B., Grootscholten, T.I.M., Buisman, C.J.N., Hamelers, H.V.M., 2016. Chain Elongation with Reactor Microbiomes: Open-Culture Biotechnology to Produce Biochemicals. Environ. Sci. Technol. 50, 2796–2810. https://doi.org/10.1021/acs.est.5b04847

Arantes, A.L., Alves, J.I., Stams, A.J.M., Alves, M.M., Sousa, D.Z., 2018. Enrichment of syngas-converting communities from a multi-orifice baffled bioreactor. Microb. Biotechnol. 11, 639–646. https://doi.org/10.1111/1751-7915.12864

Arantes, A.L., Moreira, J.P.C., Diender, M., Parshina, S.N., Stams, A.J.M., Alves, M.M., Alves, J.I., Sousa, D.Z., 2020. Enrichment of Anaerobic Syngas-Converting Communities and Isolation of a Novel Carboxydotrophic *Acetobacterium wieringae* Strain JM. Front. Microbiol. 11. https://doi.org/10.3389/fmicb.2020.00058

Arantes, V., Saddler, J.N., 2010. Access to cellulose limits the efficiency of enzymatic hydrolysis: The role of amorphogenesis. Biotechnol. Biofuels 3, 1–11. https://doi.org/10.1186/1754-6834-3-4

Aria, M., Cuccurullo, C., 2017. bibliometrix: An R-tool for comprehensive science mapping analysis. J. Informetr. 11, 959–975. https://doi.org/10.1016/j.joi.2017.08.007

Arslan, D., Steinbusch, K.J.J., Diels, L., De Wever, H., Buisman, C.J.N., Hamelers, H.V.M., 2012. Effect of hydrogen and carbon dioxide on carboxylic acids patterns in mixed culture fermentation. Bioresour. Technol. 118, 227–234. https://doi.org/10.1016/j.biortech.2012.05.003

Arslan, K., Bayar, B., Nalakath Abubackar, H., Veiga, M.C., Kennes, C., 2019. Solventogenesis in *Clostridium aceticum* producing high concentrations of ethanol from syngas. Bioresour. Technol. 292. https://doi.org/10.1016/j.biortech.2019.121941

Asimakopoulos, K., Gavala, H.N., Skiadas, I. V, 2018. Reactor systems for syngas fermentation processes: A review. Chem. Eng. J. https://doi.org/10.1016/j.cej.2018.05.003

Atasoy, M., Owusu-Agyeman, I., Plaza, E., Cetecioglu, Z., 2018. Bio-based volatile fatty acid production and recovery from waste streams: Current status and future challenges. Bioresour. Technol. 268, 773–786. https://doi.org/10.1016/j.biortech.2018.07.042

Bachirou, G.L., Shuai, Y., Zhang, J., Huang, X., Yuan, Y., Tan, H., 2016. Syngas production by simultaneous splitting of H_2O and CO_2 via iron oxide (Fe_3O_4

) redox reactions under high-pressure. Int. J. Hydrogen Energy 41, 19936–19946. https://doi.org/10.1016/j.ijhydene.2016.09.053

Bai, W., 2010. Experimental and numerical investigation of bubble column reactors.

Balch, W.E., schoberth, S., Tanner, R.S., Wolfe, R.S., 1977. *Acetobacterium*, a new genus of hydrogen-oxidizing, carbon dioxide-reducing, anaerobic bacteria. Int. J. Syst. Bacteriol. 27, 355–361. https://doi.org/10.1099/00207713-27-4-355

Banerjee, A., Leang, C., Ueki, T., Nevin, K.P., Lovley, D.R., 2014. Lactose-inducible system for metabolic engineering of *Clostridium ljungdahlii*. Appl. Environ. Microbiol. 80, 2410–2416. https://doi.org/10.1128/AEM.03666-13

Bengelsdorf, F.R., Straub, M., Dürre, P., 2013. Bacterial synthesis gas (syngas) fermentation. Environ. Technol. (United Kingdom) 34, 1639–1651. https://doi.org/10.1080/09593330.2013.827747

Bertsch, J., Müller, V., 2015. Bioenergetic constraints for conversion of syngas to biofuels in acetogenic bacteria. Biotechnol. Biofuels 8, 1–12. https://doi.org/10.1186/s13068-015-0393-x

Berzin, Vel, Kiriukhin, M., Tyurin, M., 2012. Elimination of acetate production to improve ethanol yield during continuous synthesis gas fermentation by engineered biocatalyst *Clostridium* sp. MTEtOH550. Appl. Biochem. Biotechnol. 167, 338–347. https://doi.org/10.1007/s12010-012-9697-5

Berzin, V., Kiriukhin, M., Tyurin, M., 2012. Selective production of acetone during continuous synthesis gas fermentation by engineered biocatalyst *Clostridium* sp. MAceT113. Lett. Appl. Microbiol. 55, 149–154. https://doi.org/10.1111/j.1472-765X.2012.03272.x

Berzin, V., Tyurin, M., Kiriukhin, M., 2013. Selective n-Butanol Production by *Clostridium* sp. MTButOH1365 During Continuous Synthesis Gas Fermentation Due to Expression of Synthetic Thiolase, 3-Hydroxy Butyryl-CoA Dehydrogenase, Crotonase, Butyryl-CoA Dehydrogenase, Butyraldehyde Dehydrogenase, and. Appl. Biochem. Biotechnol. 169, 950–959. https://doi.org/10.1007/s12010-012-0060-7

Blondel, V.D., Guillaume, J.L., Lambiotte, R., Lefebvre, E., 2008. Fast unfolding of communities in large networks. J. Stat. Mech. Theory Exp. 2008, 0–12. https://doi.org/10.1088/1742-5468/2008/10/P10008

Bolyen, E., Rideout, J.R., Dillon, M.R., Bokulich, N.A., Abnet, C.C., Al-Ghalith, G.A., Alexander, H., Alm, E.J., Arumugam, M., Asnicar, F., Bai, Y., Bisanz, J.E., Bittinger, K., Brejnrod, A., Brislawn, C.J., Brown, C.T., Callahan, B.J., Caraballo-Rodríguez, A.M., Chase, J., Cope, E.K., Da Silva, R., Diener, C., Dorrestein, P.C., Douglas, G.M., Durall, D.M., Duvallet, C., Edwardson, C.F., Ernst, M., Estaki, M., Fouquier, J., Gauglitz, J.M., Gibbons, S.M., Gibson, D.L., Gonzalez, A., Gorlick, K., Guo, J., Hillmann, B., Holmes, S., Holste, H., Huttenhower, C., Huttley, G.A., Janssen, S., Jarmusch, A.K., Jiang, L., Kaehler, B.D., Kang, K. Bin, Keefe, C.R., Keim, P., Kelley, S.T., Knights, D., Koester, I., Kosciolek, T., Kreps, J., Langille, M.G.I., Lee, J., Ley, R., Liu, Y.-X., Loftfield, E., Lozupone, C., Maher, M., Marotz, C., Martin, B.D., McDonald, D., McIver, L.J., Melnik, A. V., Metcalf, J.L., Morgan, S.C., Morton, J.T., Naimey, A.T., Navas-Molina, J.A., Nothias, L.F., Orchanian, S.B., Pearson, T., Peoples, S.L., Petras, D., Preuss, M.L., Pruesse, E., Rasmussen, L.B., Rivers, A., Robeson, M.S., Rosenthal, P., Segata, N., Shaffer, M., Shiffer, A., Sinha, R., Song, S.J., Spear, J.R., Swafford, A.D., Thompson, L.R., Torres, P.J., Trinh, P., Tripathi, A., Turnbaugh, P.J., Ul-Hasan, S., van der Hooft, J.J.J., Vargas, F., Vázquez-Baeza, Y., Vogtmann, E., von Hippel, M., Walters, W., Wan, Y., Wang, M., Warren, J., Weber, K.C., Williamson, C.H.D., Willis, A.D., Xu, Z.Z., Zaneveld, J.R., Zhang, Y., Zhu, Q., Knight, R., Caporaso, J.G., 2019. Reproducible, interactive, scalable and extensible microbiome data science using QIIME 2. Nat. Biotechnol. 37, 852–857. https://doi.org/10.1038/s41587-019-0209-9

Bredwell, M.D., Srivastava, P., Worden, R.M., 1999. Reactor design issues for synthesis-gas fermentations. Biotechnol. Prog. 15, 834–844. https://doi.org/10.1021/bp990108m

Calvo, D.C., Ontiveros-Valencia, A., Krajmalnik-Brown, R., Torres, C.I., Rittmann, B.E., 2021. Carboxylates and alcohols production in an autotrophic hydrogen-based membrane biofilm reactor. Biotechnol. Bioeng. https://doi.org/10.1002/bit.27745

Candry, P., Ganigué, R., 2021. Chain elongators, friends, and foes. Curr. Opin. Biotechnol. 67, 99–110. https://doi.org/10.1016/j.copbio.2021.01.005

Candry, P., Huang, S., Carvajal-Arroyo, J.M., Rabaey, K., Ganigue, R., 2020. Enrichment and characterisation of ethanol chain elongating communities from natural and engineered environments. Sci. Rep. 10, 1–10. https://doi.org/10.1038/s41598-020-60052-z

Caporaso, J.G., Lauber, C.L., Walters, W. a, Berg-Lyons, D., Huntley, J., Fierer, N., Owens, S.M., Betley, J., Fraser, L., Bauer, M., Gormley, N., Gilbert, J. a, Smith, G., Knight, R., 2012. 1. Caporaso JG, Lauber CL, Walters W a, et al. Ultra-high-throughput microbial community analysis on the Illumina HiSeq and MiSeq platforms. ISME J 2012; 6: 1621–4.Ultra-high-throughput microbial community analysis on the Illumina HiSeq and MiSeq platform. ISME J. 6, 1621–1624. https://doi.org/10.1038/ismej.2012.8

Caporaso, J.G., Lauber, C.L., Walters, W.A., Berg-Lyons, D., Lozupone, C.A., Turnbaugh, P.J., Fierer, N., Knight, R., 2011. Global patterns of 16S rRNA diversity at a depth of millions of sequences per sample. Proc. Natl. Acad. Sci. U. S. A. 108, 4516–4522. https://doi.org/10.1073/pnas.1000080107

Cavalcante, W. de A., Leitão, R.C., Gehring, T.A., Angenent, L.T., Santaella, S.T., 2017. Anaerobic fermentation for n-caproic acid production: A review. Process Biochem. 54, 106–119. https://doi.org/10.1016/j.procbio.2016.12.024

Chemical Engineering Plant Cost Index, 2021. Chem. Eng. 128, 48.

Chen, H., Jiang, W., Yang, Yu, Yang, Yan, Man, X., 2017. State of the art on food waste research: a bibliometrics study from 1997 to 2014. J. Clean. Prod. 140, 840–846. https://doi.org/10.1016/j.jclepro.2015.11.085

Chen, J., Daniell, J., Griffin, D., Li, X., Henson, M.A., 2018. Experimental testing of a spatiotemporal metabolic model for carbon monoxide fermentation with *Clostridium autoethanogenum*. Biochem. Eng. J. 129, 64–73. https://doi.org/10.1016/j.bej.2017.10.018

Chen, J., Gomez, J.A., Höffner, K., Barton, P.I., Henson, M.A., 2015. Metabolic modeling of synthesis gas fermentation in bubble column reactors. Biotechnol. Biofuels 8, 1–12. https://doi.org/10.1186/s13068-015-0272-5

Chen, J., Henson, M.A., 2016. In silico metabolic engineering of *Clostridium ljungdahlii* for synthesis gas fermentation. Metab. Eng. 38, 389–400.

https://doi.org/10.1016/j.ymben.2016.10.002

Chen, X., Ni, B.J., 2016. Anaerobic conversion of hydrogen and carbon dioxide to fatty acids production in a membrane biofilm reactor: A modeling approach. Chem. Eng. J. 306, 1092–1098. https://doi.org/10.1016/j.cej.2016.08.049

Chien, I.L., Zeng, K.L., Chao, H.Y., Liu, J.H., 2004. Design and control of acetic acid dehydration system via heterogeneous azeotropic distillation. Chem. Eng. Sci. 59, 4547–4567. https://doi.org/10.1016/j.ces.2004.06.041

Choerudin, C., Arrahmah, F.I., Daniel, J.K., Watari, T., Yamaguchi, T., Setiadi, T., 2021. Evaluation of combined anaerobic membrane bioreactor and downflow hanging sponge reactor for treatment of synthetic textile wastewater. J. Environ. Chem. Eng. 9, 105276. https://doi.org/10.1016/j.jece.2021.105276

Chu, F., Yang, L., Du, X., Yang, Y., 2017. Mass transfer and energy consumption for CO_2 absorption by ammonia solution in bubble column. Appl. Energy 190, 1068–1080. https://doi.org/10.1016/j.apenergy.2017.01.027

Chung, J., Ahn, C.H., Chen, Z., Rittmann, B.E., 2008. Bio-reduction of N-nitrosodimethylamine (NDMA) using a hydrogen-based membrane biofilm reactor. Chemosphere 70, 516–520. https://doi.org/10.1016/j.chemosphere.2007.07.016

Chung, J., Nerenberg, R., Rittmann, B.E., 2007a. Evaluation for Biological Reduction of Nitrate and Perchlorate in Brine Water Using the Hydrogen-Based Membrane Biofilm Reactor. J. Environ. Eng. 133, 157–164. https://doi.org/10.1061/(asce)0733-9372(2007)133:2(157)

Chung, J., Rittmann, B.E., Wright, W.F., Bowman, R.H., 2007b. Simultaneous bio-reduction of nitrate, perchlorate, selenate, chromate, arsenate, and dibromochloropropane using a hydrogen-based membrane biofilm reactor. Biodegradation 18, 199–209. https://doi.org/10.1007/s10532-006-9055-9

Chung, J., Ryu, H., Abbaszadegan, M., Rittmann, B.E., 2006. Community structure and function in a H_2-based membrane biofilm reactor capable of bioreduction of selenate and chromate. Appl. Microbiol. Biotechnol. 72, 1330–1339. https://doi.org/10.1007/s00253-006-0439-x

Coma, M., Vilchez-Vargas, R., Roume, H., Jauregui, R., Pieper, D.H., Rabaey, K., 2016. Product Diversity Linked to Substrate Usage in Chain Elongation by Mixed-Culture Fermentation. Environ. Sci. Technol. 50, 6467–6476. https://doi.org/10.1021/acs.est.5b06021

Daniell, J., Köpke, M., Simpson, S.D., 2012. Commercial biomass syngas fermentation, Energies. https://doi.org/10.3390/en5125372

De Klerk, A., 2012. Fischer-Tropsch Refining. John Wiley & Sons.

De Luna, P., Hahn, C., Higgins, D., Jaffer, S.A., Jaramillo, T.F., Sargent, E.H., 2019. What would it take for renewably powered electrosynthesis to displace petrochemical processes? Science (80-.). 364. https://doi.org/10.1126/science.aav3506

de Medeiros, E.M., Noorman, H., Maciel Filho, R., Posada, J.A., 2020. Production of ethanol fuel via syngas fermentation: Optimization of economic performance and energy efficiency. Chem. Eng. Sci. X 5, 100056. https://doi.org/10.1016/j.cesx.2020.100056

Delgado, A.G., Parameswaran, P., Fajardo-Williams, D., Halden, R.U., Krajmalnik-Brown, R., 2012. Role of bicarbonate as a pH buffer and electron sink in microbial dechlorination of chloroethenes. Microb. Cell Fact. 11. https://doi.org/10.1186/1475-2859-11-128

Devarapalli, M., Atiyeh, H.K., Phillips, J.R., Lewis, R.S., Huhnke, R.L., 2016. Ethanol production during semi-continuous syngas fermentation in a trickle bed reactor using *Clostridium ragsdalei*. Bioresour. Technol. 209, 56–65. https://doi.org/10.1016/j.biortech.2016.02.086

Devarapalli, M., Lewis, R.S., Atiyeh, H.K., 2017. Continuous ethanol production from synthesis gas by *Clostridium ragsdalei* in a trickle-bed reactor. Fermentation 3, 1–13. https://doi.org/10.3390/fermentation3020023

Devi, A., Niazi, A., Ramteke, M., Upadhyayula, S., 2021. Techno-economic analysis of ethanol production from lignocellulosic biomass–a comparison of fermentation, thermo catalytic, and chemocatalytic technologies. Bioprocess Biosyst. Eng. https://doi.org/10.1007/s00449-020-02504-4

Diekert, G., Wohlfarth, G., 1994. Metabolism of homoacetogens. Antonie Van Leeuwenhoek 66, 209–221. https://doi.org/10.1007/BF00871640

Diender, M., Stams, A.J.M., Sousa, D.Z., 2016. Production of medium-chain fatty acids and higher alcohols by a synthetic co-culture grown on carbon monoxide or syngas. Biotechnol. Biofuels 9, 1–11. https://doi.org/10.1186/s13068-016-0495-0

Doran, P.M., 2013. Reactor Engineering. Bioprocess Eng. Princ. 761–852. https://doi.org/10.1016/b978-0-12-220851-5.00014-9

Drake, H.L., Daniel, S.L., Küsel, K., Matthies, C., Kuhner, C., Braus-Stromeyer, S., 1997. Acetogenic bacteria: What are the in situ consequences of their diverse metabolic versatilities. BioFactors 6, 13–24. https://doi.org/10.1002/biof.5520060103

Drake, H.L., Gößner, A.S., Daniel, S.L., 2008. Old acetogens, new light. Ann. N. Y. Acad. Sci. 1125, 100–128. https://doi.org/10.1196/annals.1419.016

Drzyzga, O., Revelles, O., Durante-Rodríguez, G., Díaz, E., García, J.L., Prieto, A., 2015. New challenges for syngas fermentation: Towards production of biopolymers. J. Chem. Technol. Biotechnol. 90, 1735–1751. https://doi.org/10.1002/jctb.4721

Duyar, A., Ciftcioglu, V., Cirik, K., Civelekoglu, G., Uruş, S., 2021. Treatment of landfill leachate using single-stage anoxic moving bed biofilm reactor and aerobic membrane reactor. Sci. Total Environ. 776. https://doi.org/10.1016/j.scitotenv.2021.145919

El-Nagar, R.A., Ghanem, A.A., 2019. Syngas Production, Properties, and Its Importance. IntechOpen 1–8.

Ereña, J., 2020. Catalysts for syngas production. Catalysts 10, 1–3. https://doi.org/10.3390/catal10060657

Ermanoski, I., Siegel, N.P., Stechel, E.B., 2013. A new reactor concept for efficient solar-thermochemical fuel production. J. Sol. Energy Eng. Trans. ASME 135, 1–10. https://doi.org/10.1115/1.4023356

Esquivel-Elizondo, S., Delgado, A.G., Rittmann, B.E., Krajmalnik-Brown, R., 2017. The effects of CO_2 and H_2 on CO metabolism by pure and mixed microbial cultures. Biotechnol. Biofuels 10, 1–13. https://doi.org/10.1186/s13068-017-0910-1

Esquivel-Elizondo, S., Miceli, J., Torres, C.I., Krajmalnik-Brown, R., 2018. Impact of carbon monoxide partial pressures on methanogenesis and medium chain fatty acids production during ethanol fermentation. Biotechnol. Bioeng. 115, 341–350. https://doi.org/10.1002/bit.26471

Evans, P., Smith, J., Singh, T., Hyung, H., Arucan, C., Berokoff, D., Friese, D., Overstreet, R., Vigo, R., Rittmann, B., Ontiveros-valencia, A., Zhao, H., Tang, Y., Kim, B., Ginkel, V., Krajmalnik-brown, R., Leeson, A., St, N.S., 2013. Nitrate and Perchlorate Destruction and Potable Water Production Using Membrane Biofilm Reduction Environmental Security Technology Certification Program.

Falter, C.P., Pitz-Paal, R., 2018. Modeling counter-flow particle heat exchangers for two-step solar thermochemical syngas production. Appl. Therm. Eng. 132, 613–623. https://doi.org/10.1016/j.applthermaleng.2017.12.087

Fernández-Naveira, Á., Abubackar, H.N., Veiga, M.C., Kennes, C., 2016. Carbon monoxide bioconversion to butanol-ethanol by *Clostridium carboxidivorans*: kinetics and toxicity of alcohols. Appl. Microbiol. Biotechnol. 100, 4231–4240. https://doi.org/10.1007/s00253-016-7389-8

Fernández-Naveira, Á., Veiga, M.C., Kennes, C., 2019. Selective anaerobic fermentation of syngas into either C2-C6 organic acids or ethanol and higher alcohols. Bioresour. Technol. 280, 387–395. https://doi.org/10.1016/j.biortech.2019.02.018

Frilund, C., Tuomi, S., Kurkela, E., Simell, P., 2021. Small- to medium-scale deep syngas purification: Biomass-to-liquids multi-contaminant removal demonstration. Biomass and Bioenergy 148, 106031. https://doi.org/10.1016/j.biombioe.2021.106031

Fuchs, G., 1986. CO_2 fixation in acetogenic bacteria: Variations on a theme. FEMS Microbiol. Lett. 39, 181–213. https://doi.org/10.1016/0378-1097(86)90446-5

George Hayden, J., O'Connell, J.P., 1975. A Generalized Method for Predicting Second Virial Coefficients. Ind. Eng. Chem. Process Des. Dev. https://doi.org/10.1021/i260055a003

Gildemyn, S., Molitor, B., Usack, J.G., Nguyen, M., Rabaey, K., Angenent, L.T., 2017. Upgrading syngas fermentation effluent using *Clostridium kluyveri* in a continuous fermentation. Biotechnol. Biofuels. https://doi.org/10.1186/s13068-017-0764-6

Groher, A., Weuster-Botz, D., 2016. Comparative reaction engineering analysis of different acetogenic bacteria for gas fermentation. J. Biotechnol. 228, 82–94. https://doi.org/10.1016/j.jbiotec.2016.04.032

Grootscholten, T. I M, Kinsky dal Borgo, F., Hamelers, H.V.M., Buisman, C.J.N., 2013. Promoting chain elongation in mixed culture acidification reactors by addition of ethanol. Biomass and Bioenergy 48, 10–16. https://doi.org/10.1016/j.biombioe.2012.11.019

Grootscholten, T. I.M., Steinbusch, K.J.J., Hamelers, H.V.M., Buisman, C.J.N., 2013a. Improving medium chain fatty acid productivity using chain elongation by reducing the hydraulic retention time in an upflow anaerobic filter. Bioresour. Technol. 136, 735–738. https://doi.org/10.1016/j.biortech.2013.02.114

Grootscholten, T. I.M., Steinbusch, K.J.J., Hamelers, H.V.M., Buisman, C.J.N., 2013b. Chain elongation of acetate and ethanol in an upflow anaerobic filter for high rate MCFA production. Bioresour. Technol. 135, 440–445. https://doi.org/10.1016/j.biortech.2012.10.165

Guerrero, F., Espinoza, L., Ripoll, N., Lisbona, P., Arauzo, I., Toledo, M., 2020. Syngas Production From the Reforming of Typical Biogas Compositions in an Inert Porous Media Reactor. Front. Chem. 8, 1–12. https://doi.org/10.3389/fchem.2020.00145

Haas, T., Krause, R., Weber, R., Demler, M., Schmid, G., 2018. Technical photosynthesis involving CO_2 electrolysis and fermentation. Nat. Catal. 1, 32–39. https://doi.org/10.1038/s41929-017-0005-1

Haddad, M., Cimpoia, R., Guiot, S.R., 2014. Performance of Carboxydothermus hydrogenoformans in a gas-lift reactor for syngas upgrading into hydrogen. Int. J. Hydrogen Energy 39, 2543–2548. https://doi.org/10.1016/j.ijhydene.2013.12.022

Han, W., He, P., Shao, L., Lü, F., 2018. Metabolic interactions of a chain elongation microbiome. Appl. Environ. Microbiol. 84, 1–16. https://doi.org/10.1128/AEM.01614-18

He, M., Xiao, B., Liu, S., Hu, Z., Guo, X., Luo, S., Yang, F., 2010. Syngas production from pyrolysis of municipal solid waste (MSW) with dolomite as downstream catalysts. J. Anal. Appl. Pyrolysis 87, 181–187. https://doi.org/10.1016/j.jaap.2009.11.005

Henstra, A.M., Sipma, J., Rinzema, A., Stams, A.J., 2007. Microbiology of synthesis gas fermentation for biofuel production. Curr. Opin. Biotechnol. 18, 200–206. https://doi.org/10.1016/j.copbio.2007.03.008

Hew, J.J., 2017. Hall of fame for mobile commerce and its applications: A bibliometric evaluation of a decade and a half (2000-2015). Telemat. Informatics 34, 43–66. https://doi.org/10.1016/j.tele.2016.04.003

Huang, L., Zhou, M., Lv, J., Chen, K., 2020. Trends in global research in forest carbon sequestration: A bibliometric analysis. J. Clean. Prod. 252, 119908. https://doi.org/10.1016/j.jclepro.2019.119908

Hurst, K.M., Lewis, R.S., 2010. Carbon monoxide partial pressure effects on the metabolic process of syngas fermentation. Biochem. Eng. J. 48, 159–165. https://doi.org/10.1016/j.bej.2009.09.004

Jang, N., Yasin, M., Kang, H., Lee, Y., Park, G.W., Park, S., Chang, I.S., 2018. Bubble coalescence suppression driven carbon monoxide (CO)-water mass transfer increase by electrolyte addition in a hollow fiber membrane bioreactor (HFMBR) for microbial CO conversion to ethanol. Bioresour. Technol. 263, 375–384. https://doi.org/10.1016/j.biortech.2018.05.012

Jang, Y.S., Malaviya, A., Cho, C., Lee, J., Lee, S.Y., 2012. Butanol production from renewable biomass by clostridia. Bioresour. Technol. 123, 653–663. https://doi.org/10.1016/j.biortech.2012.07.104

Joshi, S., Robles, A., Aguiar, S., Delgado, A.G., 2021. The occurrence and ecology of microbial chain elongation of carboxylates in soils. ISME J. https://doi.org/10.1038/s41396-021-00893-2

Kantzow, C., Mayer, A., Weuster-Botz, D., 2015. Continuous gas fermentation by *Acetobacterium woodii* in a submerged membrane reactor with full cell retention. J. Biotechnol. 212, 11–18. https://doi.org/10.1016/j.jbiotec.2015.07.020

Karatzos, S., van Dyk, J.S., McMillan, J.D., Saddler, J., 2017. Drop-in biofuel production via conventional (lipid/fatty acid) and advanced (biomass) routes. Part I. Biofuels, Bioprod. Biorefining 11, 344–362. https://doi.org/DOI: 10.1002/bbb.1746

Kelley, L., 2018. Chemical profile: US acetic acid [WWW Document]. Indep. Commod. Intell. Serv. URL https://www.icis.com/explore/resources/news/2018/11/30/10288632/chemical-profile-us-acetic-acid/

Khan, M.A., Adewuyi, Y.G., 2019. Techno-economic modeling and optimization of catalytic reactive distillation for the esterification reactions in bio-oil upgradation. Chem. Eng. Res. Des. 148, 86–101. https://doi.org/10.1016/j.cherd.2019.05.037

Kim, Y.K., Park, S.E., Lee, H., Yun, J.Y., 2014. Enhancement of bioethanol production in syngas fermentation with *Clostridium ljungdahlii* using nanoparticles. Bioresour. Technol. 159, 446–450. https://doi.org/10.1016/j.biortech.2014.03.046

Klasson, K.T., Ackerson, M.D., Clausen, E.C., Gaddy, J.L., 1993. Biological conversion of coal and coal-derived synthesis gas. Fuel 72, 1673–1678. https://doi.org/10.1016/0016-2361(93)90354-5

Köpke, M., Held, C., Hujer, S., Liesegang, H., Wiezer, A., Wollherr, A., Ehrenreich, A., Liebl, W., Gottschalk, G., Dürre, P., 2010. *Clostridium ljungdahlii* represents a microbial production platform based on syngas. Proc. Natl. Acad. Sci. U. S. A. 107, 13087–13092. https://doi.org/10.1073/pnas.1004716107

Kosuri, M.R., Koros, W.J., 2008. Defect-free asymmetric hollow fiber membranes from Torlon®, a polyamide-imide polymer, for high-pressure CO_2 separations. J. Memb. Sci. 320, 65–72. https://doi.org/10.1016/j.memsci.2008.03.062

Kucek, L.A., Spirito, C.M., Angenent, L.T., 2016. High n-caprylate productivities and specificities from dilute ethanol and acetate: Chain elongation with microbiomes to upgrade products from syngas fermentation. Energy Environ. Sci. 9, 3482–3494. https://doi.org/10.1039/c6ee01487a

Kurucz, A., Bencik, I. (Eds.), 2009. Syngas : Production Methods, Post Treatment and Economics, Environmen. ed. Nova Science Publishers, Incorporated, New York, USA.

Lagoa-Costa, B., Abubackar, H.N., Fernández-Romasanta, M., Kennes, C., Veiga, M.C., 2017. Integrated bioconversion of syngas into bioethanol and biopolymers. Bioresour. Technol. 239, 244–249. https://doi.org/10.1016/j.biortech.2017.05.019

Lai, C.Y., Wen, L.L., Zhang, Y., Luo, S.S., Wang, Q.Y., Luo, Y.H., Chen, R., Yang, X., Rittmann, B.E., Zhao, H.P., 2016. Autotrophic antimonate bio-reduction using hydrogen as the electron donor. Water Res. 88, 467–474.

https://doi.org/10.1016/j.watres.2015.10.042

Lan, E.I., Liao, J.C., 2013. Microbial synthesis of n-butanol, isobutanol, and other higher alcohols from diverse resources. Bioresour. Technol. 135, 339–349. https://doi.org/10.1016/j.biortech.2012.09.104

Latif, H., Zeidan, A.A., Nielsen, A.T., Zengler, K., 2014. Trash to treasure: Production of biofuels and commodity chemicals via syngas fermenting microorganisms. Curr. Opin. Biotechnol. 27, 79–87. https://doi.org/10.1016/j.copbio.2013.12.001

Lee, E.J., Kim, Y.H., 2018. Energy saving in acetic acid process using an azeotropic distillation column with a side stripper. Chem. Eng. Commun. 205, 1311–1322. https://doi.org/10.1080/00986445.2018.1446426

Lee, K.-C., Rittmann, B.E., 2000. A novel hollow-fibre membrane biofilm reactor for autohydrogenotrophic denitrification of drinking water. Water Sci. Technol. 41, 219–226. https://doi.org/10.2166/wst.2000.0448

Lee, K.C., Rittmann, B.E., 2002. Applying a novel autohydrogenotrophic hollow-fiber membrane biofilm reactor for denitrification of drinking water. Water Res. 36, 2040–2052. https://doi.org/10.1016/S0043-1354(01)00425-0

Li, D., Hu, N., Ding, D., Li, S., Li, G., Wang, Y., 2016. An experimental study on the inhibitory effect of high concentration bicarbonate on the reduction of U(VI) in groundwater by functionalized indigenous microbial communities. J. Radioanal. Nucl. Chem. 307, 1011–1019. https://doi.org/10.1007/s10967-015-4427-4

Li, K., Chien, I., Chen, C., 2014. Design and Optimization of Acetic Acid Dehydration Processes. 5th Int. Symp. Adv. Control Ind. Process. 126–131.

Li, N., Yang, J., Chai, C., Yang, S., Jiang, W., Gu, Y., 2015. Complete genome sequence of *Clostridium carboxidivorans* P7T, a syngas-fermenting bacterium capable of producing long-chain alcohols. J. Biotechnol. 211, 44–45. https://doi.org/10.1016/j.jbiotec.2015.06.430

Liakakou, E.T., Infantes, A., Neumann, A., Vreugdenhil, B.J., 2021. Connecting gasification with syngas fermentation: Comparison of the performance of lignin and beech wood. Fuel 290, 120054. https://doi.org/10.1016/j.fuel.2020.120054

Liew, F.M., Martin, M.E., Tappel, R.C., Heijstra, B.D., Mihalcea, C., Köpke, M., 2016. Gas Fermentation-A flexible platform for commercial scale production of low-carbon-fuels and chemicals from waste and renewable feedstocks. Front. Microbiol. 7. https://doi.org/10.3389/fmicb.2016.00694

Liu, C., Dong, G., Tsuru, T., Matsuyama, H., 2020. Organic solvent reverse osmosis membranes for organic liquid mixture separation: A review. J. Memb. Sci. 118882.

https://doi.org/10.1016/j.memsci.2020.118882

Liu, K., Atiyeh, H.K., Stevenson, B.S., Tanner, R.S., Wilkins, M.R., Huhnke, R.L., 2014a. Continuous syngas fermentation for the production of ethanol, n-propanol and n-butanol. Bioresour. Technol. 151, 69–77. https://doi.org/10.1016/j.biortech.2013.10.059

Liu, K., Atiyeh, H.K., Stevenson, B.S., Tanner, R.S., Wilkins, M.R., Huhnke, R.L., 2014b. Mixed culture syngas fermentation and conversion of carboxylic acids into alcohols. Bioresour. Technol. 152, 337–346. https://doi.org/10.1016/j.biortech.2013.11.015

Liu, K., Atiyeh, H.K., Tanner, R.S., Wilkins, M.R., Huhnke, R.L., 2012. Fermentative production of ethanol from syngas using novel moderately alkaliphilic strains of Alkalibaculum bacchi. Bioresour. Technol. 104, 336–341. https://doi.org/10.1016/j.biortech.2011.10.054

López-Garzón, C.S., Straathof, A.J.J., 2014. Recovery of carboxylic acids produced by fermentation. Biotechnol. Adv. 32, 873–904. https://doi.org/10.1016/j.biotechadv.2014.04.002

Lovley, D.R., Nevin, K.P., 2013. Electrobiocommodities: Powering microbial production of fuels and commodity chemicals from carbon dioxide with electricity. Curr. Opin. Biotechnol. 24, 385–390. https://doi.org/10.1016/j.copbio.2013.02.012

Lynd, L.R., Van Zyl, W.H., McBride, J.E., Laser, M., 2005. Consolidated bioprocessing of cellulosic biomass: An update. Curr. Opin. Biotechnol. 16, 577–583. https://doi.org/10.1016/j.copbio.2005.08.009

Maddipati, P., Atiyeh, H.K., Bellmer, D.D., Huhnke, R.L., 2011. Ethanol production from syngas by *Clostridium* strain P11 using corn steep liquor as a nutrient replacement to yeast extract. Bioresour. Technol. 102, 6494–6501. https://doi.org/10.1016/j.biortech.2011.03.047

Makshina, E. V., Dusselier, M., Janssens, W., Degrève, J., Jacobs, P.A., Sels, B.F., 2014. Review of old chemistry and new catalytic advances in the on-purpose synthesis of butadiene. Chem. Soc. Rev. 43, 7917–7953. https://doi.org/10.1039/c4cs00105b

Mallawaarachchi, H., Sandanayake, Y., Karunasena, G., Liu, C., 2020. Unveiling the conceptual development of industrial symbiosis: Bibliometric analysis. J. Clean. Prod. 258, 120618. https://doi.org/10.1016/j.jclepro.2020.120618

Martin, K.J., Nerenberg, R., 2012. The membrane biofilm reactor (MBfR) for water and wastewater treatment: Principles, applications, and recent developments. Bioresour. Technol. 122, 83–94. https://doi.org/10.1016/j.biortech.2012.02.110

Martin, M.E., Richter, H., Saha, S., Angenent, L.T., 2016. Traits of selected *Clostridium* strains for syngas fermentation to ethanol. Biotechnol. Bioeng. 113, 531–539. https://doi.org/10.1002/bit.25827

Martinez-Gomez, J., Nápoles-Rivera, F., Ponce-Ortega, J.M., El-Halwagi, M.M., 2017. Optimization of the production of syngas from shale gas with economic and safety considerations. Appl. Therm. Eng. 110, 678–685. https://doi.org/10.1016/j.applthermaleng.2016.08.201

Marxer, D., Furler, P., Takacs, M., Steinfeld, A., 2017. Solar thermochemical splitting of CO_2 into separate streams of CO and O_2 with high selectivity, stability, conversion, and efficiency. Energy Environ. Sci. 10, 1142–1149. https://doi.org/10.1039/c6ee03776c

Mohammadi, M., Najafpour, G.D., Younesi, H., Lahijani, P., Uzir, M.H., Mohamed, A.R., 2011. Bioconversion of synthesis gas to second generation biofuels: A review. Renew. Sustain. Energy Rev. 15, 4255–4273. https://doi.org/10.1016/j.rser.2011.07.124

Mohammadi, M., Younesi, H., Najafpour, G., Mohamed, A.R., 2012. Sustainable ethanol fermentation from synthesis gas by *Clostridium ljungdahlii* in a continuous stirred tank bioreactor. J. Chem. Technol. Biotechnol. 87, 837–843. https://doi.org/10.1002/jctb.3712

Molino, A., Chianese, S., Musmarra, D., 2016. Biomass gasification technology: The state of the art overview. J. Energy Chem. 25, 10–25. https://doi.org/10.1016/j.jechem.2015.11.005

Molitor, B., Marcellin, E., Angenent, L.T., 2017. Overcoming the energetic limitations of syngas fermentation. Curr. Opin. Chem. Biol. 41, 84–92. https://doi.org/10.1016/j.cbpa.2017.10.003

Munasinghe, P.C., Khanal, S.K., 2012. Syngas fermentation to biofuel: Evaluation of carbon monoxide mass transfer and analytical modeling using a composite hollow fiber (CHF) membrane bioreactor. Bioresour. Technol. 122, 130–136. https://doi.org/10.1016/j.biortech.2012.03.053

Munasinghe, P.C., Khanal, S.K., 2010. Biomass-derived syngas fermentation into biofuels: Opportunities and challenges. Bioresour. Technol. 101, 5013–5022. https://doi.org/10.1016/j.biortech.2009.12.098

Murali, N., Srinivas, K., Ahring, B.K., 2017. Biochemical production and separation of carboxylic acids for biorefinery applications. Fermentation 3, 1–25. https://doi.org/10.3390/fermentation3020022

Naik, S.N., Goud, V. V., Rout, P.K., Dalai, A.K., 2010. Production of first and second

generation biofuels: A comprehensive review. Renew. Sustain. Energy Rev. 14, 578–597. https://doi.org/10.1016/j.rser.2009.10.003

Nayak, J., Pal, M., Pal, P., 2015. Modeling and simulation of direct production of acetic acid from cheese whey in a multi-stage membrane-integrated bioreactor. Biochem. Eng. J. 93, 179–195. https://doi.org/10.1016/j.bej.2014.10.002

Ontiveros-Valencia, A., Ilhan, Z.E., Kang, D.W., Rittmann, B., Krajmalnik-Brown, R., 2013. Phylogenetic analysis of nitrate- and sulfate-reducing bacteria in a hydrogen-fed biofilm. FEMS Microbiol. Ecol. 85, 158–167. https://doi.org/10.1111/1574-6941.12107

Ontiveros-Valencia, A., Tang, Y., Krajmalnik-Brown, R., Rittmann, B.E., 2014. Managing the interactions between sulfate- and perchlorate-reducing bacteria when using hydrogen-fed biofilms to treat a groundwater with a high perchlorate concentration. Water Res. 55, 215–224. https://doi.org/10.1016/j.watres.2014.02.020

Orgill, J.J., Atiyeh, H.K., Devarapalli, M., Phillips, J.R., Lewis, R.S., Huhnke, R.L., 2013. A comparison of mass transfer coefficients between trickle-bed, Hollow fiber membrane and stirred tank reactors. Bioresour. Technol. 133, 340–346. https://doi.org/10.1016/j.biortech.2013.01.124

Overett, M.J., Hill, R.O., Moss, J.R., 2000. Organometallic chemistry and surface science: Mechanistic models for the Fischer-Tropsch synthesis. Coord. Chem. Rev. 206–207, 581–605. https://doi.org/10.1016/S0010-8545(00)00249-6

Pal, P., Nayak, J., 2017. Acetic Acid Production and Purification: Critical Review Towards Process Intensification. Sep. Purif. Rev. 46, 44–61. https://doi.org/10.1080/15422119.2016.1185017

Park, S., Ahn, B., Kim, Y.-K., 2019. Growth enhancement of bioethanol-producing microbe *Clostridium autoethanogenum* by changing culture medium composition. Bioresour. Technol. Reports 6, 237–240. https://doi.org/10.1016/j.biteb.2019.03.012

Perez, J.M., Richter, H., Loftus, S.E., Angenent, L.T., 2013. Biocatalytic reduction of short-chain carboxylic acids into their corresponding alcohols with syngas fermentation. Biotechnol. Bioeng. 110, 1066–1077. https://doi.org/10.1002/bit.24786

Persson, O., Danell, R., Schneider, J.W., 2009. How to use Bibexcel for vatious types of bibliometric analysis, in: Astrom, F., Danell, R., Larsen, B., Schneider, J.W. (Eds.), Celebrating Scholarly Communication Studies: A Festschrift for Olle Persson at His 60th Birthday. International Society for Scientometrics and Informetrics, Leuven, Belgium, pp. 9–24.

Pesek, S.C., Koros, W.J., 1994. Aqueous quenched asymmetric polysulfone hollow fibers

prepared by dry/wet phase separation. J. Memb. Sci. 88, 1–19. https://doi.org/10.1016/0376-7388(93)E0150-I

Peters, M.S., Timmerhaus, K.D., 2014. Plant design and economics for chemical engineers. New York, NY.

Petersen, A.M., Franco, T., Görgens, J.F., 2018. Comparison of recovery of volatile fatty acids and mixed ketones as alternative downstream processes for acetogenisis fermentation. Biofuels, Bioprod. Biorefining 12, 882–898. https://doi.org/10.1002/bbb.1901

Phillips, J.R., Atiyeh, H.K., Tanner, R.S., Torres, J.R., Saxena, J., Wilkins, M.R., Huhnke, R.L., 2015. Butanol and hexanol production in *Clostridium carboxidivorans* syngas fermentation: Medium development and culture techniques. Bioresour. Technol. 190, 114–121. https://doi.org/10.1016/j.biortech.2015.04.043

Phillips, J.R., Huhnke, R.L., Atiyeh, H.K., 2017. Syngas fermentation: A microbial conversion process of gaseous substrates to various products. Fermentation 3. https://doi.org/10.3390/fermentation3020028

Piccolo, C., Bezzo, F., 2009. A techno-economic comparison between two technologies for bioethanol production from lignocellulose. Biomass and Bioenergy 33, 478–491. https://doi.org/10.1016/j.biombioe.2008.08.008

Ramí O-Pujol, S., Ganigú, R., Bã Neras, L., Jes´, J., Colprim, J., 2018. Effect of ethanol and butanol on autotrophic growth of model homoacetogens. FEMS Microbiol. Lett. 365, 84. https://doi.org/10.1093/femsle/fny084

Ramió-Pujol, S., Ganigué, R., Bañeras, L., Colprim, J., 2015a. Incubation at 25°C prevents acid crash and enhances alcohol production in *Clostridium carboxidivorans* P7. Bioresour. Technol. 192, 296–303. https://doi.org/10.1016/j.biortech.2015.05.077

Ramió-Pujol, S., Ganigué, R., Bañeras, L., Colprim, J., 2015b. How can alcohol production be improved in carboxydotrophic clostridia? Process Biochem. 50, 1047–1055. https://doi.org/10.1016/j.procbio.2015.03.019

Rastogi, M., Shrivastava, S., 2017. Recent advances in second generation bioethanol production: An insight to pretreatment, saccharification and fermentation processes. Renew. Sustain. Energy Rev. 80, 330–340. https://doi.org/10.1016/j.rser.2017.05.225

Reyes, S.C., Sinfelt, J.H., Feeley, J.S., 2003. Evolution of processes for synthesis gas production: Recent developments in an old technology. Ind. Eng. Chem. Res. 42, 1588–1597. https://doi.org/10.1021/ie0206913

Richter, H., Martin, M.E., Angenent, L.T., 2013. A two-stage continuous fermentation system for conversion of syngas into ethanol. Energies 6, 3987–4000. https://doi.org/10.3390/en6083987

Richter, Hanno, Molitor, B., Diender, M., Sousa, D.Z., Angenent, L.T., 2016. A narrow pH range supports butanol, hexanol, and octanol production from syngas in a continuous co-culture of *Clostridium ljungdahlii* and *Clostridium kluyveri* with in-line product extraction. Front. Microbiol. 7. https://doi.org/10.3389/fmicb.2016.01773

Richter, H., Molitor, B., Wei, H., Chen, W., Aristilde, L., Angenent, L.T., 2016. Ethanol production in syngas-fermenting: *Clostridium ljungdahlii* is controlled by thermodynamics rather than by enzyme expression. Energy Environ. Sci. 9, 2392–2399. https://doi.org/10.1039/c6ee01108j

Riggs, S.S., Heindel, T.J., 2006. Measuring carbon monoxide gas-liquid mass transfer in a stirred tank reactor for syngas fermentation. Biotechnol. Prog. 22, 903–906. https://doi.org/10.1021/bp050352f

Rittmann, B.E., 2018. Biofilms, active substrata, and me. Water Res. 132, 135–145. https://doi.org/10.1016/j.watres.2017.12.043

Rittmann, B.E., 2006. The membrane biofilm reactor: the natural partnership of membranes and biofilm. Water Sci. Technol. 53, 219–225. https://doi.org/10.2166/wst.2006.096

Rittmann, B.E., McCarty, P.L., 2020. Environmental Biotechnology: Principles and Applications, Second Edi. ed. McGraw-Hill Education, New York, NY.

Rostrup-Nielsen, J.R., 2000. New aspects of syngas production and use. Catal. Today 63, 159–164. https://doi.org/10.1016/S0920-5861(00)00455-7

Sander, R., 2015. Compilation of Henry's law constants (version 4.0) for water as solvent. Atmos. Chem. Phys. 15, 4399–4981. https://doi.org/10.5194/acp-15-4399-2015

Santos, R.G. dos, Alencar, A.C., 2020. Biomass-derived syngas production via gasification process and its catalytic conversion into fuels by Fischer Tropsch synthesis: A review. Int. J. Hydrogen Energy 45, 18114–18132. https://doi.org/10.1016/j.ijhydene.2019.07.133

Saxena, J., Tanner, R.S., 2012. Optimization of a corn steep medium for production of ethanol from synthesis gas fermentation by *Clostridium ragsdalei*. World J. Microbiol. Biotechnol. 28, 1553–1561. https://doi.org/10.1007/s11274-011-0959-0

Scarborough, M.J., Lynch, G., Dickson, M., McGee, M., Donohue, T.J., Noguera, D.R.,

2018. Increasing the economic value of lignocellulosic stillage through medium-chain fatty acid production. Biotechnol. Biofuels 11, 1–17. https://doi.org/10.1186/s13068-018-1193-x

Scholes, C.A., Ghosh, U.K., 2017. Review of membranes for helium separation and purification. Membranes (Basel). 7, 1–13. https://doi.org/10.3390/membranes7010009

Scholes, C.A., Kentish, S.E., Stevens, G.W., deMontigny, D., 2015. Comparison of thin film composite and microporous membrane contactors for CO_2 absorption into monoethanolamine. Int. J. Greenh. Gas Control 42, 66–74. https://doi.org/10.1016/j.ijggc.2015.07.032

Seader, J.D., Henley, E.J., Roper, D.K., 2011. Separation process principles: Chemical and biochemical operations. Wiley, Hoboken, NJ.

Seedorf, H., Fricke, W.F., Veith, B., Brüggemann, H., Liesegang, H., Strittmatter, A., Miethke, M., Buckel, W., Hinderberger, J., Li, F., Hagemeier, C., Thauer, R.K., Gottschalk, G., 2008. The genome of *Clostridium kluyveri*, a strict anaerobe with unique metabolic features. Proc. Natl. Acad. Sci. U. S. A. 105, 2128–2133. https://doi.org/10.1073/pnas.0711093105

Shen, N., Dai, K., Xia, X.Y., Zeng, R.J., Zhang, F., 2018. Conversion of syngas (CO and H_2) to biochemicals by mixed culture fermentation in mesophilic and thermophilic hollow-fiber membrane biofilm reactors. J. Clean. Prod. 202, 536–542. https://doi.org/10.1016/j.jclepro.2018.08.162

Shen, Y., Brown, R., Wen, Z., 2014. Syngas fermentation of *Clostridium carboxidivorans* P7 in a hollow fiber membrane biofilm reactor: Evaluating the mass transfer coefficient and ethanol production performance. Biochem. Eng. J. 85, 21–29. https://doi.org/10.1016/j.bej.2014.01.010

Sims, R.E.H., Mabee, W., Saddler, J.N., Taylor, M., 2010. An overview of second generation biofuel technologies. Bioresour. Technol. 101, 1570–1580. https://doi.org/10.1016/j.biortech.2009.11.046

Skidmore, B.E., Baker, R.A., Banjade, D.R., Bray, J.M., Tree, D.R., Lewis, R.S., 2013. Syngas fermentation to biofuels: Effects of hydrogen partial pressure on hydrogenase efficiency. Biomass and Bioenergy 55, 156–162. https://doi.org/10.1016/j.biombioe.2013.01.034

Speight, J.G., 2019. 3 - Unconventional gas, in: Speight, J.G.B.T.-N.G. (Second E. (Ed.), . Gulf Professional Publishing, Boston, pp. 59–98. https://doi.org/https://doi.org/10.1016/B978-0-12-809570-6.00003-5

Spirito, C.M., Marzilli, A.M., Angenent, L.T., 2018. Higher Substrate Ratios of Ethanol

to Acetate Steered Chain Elongation toward n-Caprylate in a Bioreactor with Product Extraction. Environ. Sci. Technol. 52, 13438–13447. https://doi.org/10.1021/acs.est.8b03856

Spirito, C.M., Richter, H., Rabaey, K., Stams, A.J.M., Angenent, L.T., 2014. Chain elongation in anaerobic reactor microbiomes to recover resources from waste. Curr. Opin. Biotechnol. 27, 115–122. https://doi.org/10.1016/j.copbio.2014.01.003

Steinbusch, K.J.J., Hamelers, H.V.M., Buisman, C.J.N., 2008. Alcohol production through volatile fatty acids reduction with hydrogen as electron donor by mixed cultures. Water Res. 42, 4059–4066. https://doi.org/10.1016/j.watres.2008.05.032

Steinbusch, K.J.J., Hamelers, H.V.M., Plugge, C.M., Buisman, C.J.N., 2011. Biological formation of caproate and caprylate from acetate: Fuel and chemical production from low grade biomass. Energy Environ. Sci. 4, 216–224. https://doi.org/10.1039/c0ee00282h

Straub, M., Demler, M., Weuster-Botz, D., Dürre, P., 2014. Selective enhancement of autotrophic acetate production with genetically modified *Acetobacterium woodii*. J. Biotechnol. 178, 67–72. https://doi.org/10.1016/j.jbiotec.2014.03.005

Sun, X., Atiyeh, H.K., Huhnke, R.L., Tanner, R.S., 2019. Syngas fermentation process development for production of biofuels and chemicals: A review. Bioresour. Technol. Reports 7, 100279. https://doi.org/10.1016/j.biteb.2019.100279

Sun, X., Atiyeh, H.K., Kumar, A., Zhang, H., 2018a. Enhanced ethanol production by *Clostridium ragsdalei* from syngas by incorporating biochar in the fermentation medium. Bioresour. Technol. 247, 291–301. https://doi.org/10.1016/j.biortech.2017.09.060

Sun, X., Atiyeh, H.K., Kumar, A., Zhang, H., Tanner, R.S., 2018b. Biochar enhanced ethanol and butanol production by *Clostridium carboxidivorans* from syngas. Bioresour. Technol. 265, 128–138. https://doi.org/10.1016/j.biortech.2018.05.106

Tan, E.C.D., Snowden-Swan, L.J., Talmadge, M., Dutta, A., Jones, S., Ramasamy, K.K., Gray, M., Dagle, R., Padmaperuma, A., Gerber, M., Sahir, A.H., Tao, L., Zhang, Y., 2017. Comparative techno-economic analysis and process design for indirect liquefaction pathways to distillate-range fuels via biomass-derived oxygenated intermediates upgrading. Biofuels, Bioprod. Biorefining 11, 41–66. https://doi.org/10.1002/bbb.1710

Tang, Y., Zhou, C., Van Ginkel, S.W., Ontiveros-Valencia, A., Shin, J., Rittmann, B.E., 2012. Hydrogen permeability of the hollow fibers used in H 2-based membrane biofilm reactors. J. Memb. Sci. 407–408, 176–183. https://doi.org/10.1016/j.memsci.2012.03.040

Tanner, R.S., Miller, Letrisa, M., Yang, D., 1993. *Clostridium ljungdahlii* sp. nov., an acetogenic species in clostridial rRNA homology group I. Int. J. Syst. Bacteriol. 43, 232–236.

Techtmann, S.M., Colman, A.S., Robb, F.T., 2009. "That which does not kill us only makes us stronger": The role of carbon monoxide in thermophilic microbial consortia: Minireview. Environ. Microbiol. 11, 1027–1037. https://doi.org/10.1111/j.1462-2920.2009.01865.x

Terada, A., Yamamoto, T., Hibiya, K., Tsuneda, S., Hirata, A., 2004. Enhancement of biofilm formation onto surface-modified hollow-fiber membranes and its application to a membrane-aerated biofilm reactor. Water Sci. Technol. 49, 263–268. https://doi.org/10.2166/wst.2004.0857

U.S. Bureau of Labor Statistics, n.d. Occupational Employment and Wage Statistics (OEWS) [WWW Document]. URL https://www.bls.gov/oes/

U.S. Secretary of Commerce, 2018. NIST Chemistry WebBook. https://doi.org/https://doi.org/10.18434/T4D303

Ungerman, A.J., Heindel, T.J., 2007. Carbon monoxide mass transfer for syngas fermentation in a stirred tank reactor with dual impeller configurations. Biotechnol. Prog. 23, 613–620. https://doi.org/10.1021/bp060311z

Valgepea, K., de Souza Pinto Lemgruber, R., Meaghan, K., Palfreyman, R.W., Abdalla, T., Heijstra, B.D., Behrendorff, J.B., Tappel, R., Köpke, M., Simpson, S.D., Nielsen, L.K., Marcellin, E., 2017. Maintenance of ATP Homeostasis Triggers Metabolic Shifts in Gas-Fermenting Acetogens. Cell Syst. 4, 505-515.e5. https://doi.org/10.1016/j.cels.2017.04.008

van Eck, N.J., Waltman, L., 2010. Software survey: VOSviewer, a computer program for bibliometric mapping. Scientometrics 84, 523–538. https://doi.org/10.1007/s11192-009-0146-3

Van Ginkel, S.W., Ahn, C.H., Badruzzaman, M., Roberts, D.J., Lehman, S.G., Adham, S.S., Rittmann, B.E., 2008. Kinetics of nitrate and perchlorate reduction in ion-exchange brine using the membrane biofilm reactor (MBfR). Water Res. 42, 4197–4205. https://doi.org/10.1016/j.watres.2008.07.012

Van Ginkel, S.W., Lamendella, R., Kovacik, W.P., Santo Domingo, J.W., Rittmann, B.E., 2010. Microbial community structure during nitrate and perchlorate reduction in ion-exchange brine using the hydrogen-based membrane biofilm reactor (MBfR). Bioresour. Technol. 101, 3747–3750. https://doi.org/10.1016/j.biortech.2009.12.028

Vasudevan, D., Richter, H., Angenent, L.T., 2014. Upgrading dilute ethanol from syngas fermentation to n-caproate with reactor microbiomes. Bioresour. Technol. 151, 378–

382. https://doi.org/10.1016/j.biortech.2013.09.105

Wang, H.-J., Dai, K., Wang, Y.-Q., Wang, H.-F., Zhang, F., Zeng, R.J., 2018. Mixed culture fermentation of synthesis gas in the microfiltration and ultrafiltration hollow-fiber membrane biofilm reactors. Bioresour. Technol. 267, 650–656. https://doi.org/10.1016/j.biortech.2018.07.098

Wang, H.J., Dai, K., Xia, X.Y., Wang, Y.Q., Zeng, R.J., Zhang, F., 2018. Tunable production of ethanol and acetate from synthesis gas by mesophilic mixed culture fermentation in a hollow fiber membrane biofilm reactor. J. Clean. Prod. 187, 165–170. https://doi.org/10.1016/j.jclepro.2018.03.193

Wang, J., Yang, X., Chen, C.C., Yang, S.T., 2014. Engineering clostridia for butanol production from biorenewable resources: From cells to process integration. Curr. Opin. Chem. Eng. 6, 43–54. https://doi.org/10.1016/j.coche.2014.09.003

Wang, L., Boutilier, M.S.H., Kidambi, P.R., Jang, D., Hadjiconstantinou, N.G., Karnik, R., 2017. Fundamental transport mechanisms, fabrication and potential applications of nanoporous atomically thin membranes. Nat. Nanotechnol. 12, 509–522. https://doi.org/10.1038/nnano.2017.72

Wang, Y.Q., Yu, S.J., Zhang, F., Xia, X.Y., Zeng, R.J., 2017. Enhancement of acetate productivity in a thermophilic (55 °C) hollow-fiber membrane biofilm reactor with mixed culture syngas (H_2/CO_2) fermentation. Appl. Microbiol. Biotechnol. 101, 2619–2627. https://doi.org/10.1007/s00253-017-8124-9

Wang, Y.Q., Zhang, F., Zhang, W., Dai, K., Wang, H.J., Li, X., Zeng, R.J., 2018. Hydrogen and carbon dioxide mixed culture fermentation in a hollow-fiber membrane biofilm reactor at 25 °C. Bioresour. Technol. 249, 659–665. https://doi.org/10.1016/j.biortech.2017.10.054

Weimer, P.J., Nerdahl, M., Brandl, D.J., 2015. Production of medium-chain volatile fatty acids by mixed ruminal microorganisms is enhanced by ethanol in co-culture with *Clostridium kluyveri*. Bioresour. Technol. 175, 97–101. https://doi.org/10.1016/j.biortech.2014.10.054

Wender, I., 1996. Reactions of synthesis gas. Fuel Process. Technol. 48, 189–297. https://doi.org/10.1016/S0378-3820(96)01048-X

Wilhelm, Simbeck, Karp, Dickenson, 2001. Syngas production for gas-to-liquids applications: technologies, issues and outlook. Fuel Process. Technol. 71, 139/148. https://doi.org/10.1016/j.joule.2017.08.010

Wu, Y., Wu, Z., Chu, H., Li, J., Ngo, H.H., Guo, W., Zhang, N., Zhang, H., 2019. Comparison study on the performance of two different gas-permeable membranes used in a membrane-aerated biofilm reactor. Sci. Total Environ. 658, 1219–1227.

https://doi.org/10.1016/j.scitotenv.2018.12.121

Xiao, P.Y., Zhou, J., Luo, X., Kang, B., Guo, L., Yuan, G., Zhang, L., Zhao, T., 2021. Enhanced nitrogen removal from high-strength ammonium wastewater by improving heterotrophic nitrification-aerobic denitrification process: Insight into the influence of dissolved oxygen in the outer layer of the biofilm. J. Clean. Prod. 297, 126658. https://doi.org/10.1016/j.jclepro.2021.126658

Xie, H., Zhang, Y., Zeng, X., He, Y., 2020. Sustainable land use and management research: a scientometric review, Landscape Ecology. Springer Netherlands. https://doi.org/10.1007/s10980-020-01002-y

Xu, J., Guzman, J.J.L., Andersen, S.J., Rabaey, K., Angenent, L.T., 2015. In-line and selective phase separation of medium-chain carboxylic acids using membrane electrolysis. Chem. Commun. 51, 6847–6850. https://doi.org/10.1039/c5cc01897h

Yang, B., Wynman, C., 2012. Pretreatment: the key to unlocking low-cost cellulosic ethanol Bin. Biofuels, Bioprod. Biorefining 6, 246–256. https://doi.org/10.1002/bbb

Yang, L., Ge, X., Wan, C., Yu, F., Li, Y., 2014. Progress and perspectives in converting biogas to transportation fuels. Renew. Sustain. Energy Rev. 40, 1133–1152. https://doi.org/10.1016/j.rser.2014.08.008

Yao, Z., You, S., Ge, T., Wang, C.H., 2018. Biomass gasification for syngas and biochar co-production: Energy application and economic evaluation. Appl. Energy 209, 43–55. https://doi.org/10.1016/j.apenergy.2017.10.077

Yasin, M., Jeong, Y., Park, S., Jeong, J., Lee, E.Y., Lovitt, R.W., Kim, B.H., Lee, J., Chang, I.S., 2015. Microbial synthesis gas utilization and ways to resolve kinetic and mass-transfer limitations. Bioresour. Technol. 177, 361–374. https://doi.org/10.1016/j.biortech.2014.11.022

Yasin, M., Park, S., Jeong, Y., Lee, E.Y., Lee, J., Chang, I.S., 2014. Effect of internal pressure and gas/liquid interface area on the CO mass transfer coefficient using hollow fibre membranes as a high mass transfer gas diffusing system for microbial syngas fermentation. Bioresour. Technol. 169, 637–643. https://doi.org/10.1016/j.biortech.2014.07.026

Zhang, F., Ding, J., Shen, N., Zhang, Y., Ding, Z., Dai, K., Zeng, R.J., 2013a. In situ hydrogen utilization for high fraction acetate production in mixed culture hollow-fiber membrane biofilm reactor. Appl. Microbiol. Biotechnol. 97, 10233–10240. https://doi.org/10.1007/s00253-013-5281-3

Zhang, F., Ding, J., Zhang, Y., Chen, M., Ding, Z.W., van Loosdrecht, M.C.M., Zeng, R.J., 2013b. Fatty acids production from hydrogen and carbon dioxide by mixed culture in the membrane biofilm reactor. Water Res. 47, 6122–6129.

https://doi.org/10.1016/j.watres.2013.07.033

Zhao, H.P., Ilhan, Z.E., Ontiveros-Valencia, A., Tang, Y., Rittmann, B.E., Krajmalnik-Brown, R., 2013a. Effects of multiple electron acceptors on microbial interactions in a hydrogen-based biofilm. Environ. Sci. Technol. 47, 7396–7403. https://doi.org/10.1021/es401310j

Zhao, H.P., Ontiveros-Valencia, A., Tang, Y., Kim, B.O., Ilhan, Z.E., Krajmalnik-Brown, R., Rittmann, B., 2013b. Using a two-stage hydrogen-based membrane biofilm reactor (MBfR) to achieve complete perchlorate reduction in the presence of nitrate and sulfate. Environ. Sci. Technol. 47, 1565–1572. https://doi.org/10.1021/es303823n

Zhao, L., Deng, J., Sun, P., Liu, J., Ji, Y., Nakada, N., Qiao, Z., Tanaka, H., Yang, Y., 2018. Nanomaterials for treating emerging contaminants in water by adsorption and photocatalysis: Systematic review and bibliometric analysis. Sci. Total Environ. 627, 1253–1263. https://doi.org/10.1016/j.scitotenv.2018.02.006

Zhao, R., Liu, Y., Zhang, H., Chai, C., Wang, J., Jiang, W., Gu, Y., 2019. CRISPR-Cas12a-Mediated Gene Deletion and Regulation in *Clostridium ljungdahlii* and Its Application in Carbon Flux Redirection in Synthesis Gas Fermentation. https://doi.org/10.1021/acssynbio.9b00033

Zhong, S., Geng, Y., Liu, W., Gao, C., Chen, W., 2016. A bibliometric review on natural resource accounting during 1995–2014. J. Clean. Prod. 139, 122–132. https://doi.org/10.1016/j.jclepro.2016.08.039

Zhou, C., Ontiveros-Valencia, A., Cornette de Saint Cyr, L., Zevin, A.S., Carey, S.E., Krajmalnik-Brown, R., Rittmann, B.E., 2014. Uranium removal and microbial community in a H_2-based membrane biofilm reactor. Water Res. 64, 255–264. https://doi.org/10.1016/j.watres.2014.07.013

Zhu, H., Shanks, B.H., Heindel, T.J., 2008. Enhancing CO - Water Mass Transfer by Functionalized MCM41 Nanoparticles 7881–7887.

Zhu, J., Dressel, W., Pacion, K., Ren, Z.J., 2021. ES & T in the 21st Century : A Data-Driven Analysis of Research Topics , Interconnections , And Trends in the Past 20 Years. https://doi.org/10.1021/acs.est.0c07551

Ziv-El, M., Popat, S.C., Cai, K., Halden, R.U., Krajmalnik-Brown, R., Rittmann, B.E., 2012. Managing methanogens and homoacetogens to promote reductive dechlorination of trichloroethene with direct delivery of H_2 in a membrane biofilm reactor. Biotechnol. Bioeng. 109, 2200–2210. https://doi.org/10.1002/bit.24487

Ziv-El, M.C., Rittmann, B.E., 2009. Systematic evaluation of nitrate and perchlorate bioreduction kinetics in groundwater using a hydrogen-based membrane biofilm

reactor. Water Res. 43, 173–181. https://doi.org/10.1016/j.watres.2008.09.035